I. Enantioselective Acylation of Silyl Ketene Acetals through Fluoride Anion-Binding Catalysis II. Development of a Practical Method for the Synthesis of Highly Enantioenriched Trans-1,2-Amino Alcohols

I. Enantioselective Acylation of Silyl Ketene Acetals through Fluoride Anion-Binding Catalysis

II. Development of a Practical Method for the Synthesis of Highly Enantioenriched *trans*-1,2-Amino Alcohols

A thesis presented

by

James Andrew Birrell

to

The Department of Chemistry and Chemical Biology

in partial fulfillment of the requirements

for the degree of

Doctor of Philosophy

in the subject of

Chemistry

Harvard University

Cambridge, Massachusetts

May, 2013

Research Advisor: Professor Eric N. Jacobsen *James Andrew Birrell*

I. Enantioselective Acylation of Silyl Ketene Acetals through Fluoride Anion-Binding Catalysis

II. Development of a Practical Method for the Synthesis of Highly Enantioenriched *trans*-1,2-Amino Alcohols

Abstract

A highly enantioselective acylation of silyl ketene acetals with acyl fluorides was developed to generate useful α,α-disubstituted butyrolactone products in high yield and excellent enantioselectivities. This transformation is promoted by an arylpyrrolidino thiourea catalyst and 4-pyrrolidinopyridine and represents the first example of enantioselective thiourea anion-binding catalysis with fluoride. Mechanistic investigations revealed both catalysts to be necessary for reaction to occur, suggesting the thiourea aids in the generation of the key *N*-acylpyridinium/fluoride ion pair. The outstanding hydrogen-bond-accepting ability of fluoride is likely important in this regard. In addition, a strong dependence on both the *N*-acylpyridinium counteranion and the substituents on the silicon group of the silyl ketene acetal were observed, highlighting the importance of the silicon-fluoride interaction.

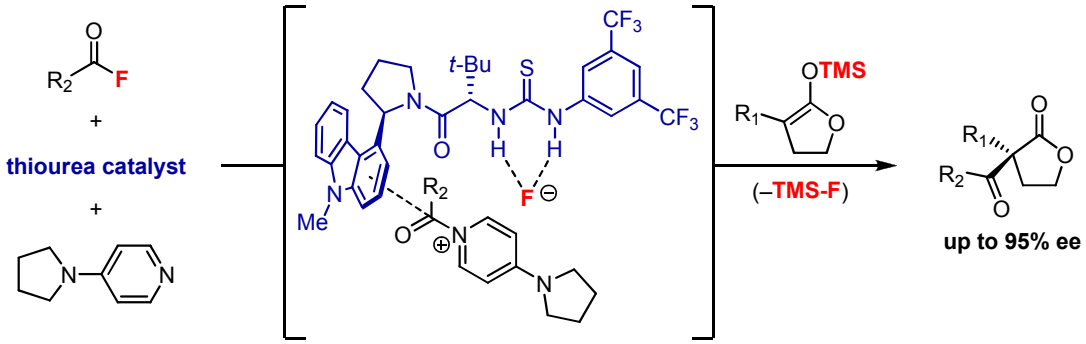

A cyclic oligomeric (salen)Co–OTf complex was used to catalyze a highly enantioselective addition of phenyl carbamate to *meso*-epoxides to afford protected *trans*-1,2-amino alcohols. The use of an oligomeric (salen)Co–OTf complex as the catalyst and aryl carbamates as nucleophiles was crucial to the development of this reaction protocol. This method is amenable to large-scale synthesis due to the low catalyst loadings and high concentration used, its operational simplicity, and the use of inexpensive, commercially-available starting materials. To demonstrate the synthetic utility of this protocol, optically pure *trans*-2-aminocyclohexanol hydrochloride and *trans*-2-aminocyclopentanol hydrochloride were prepared on a multigram scale using only 0.5 and 1 mol% catalyst loading, respectively.

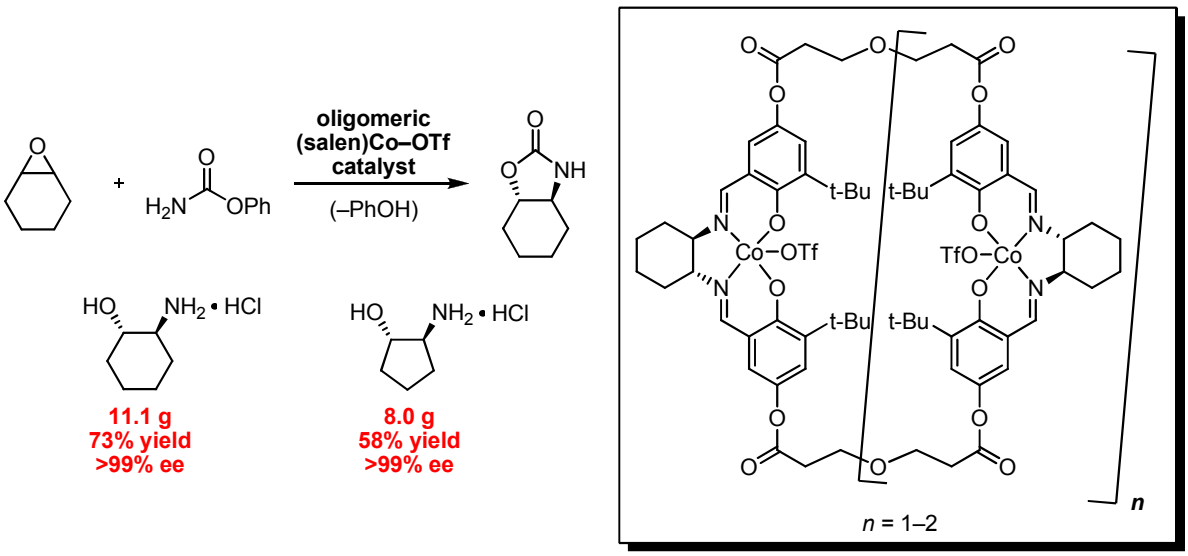

Table of Contents

Acknowledgments

I am deeply grateful for the opportunity and guidance provided to me by Professor Eric Jacobsen. I was ecstatic when I joined his lab in the winter of 2008, and it has proven to be a perfect place for me to develop professionally. Eric has cultivated an atmosphere of scientific rigor while always allowing his students to be creative and explore their own ideas. There have been numerous conversations we have had at pivotal moments in my graduate career where Eric has motivated me and guided my future progress by telling me exactly what I needed to hear. I have grown tremendously from his guidance and will use the lessons I've learned from him throughout the rest of my career.

Professors Andrew Myers and Emily Balskus served on my graduate advising committee and provided useful guidance in intermediate committee meetings during graduate school as well as at my Ph.D. defense. I'm grateful for the time they spent thinking about my chemistry and the contributions they have made to my research. Professors Dave Evans and Ted Betley helped me early in graduate school and provided the foundation for my future growth as a scientist.

I would not have attended graduate school at all if it wasn't for the opportunity given to me by Professor Steve Burke at the University of Wisconsin – Madison. As a junior I was very excited about the idea of doing organic chemistry research and only wanted to work with Professor Burke. He graciously accepted me into his lab and spent many hours patiently talking with me about graduate school, academia, and the pharmaceutical industry and how these options might appeal to me. I was also paired with two outstanding graduate student mentors in the Burke lab: Chris Marvin and Andrew Dilger. These guys showed me that in addition to being interesting and useful, chemistry can also be cool and fun (despite the constant Jimmy Buffet and Indie music).

At Harvard my graduate career accelerated dramatically after I was lucky enough to begin working with Jean-Nic Desrosiers. Jean-Nic welcomed me onto his can't-miss project when I was a second-year graduate student. He treated me as an intellectual equal while also teaching me how to think about reaction optimization, synthesis, strategy, and presentation. In addition, he entrusted me with the project after he completed his postdoc and left the group to work in industry. His guidance throughout the acylation project was instrumental to my development, and I'm extremely grateful for everything he taught me early in my career. Attending Jean-Nic's all-French wedding ceremony in Montreal was also an entertaining and memorable cultural experience.

As a young graduate student, I looked up to the senior students as models for how to perform scientific research and act as a professional. Stephan Zuend, Meredith McGowan, Rebecca Loy, Chris Uyeda, and Bekka Klausen each taught me a great deal about science and contributed to the positive culture of the lab. Weekly ultimate games, training runs for the annual 5k, and having drinks at the Cellar were spearheaded by this group of scholar-athlete-drinkers.

During graduate school I was lucky to be able to work next to Adam Brown and Naomi Rajapaksa. Adam and Naomi were in the class a year ahead of me and were true leaders and role models in the lab. They were thrust into the senior ranks of the group early in graduate school and set a balanced tone of working hard while maintaining a well-rounded life outside of lab. Naomi and I worked for so long together that we developed a sibling-type relationship, complete with both a lot of great memories as well as a few Naomi daggers along the way. I couldn't have chosen a better guy than ARB to share an office with. Whether it was in lab, on the golf course, or taking a detour to Browntown we always had a great time.

Dave Ford, Song Lin, and Andy Röetheli were colleagues and friends that made coming to work easy and enjoyable every day. They set a fast pace for our class as intellectuals and scientists that kept me motivated throughout graduate school. I had the pleasure of sharing an apartment for two years on Carlos Medeiros with Dave as well as countless beers and late-night Hong Kong combination platters. Song made graduate school and acclimating to a new country look extremely easy and also is one of the funniest guys I've met. His one-liners during group meetings and presentations were always dead on, and if he wasn't such a great chemist I would try to persuade him to go into stand-up comedy. Andy is perhaps the smoothest guy I know and is also a great scientist. He taught me about many of the finer things in life such as Jacques Cousteau, Dom Rose, and of course, Saint Tropez. I'm grateful for the friendships we have all developed and know they will last many years into the future. In addition to being great people, these are also some exceptional scientists, and I look forward to seeing the impact they will have in their future careers.

The postdocs in the lab were instrumental to both the culture and the research in the Jacobsen lab. As one of them pointed out, we truly do have "the most talented postdocs in the world." Specifically, I'm thankful to Rob Knowles, Noah Burns, and Sean Kedrowski for spending countless hours talking about both chemistry and a wide range of other subjects as well as reliving their glory days every once in a while on the streets of Cambridge.

With the departure of five senior graduate students in a short period of time, I know the lab is in good hands with a talented group of younger graduate students that will quickly become leaders as Adam and Naomi did two years ago. Mike Witten, Amanda Turek, Yongho Park, Gary Zhang, Steven Banik, Rose Kennedy, Baye Galligan, and Ania Levina have promising careers ahead of them, and it's been a pleasure for me to work with each of them. In particular,

sharing an office with Steven was always entertaining. Steven can both talk the talk and walk the walk, as well as being a great guy and a Badger. I look forward to all the great research he will do over the course of his graduate and professional career.

All of my other friends in Cambridge and Boston have made my five years here extremely enjoyable and rewarding. From playing basketball to going out for food and drinks or going on weekend trips, I have had a truly phenomenal group of people around me both inside and outside of lab. I'm extremely grateful to have met each of them and will always have positive memories of my time in Cambridge and Boston because of these people.

Finally, I'm extremely lucky to have such a close and supportive family. My dad, mom and brother were instrumental in keeping me happy and focused during the past five years. The time they spent traveling to Cambridge to stay in the Kendall Square Marriot, welcoming me back home, and calling to stay in touch is greatly appreciated. Their love and support allowed me to keep my work in perspective and continually strive to be my best.

for my mother and father

List of Abbreviations

Ac	acetyl
Ada	adamantyl
APCI	atmospheric pressure chemical ionization
Ar	aryl
Bn	benzyl
Boc	*tert*-butoxycarbonyl
Bu	butyl
Bz	benzoyl
Cbz	benzyloxycarbonyl
conv	conversion
CSA	camphorsulfonic acid
DIPEA	*N*,*N*-diisopropylethylamine
DMA	*N*,*N*-dimethylacetamide
DMAP	*N*,*N*-4-dimethylaminopyridine
DME	1,2-dimethoxyethane
ee	enantiomeric excess
ent	enantiomer
Et	ethyl
equiv	equivalents
ESI	electrospray ionization
Fmoc	9-fluorenylmethoxycarbonyl
FTIR	Fourier transform infrared spectroscopy

g	grams
GC	gas chromatography
gem	geminal
h	hours
HBTU	*O*-(Benzotriazol-1-yl)-*N*,*N*,*N*',*N*'-tetramethyluronium hexafluorophosphate
HPLC	high-performance liquid chromatography
Hz	hertz
i-Pr	isopropyl
IPA	isopropylalcohol
IR	infrared
L	ligand
LC	liquid chromatography
LDA	lithium *N*,*N*-diisopropylamide
M	molar
Me	methyl
min	minutes
mol	mole
MOM	methoxymethyl
MS	molecular sieves
MS	mass spectrometry
NMR	nuclear magnetic resonance
Ph	phenyl
PPY	4-pyrrolidinopyridine

s	second
s-Bu	*sec*-butyl
SKA	silyl ketene acetal
t-Bu	*tert*-butyl
TBME	*tert*-butyl methyl ether
TBS	*tert*-butyldimethylsilyl
TES	triethylsilyl
Tf	trifluoromethanesulfonyl
TFA	trifluoroacetic acid
THF	tetrahydrofuran
TMB	3,4,5-trimethoxybenzoyl
TMS	trimethylsilyl
Ts	*para*-toluenesulfonyl
salen	a contraction of salicylaldehyde and ethylenediamine

Chapter One

Enantioselective Acylation of Silyl Ketene Acetals through Fluoride Anion-Binding Catalysis[1]

1.1 Introduction

1.1.1 Pyridine-Based Nucleophilic Catalysis

Pyridine derivatives induce significant rate accelerations in acyl transfer reactions through the generation of electrophilic *N*-acylpyridinium ion intermediates (Scheme 1.1).[2] While pyridine itself is a competent nucleophilic catalyst, analogs bearing strongly electron-donating substituents such as 4-(dimethylamino)pyridine (DMAP) and 4-pyrrolidinopyridine (PPY) are up to four orders of magnitude more reactive in representative acyl transfer reactions.[3,4] The

[1] Portions of this chapter have been published: Birrell, J. A.; Desrosiers, J.-N.; Jacobsen, E. N. *J. Am. Chem. Soc.* **2011**, *133*, 13872-13875.

[2] (a) Fersht, A. R.; Jencks, W. P. *J. Am. Chem. Soc.* **1969**, *91*, 2125-2126. (b) Fersht, A. R.; Jencks, W. P. *J. Am. Chem. Coc.* **1970**, *92*, 5432-5442.

[3] For pioneering reports on DMAP as a nucleophilic catalyst, see: (a) Litvinenko, L. M.; Kirichenko, A. I. *Dokl. Akad. Nauk. SSSR, Ser. Khim.* **1967**, *176*, 97-100. (b) Steglich, W.; Höfle, G. *Angew. Chem., Int. Ed.* **1969**, *8*, 981.

[4] For reviews on DMAP catalysis, see: (a) Hassner, A.; Krepski, L. R.; Alexanian, V. *Tetrahedron* **1978**, *34*, 2069-2076. (b) Höfle, G.; Steglich, W.; Vorbrüggen, H. *Angew. Chem., Int. Ed.* **1978**, *17*, 569-583. (c) Scriven, E. F. V. *Chem. Soc. Rev.* **1983**, *12*, 129-161. (d) Murugan, R.; Scriven, E. F. V. *Aldrichimica Acta* **2003**, *36*, 21-27.

amplified reactivity of 4-aminopyridine derivatives is ascribable to stabilization of the *N*-acylpyridinium cation through resonance donation from the strongly electron-donating dialkylamino substituent. This stabilization leads to both a greater equilibrium concentration of the key *N*-acylpyridinium ion pair intermediate and increased electrophilicity of that intermediate as a result of looser ion pairing.[5] The greater ion mobility of stabilized pyridinium salts was demonstrated by Steglich through the comparison of the specific conductivity of the acetate salts of *N*-methylpyridinium and *N*-methyl-4-(dimethylamino)pyridinium.[4b] It was found that the highly stabilized *N*-methyl-4-(dimethylamino)pyridinium ion pair (Scheme 1.1B) exhibited a specific conductivity almost five times greater than the unstabilized *N*-methylpyridinium ion pair, indicating that the presence of the dimethylamino group leads to a more loosely associated ion pair.

[5] For discussions on the mechanism of DMAP catalysis, see ref 4a and the following: (a) Spivey, A. C.; Arseniyadis, S. *Angew. Chem., Int. Ed*. **2004**, *43*, 5436-5441. (b) Xu, S.; Held, I.; Kempf, B.; Mayr, H.; Steglich, W.; Zipse, H. *Chem. Eur. J.* **2005**, *11*, 4751-4757. (c) Held, I.; Villinger, A.; Zipse, H. *Synthesis* **2005**, *9*, 1425-1430. (d) Lutz, V.; Glatthaar, J.; Würtele, C.; Serafin, M.; Hausmann, H.; Schreiner, P. R. *Chem. Eur. J.* **2009**, *15*, 8548-8557.

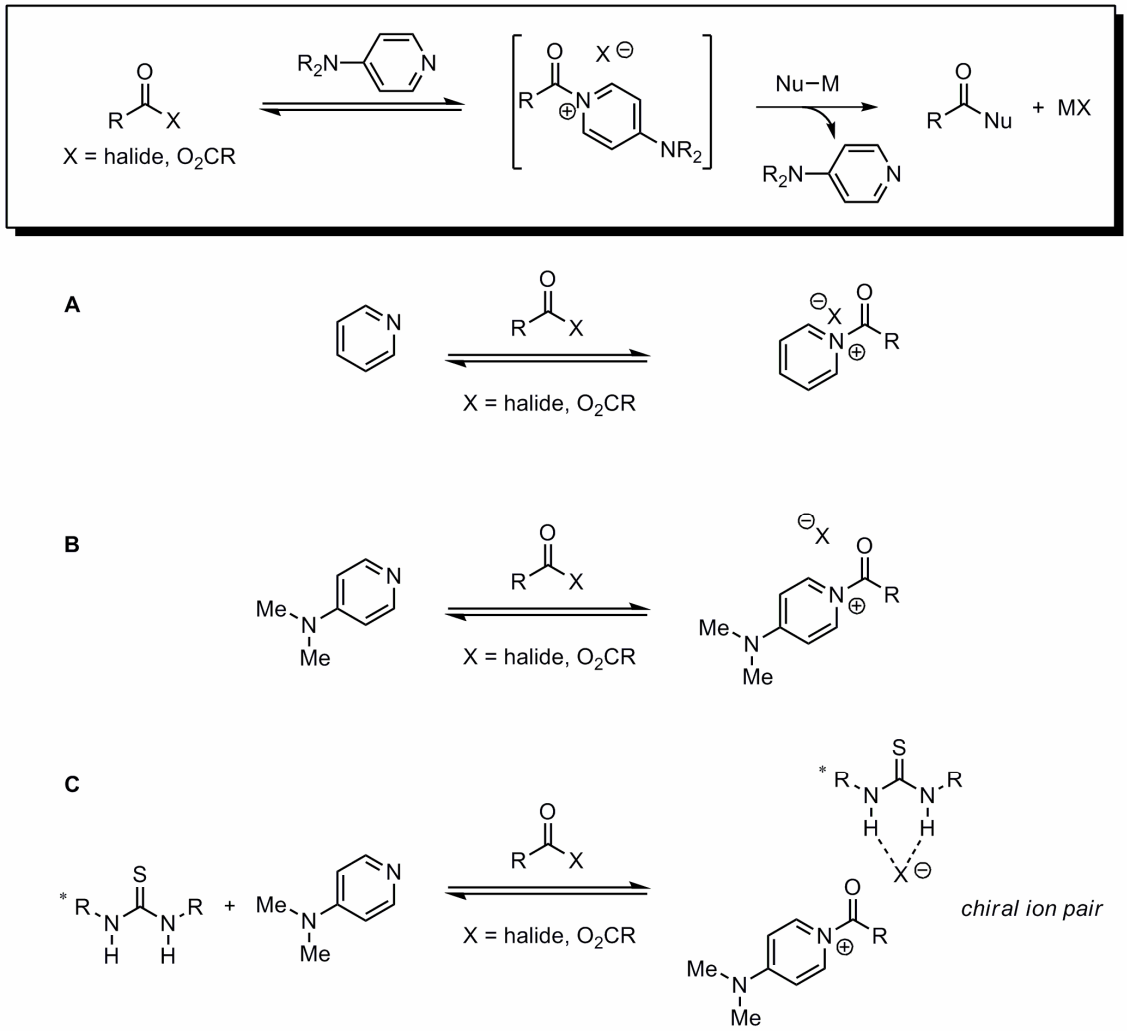

Scheme 1.1. Mechanism of DMAP catalysis and expansion of the *N*-acylpyridinium ion pair

An increase in the equilibrium concentration of an *N*-acylpyridinium ion pair and a looser association of this species can be achieved, in principle, through stabilization of the counteranion by a specific hydrogen-bond donor (Scheme 1.1C).[6] Both of these effects are expected to accelerate the reaction and should be achieved in the presence of a hydrogen-bond donor catalyst such as a urea or thiourea. In addition, opportunities for asymmetric induction exist via the generation of a chiral ion pair if a chiral hydrogen-bond donor catalyst is used. Our group has shown that chiral urea and thiourea derivatives can catalyze enantioselective reactions via

[6] For a review on thiourea anion-binding catalysis, see: Zhang, Z.; Schreiner, P. R. *Chem. Soc. Rev.* **2009**, *38*, 1187-1198.

mechanisms involving anion binding. This concept has been applied broadly to a range of thiourea-catalyzed enantioselective transformations including Pictet–Spengler-type cyclizations, nucleophilic additions to oxocarbenium ions, polycyclization reactions, and α-alkylations of aldehydes via an S_N1-type mechanism (Scheme 1.2).[7]

[7] (a) Raheem, I. T.; Thiara, P. S.; Peterson, E. A.; Jacobsen, E. N. *J. Am. Chem. Soc.* **2007**, *129*, 13404-13405. (b) Reisman, S. E.; Doyle, A. G.; Jacobsen, E. N. *J. Am. Chem. Soc.* **2008**, *130*, 7198-7199. (c) Klausen, R. S.; Jacobsen, E. N. *Org. Lett.* **2009**, *11*, 887-890. (d) Zuend, S. J.; Coughlin, M. P.; Lalonde, M. P.; Jacobsen, E. N. *Nature* **2009**, *461*, 968–970. (e) Knowles, R. R.; Lin, S.; Jacobsen, E. N. *J. Am. Chem. Soc.* **2010**, *132*, 5030-5032. (f) Brown, A. R.; Kuo, W.-H.; Jacobsen, E. N. *J. Am. Chem. Soc.* **2010**, *132*, 9286-9288.

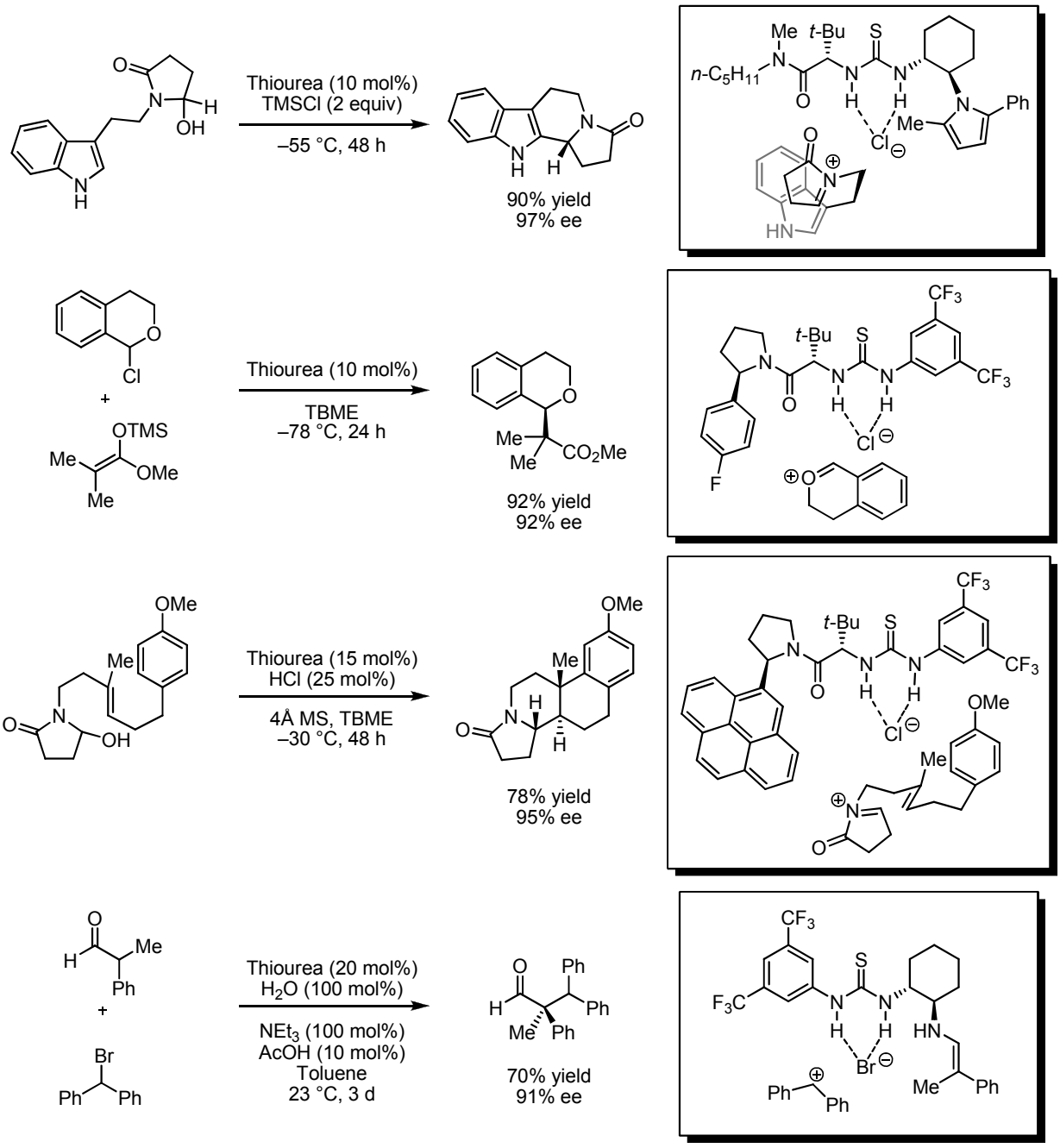

Scheme 1.2 Examples of enantioselective transformations proceeding via anion-binding catalysis

1.1.2 Thiourea-DMAP Co-catalyzed Acylative Kinetic Resolutions

Seidel has demonstrated the successful application of asymmetric hydrogen-bond donor catalysis using *N*-acylpyridinium ion pair intermediates in the context of chiral thiourea-DMAP

co-catalyzed acylative kinetic resolutions of primary amines (Scheme 1.3).[8] In this approach, the *N*-acylpyridinium ion pair is rendered chiral through association of the achiral ion pair with a chiral hydrogen-bond donor catalyst. Asymmetric induction was achieved in a variety of acylation reactions including the kinetic resolution of benzylic,[8a] propargylic,[8b] and allylic[8c] amines. A variety of hydrogen-bond donor catalysts were examined, with bis(thiourea) **1** and amidothiourea **2** proving optimal.

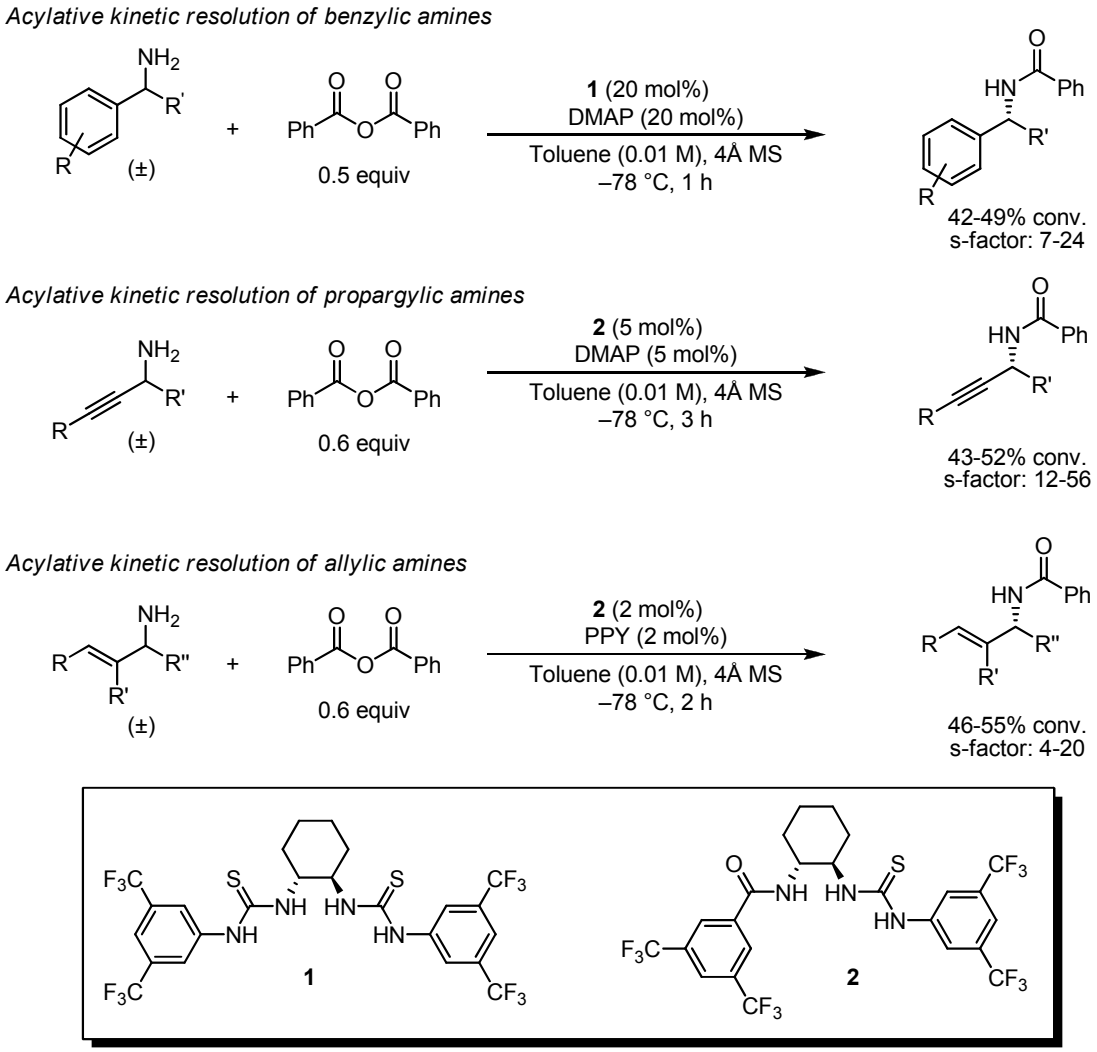

Scheme 1.3. Enantioselective hydrogen-bond donor catalysis using *N*-acylpyridinium ion pairs

[8] (a) De, C. K.; Klauber, E. G.; Seidel, D. *J. Am. Chem. Soc.* **2009**, *131*, 17060-17061. (b) Klauber, E. G.; De, C. K.; Shah, T. K.; Seidel, D. *J. Am. Chem. Soc.* **2010**, *132*, 13624-13626. (c) Klauber, E. G.; Mittal, N.; Shah, T. K.; Seidel, D. *Org. Lett.* **2011**, *13*, 2464-2467.

1.1.3 Chiral-DMAP Catalysis

Using a chiral hydrogen-bond donor catalyst to bind the counteranion of an *N*-acylpyridinium ion pair is fundamentally different from classical approaches to catalytic asymmetric acyl transfer reactions that employ chiral nucleophilic catalysts.[9] A variety of chiral DMAP derivatives have been developed and used as nucleophilic catalysts to promote asymmetric transformations. In these transformations, the *N*-acylpyridinium that is generated is chiral by virtue of the cationic component and can induce asymmetry in the subsequent acylation. Fu and others have pioneered this approach with great success. Selected examples include the planar-chiral-DMAP-catalyzed kinetic resolution of alcohols,[10] addition of alcohols to ketenes,[11] and the rearrangement of *O*-acylated enolates (Scheme 1.4).[12]

[9] For reviews on catalytic asymmetric acyl transfer reactions, see: (a) Fu, G. C. *Acc. Chem. Res.* **2004**, *37*, 542-547. (b) Wurz, R. P. *Chem. Rev.* **2007**, *107*, 5570-5595. (c) Spivey, A. C.; Arseniyadis, S. *Top. Curr. Chem.* **2010**, *291*, 233-280. (d) Müller, C. E.; Schreiner, P. R. *Angew. Chem. Int. Ed.* **2011**, *50*, 6012-6042.

[10] Ruble, J. C.; Latham, H. A.; Fu, G. C. *J. Am. Chem. Soc.* **1997**, *119*, 1492-1493.

[11] Hodous, B. L.; Ruble, J. C.; Fu, G. C. *J. Am. Chem. Soc.* **1999**, *121*, 2637-2638.

[12] (a) Ruble, J. C.; Fu, G. C. *J. Am. Chem. Soc.* **1998**, *120*, 11532-11533. (b) Hills, I. D.; Fu, G. C. *Angew. Chem., Int. Ed.* **2003**, *42*, 3921-3924.

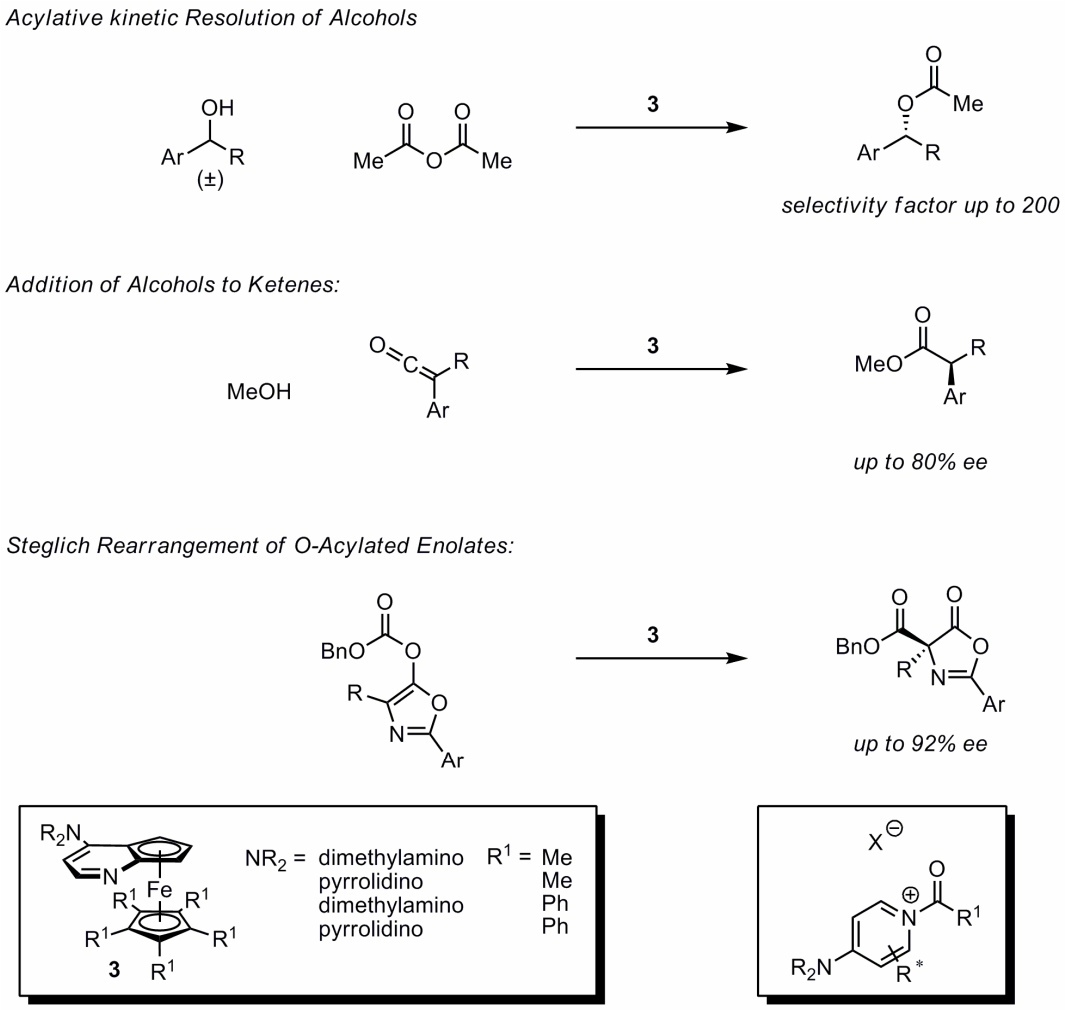

Scheme 1.4. Representative chiral-DMAP-catalyzed transformations

1.2 Results and Discussion

1.2.1 Identification of Mono-thiourea for *N*-Acylpyridinium Ion Catalysis

with Jean-Nicolas Desrosiers

We decided to further explore the opportunities for asymmetric hydrogen-bond donor catalysis using *N*-acylpyridinium ion pairs.[13] Our initial objective was to examine which of the catalysts developed in our group were capable of stabilizing an *N*-acylpyridinium ion pair and

[13] This project was initiated by a former postdoctoral researcher, Jean-Nicolas Desrosiers. Sections of this thesis where his experimental work is included are noted.

inducing asymmetry in a known transformation. A survey of representative chiral thiourea catalysts were examined in the kinetic resolution of benzylic amine **4** with benzoic anhydride under the conditions reported by Seidel.[8a] Of the various classes of mono-thiourea catalysts examined, phenylpyrrolidino thiourea **12** provided the highest enantioinduction (Scheme 1.5). An evaluation of arylpyrrolidino thioureas with expanded aromatic substituents identified 1-napthylpyrrolidino thiourea **13** as most effective, generating the product in 50% yield and 55% ee. With the identification of a chiral mono-thiourea catalyst capable of achieving catalysis and enantioinduction in a transformation involving an *N*-acylpyridinium ion pair intermediate,[14] we decided to examine a transformation of synthetic interest for which this approach had not been applied.

[14] For examples of stabilizing non-covalent interactions involving pyridinium ions in asymmetric catalysis, see: (a) Kawabata, T.; Nagato, M.; Takasu, K.; Fuji, K. *J. Am. Chem. Soc.* **1997**, *119*, 3169-3170. (b) Birman, V. B.; Uffman, E. W.; Jiang, H.; Kilbane, C. J. *J. Am. Chem. Soc.* **2004**, *126*, 12226-12227. (c) Wei, Y.; Held, I.; Zipse, H. *Org. Biomol. Chem.* **2006**, *4*, 4223-4230. (d) Li, X.; Houk, K. N.; Birman, V. B. *J. Am. Chem. Soc.* **2008**, *130*, 13836-13837. (e) Hu, B.; Meng, M.; Du, W.; Fossey, J. S.; Hu, X.; Deng, W. P. *J. Am. Chem. Soc.* **2010**, *132*, 17041-17044.

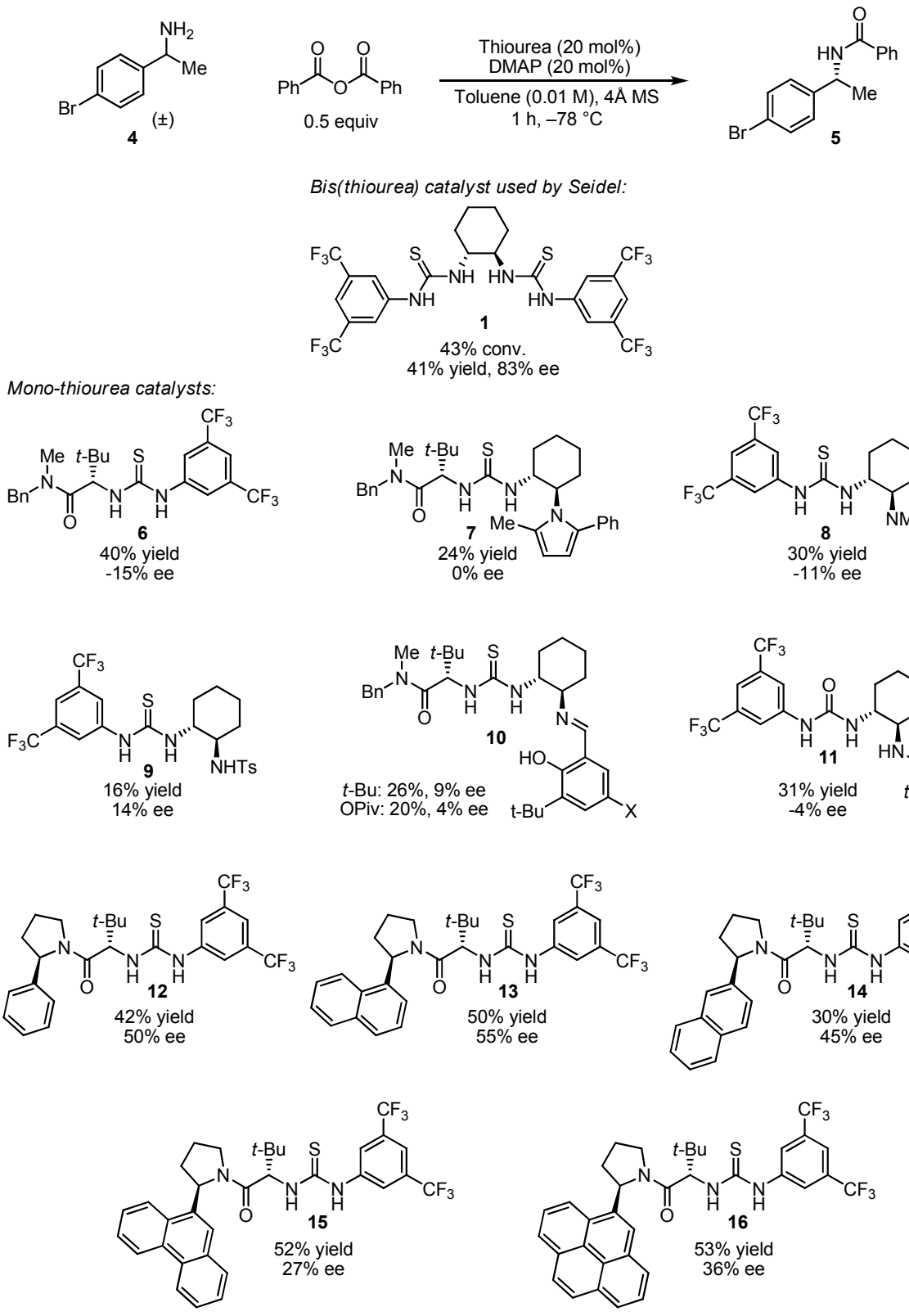

Scheme 1.5. Examination of thiourea catalysts in acylative kinetic resolution

1.2.2 Asymmetric Catalytic Methods toward α,α-Disubstituted Lactones

We sought to apply this reactivity principle to the *C*-acylation of enolate equivalents, a transformation that affords versatile β-dicarbonyl derivatives with a quaternary stereogenic center. Elegant asymmetric catalytic approaches to α,α-disubstituted butyrolactones had been developed previously,[15] however gaps in the synthetic methodology existed. Fu reported an efficient and highly enantioselective acylation of silyl ketene acetals using catalyst **3** (Scheme 1.6).[15b] While useful, many of the products reported contain a gem-dimethyl substituent, which may not be desired. In addition, acetic anhydride was the only acylating reagent reported, limiting the substituent that could be incorporated as the acyl portion of the product to an acetyl group. Maruoka reported a phase-transfer-catalysis approach to these compounds, however most of the products were generated in moderate enantiomeric excess.[15c] Furthermore, due to the use of primary alkyl bromides as the electrophilic species in this transformation only α-alkyl substituted products were able to be synthesized.

[15] For selected examples, see: (a) Spielvogel, D. J.; Buchwald, S. L. *J. Am. Chem. Soc.* **2002**, *124*, 3500-3501. (b) Mermerian, A. H.; Fu, G. C. *J. Am. Chem. Soc.* **2003**, *125*, 4050-4051. (c) Ooi, T.; Miki, T.; Fukumoto, K.; Maruoka, K. *Adv. Synth. Catal.* **2006**, *348*, 1539-1542.

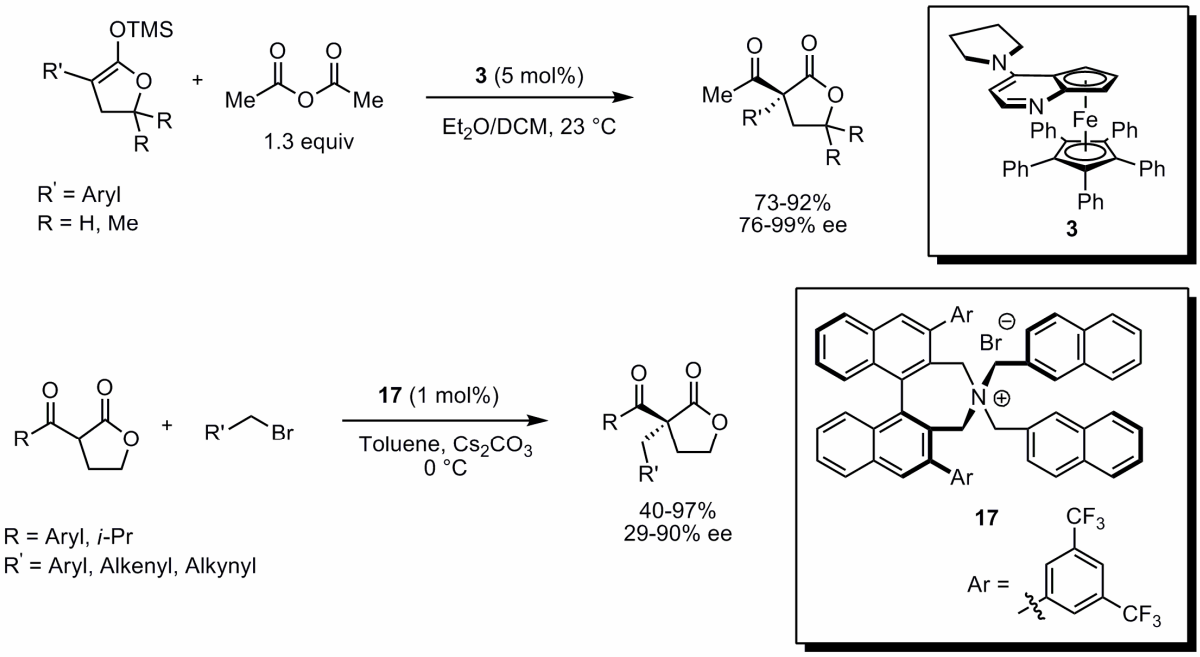

Scheme 1.6. Asymmetric catalytic methods to synthesize α,α-disubstituted-γ-butyrolactones

1.2.3 Lead Result and Reaction Optimization

with Jean-Nicolas Desrosiers

We chose to examine the thiourea-DMAP co-catalyzed acylation of substituted silyl ketene acetals to generate enantioenriched α,α-disubstituted carbonyl products. A lead result was obtained in the benzoylation of silyl ketene acetal **18** using benzoic anhydride in the presence of thiourea catalyst **13** and DMAP to provide lactone **19** in 59% yield and 37% ee (Scheme 1.7).[16] Notably, bis(thiourea) **1**, which was used in Seidel's kinetic resolution of benzylic amines, was ineffective in this transformation, generating the desired product in 1% ee.

[16] For related racemic and diastereoselective methods, see: (a) Poisson, T.; Dalla, V.; Papamicaël, C.; Dupas, G.; Marsais, F.; Levacher, V. *Synlett* **2007**, 381-386. (b) Woods, P. A.; Morrill, L. C.; Lebl, T.; Slawin, A. M. Z.; Bragg, R. A.; Smith, A. D. *Org. Lett.* **2010**, *12*, 2660-2663.

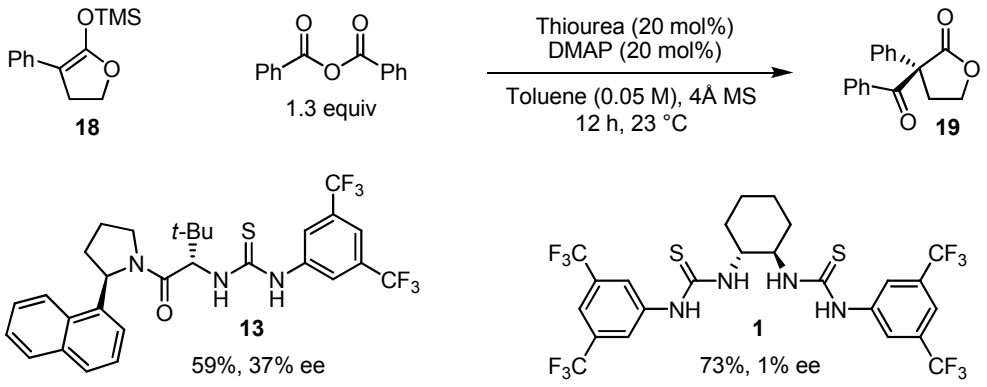

Scheme 1.7. Lead result in acylation of silyl ketene acetals

An evaluation of acylating agents identified benzoyl fluoride as optimal with regard to both rate and selectivity in comparison with benzoyl chloride and benzoic anhydride.[17] Examination of temperature and concentration led to the observation that enantioselectivity was enhanced at lower temperature and higher dilution. More electron-rich PPY was identified as a superior nucleophilic catalyst to DMAP, providing the acylation product in higher yield and enantioselectivity. Highly reactive nucleophilic catalyst **20**[18] promoted the transformation with good yield even at reduced temperature, albeit with lower enantioselectivity than DMAP or PPY. Imidazole, isoquinoline, and substituted quinoline derivatives provided no conversion of the silyl ketene acetal when used in combination with thiourea catalyst **13**. The acylation displayed a significant dependence on the solvent used, with ethereal solvents providing the highest enantioselectivity (Scheme 1.9).

[17] See Section 1.2.6 for a detailed analysis of the influence of the *N*-acylpyridinium counteranion.

[18] Held, I.; Xu, S.; Zipse, H. *Synthesis*, **2007**, 1185-1196.

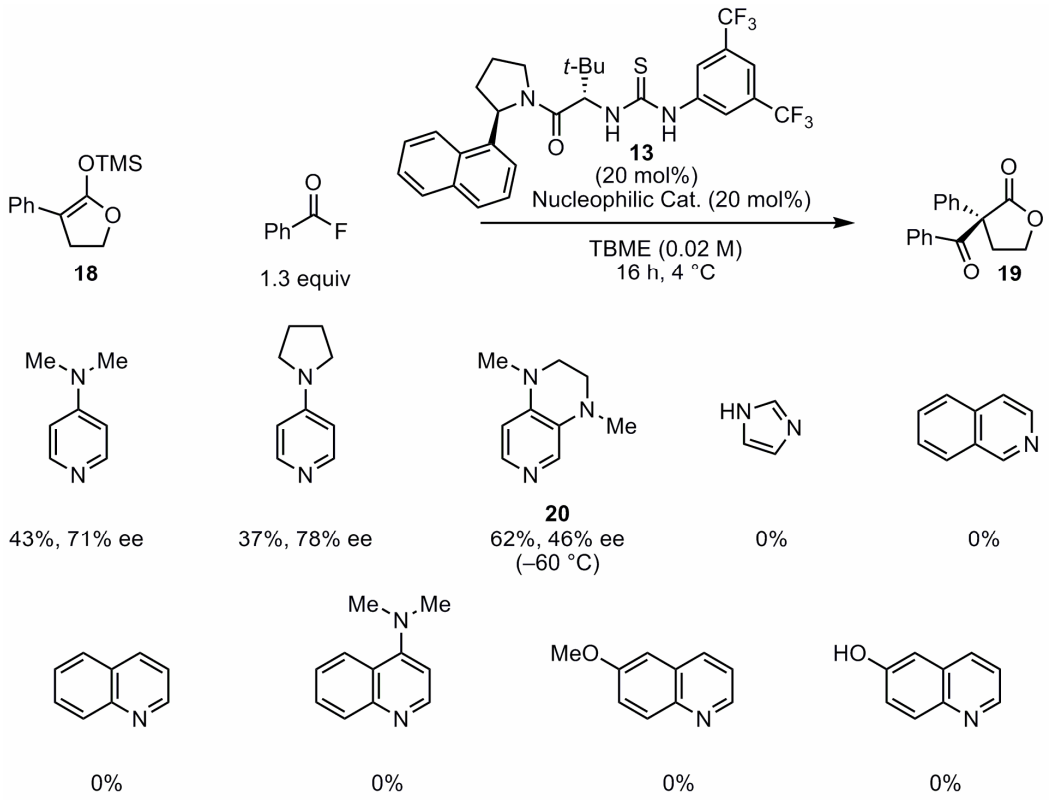

Scheme 1.8. Examination of nucleophilic catalysts

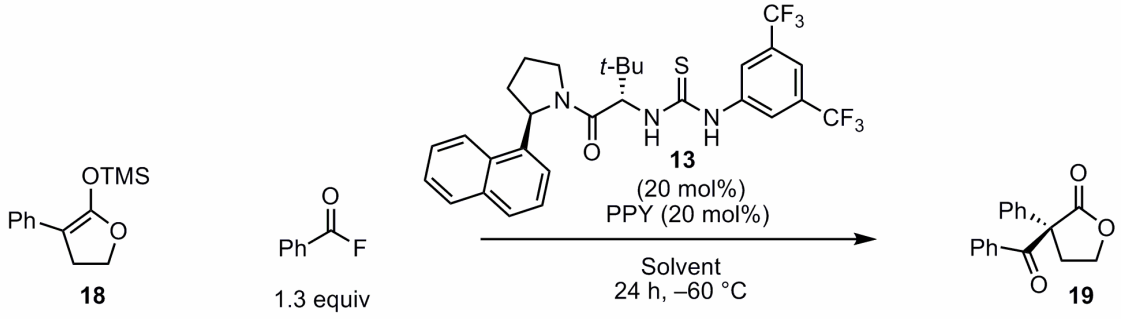

Solvent Screen (0.05 M):

Solvent	Yield	ee
Toluene	62%	76%
Hexane	21%	69%
DME	57%	12%
Et_2O	58%	84%
TBME	47%	86%

Ethereal Solvent Screen (0.02 M)

Solvent	Yield	ee
TBME	75%	88%
Et_2O	77%	87%
THF	58%	32%
n-Bu_2O	51%	84%
i-Pr_2O	80%	87%

Scheme 1.9. Examination of reaction solvent

1.2.4 Thiourea Catalyst Structure-Activity Relationships

Extensive structure-activity relationship analysis of the hydrogen-bond donor catalyst identified numerous insights about the necessary features for effective catalysis and enantioinduction.[19] Variation of the substituents on the right-hand anilide portion of the catalyst revealed a strong influence of the electronics on both reaction rate and enantioselectivity, with highly electron-deficient 3,5-bis(trifluoromethyl)phenyl-substituted thiourea **13** providing the highest enantioselectivity (Scheme 1.10). Interestingly, urea **21** provided the acylation product in the same enantioselectivity as the corresponding thiourea catalyst, whereas selenourea **22** was significantly less selective. The comparable enantioselectivity induced by **13** and **21** stands in contrast to many other asymmetric hydrogen-bond donor-catalyzed transformations in our group where thiourea catalysts are generally more enantioselective than their urea counterparts. Cyclohexyl- and phenyl-substituted thioureas, **24** and **25**, were poorly selective catalysts and also proceeded with slower rates than catalyst **13**. These results suggest the electron-withdrawing ability of the arene plays a crucial role in both the rate and enantioselectivity of the acylation.

[19] The yields of these reactions are generally high and are omitted in this analysis since they were not the focus of the optimization.

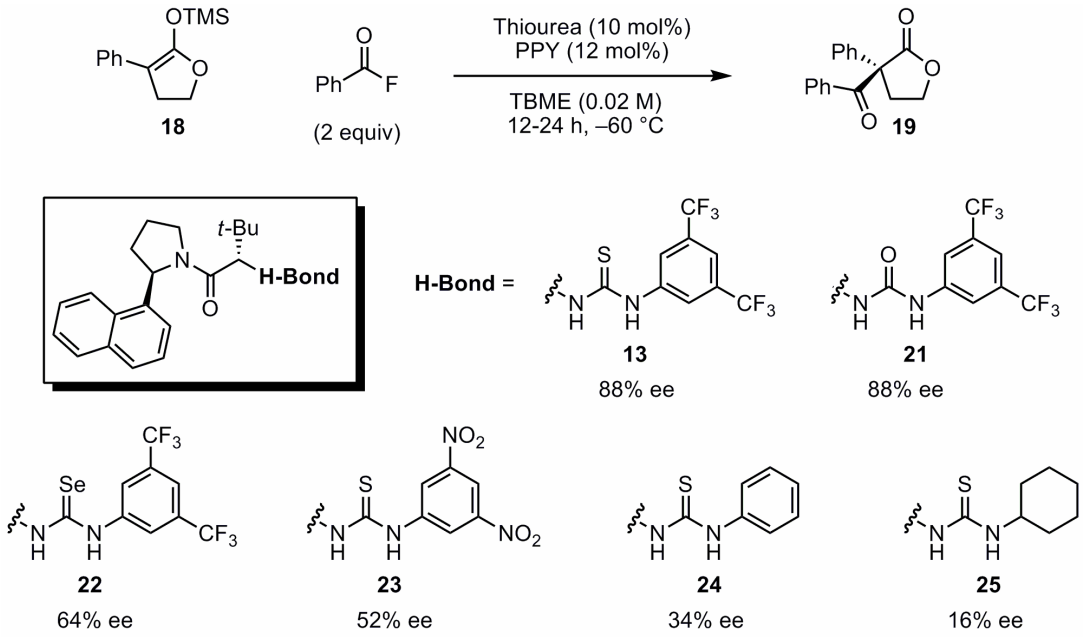

Scheme 1.10. Examination of the catalyst hydrogen-bond donor component

The amino-acid-containing portion of the catalyst was evaluated in a series of thioureas containing identical anilide and amide fragments (Scheme 1.11). Thiourea catalysts containing sterically-bulky amino acids (**26**–**29**) promoted the acylation with comparable enantioselectivity to the model *tert*-leucine-derived catalyst **13**. Catalysts incorporating smaller amino acids valine (**30**) and phenylalanine (**31**) demonstrated a marked decrease in both enantioselectivity and rate. Based on these results and the commercial availability of Boc-L-*tert*-leucine, the *tert*-lecuine-thiourea-3,5-bis(trifluoromethyl)anilide core was identified as strictly superior to other amino acid-anilide combinations and was incorporated in all remaining catalysts as the amide substitution was evaluated.

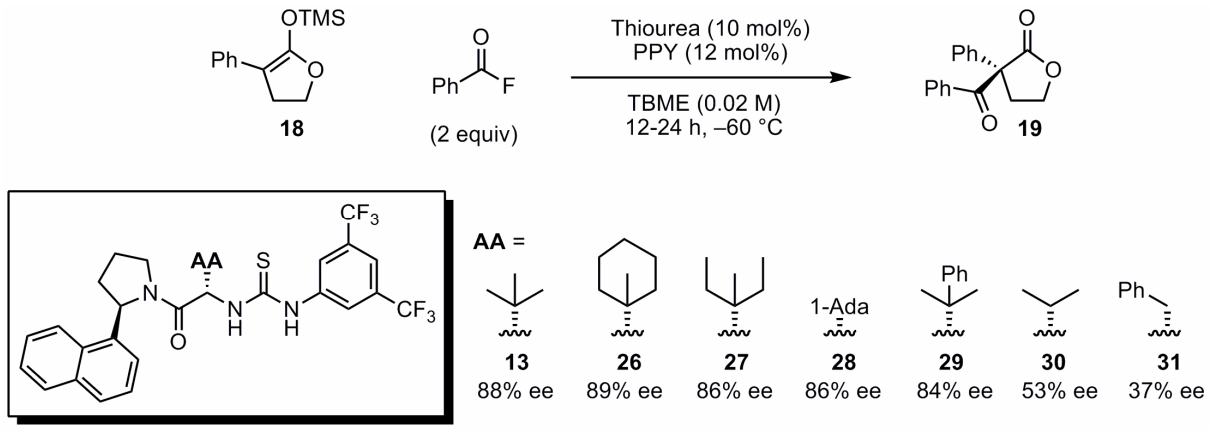

Scheme 1.11. Examination of the catalyst amino-acid substituent

Systematic variation of the amide substituents on the catalyst revealed a significant dependence on the substitution at this position (Scheme 1.12). Thioureas **32**–**34**, derived from amides that do not contain a stereogenic center, generated the acylation product in enantioselectivities of 72–73% ee. These results demonstrate that the single amino acid stereogenic center is sufficient to induce moderate levels of selectivity in the acylation but that the secondary functionality plays a significant role in asymmetric induction. Incorporation of an amide at the 2-position of the pyrrolidine was detrimental to enantioselectivity, while the addition of a benzhydryl group led to a marked increase in selectivity. Thiourea catalysts **37**–**47**, synthesized through a Mitsunobu reaction with prolinol, were effective catalysts, forming the product in generally high enantioselectivity with no clear electronic trend observed. This class of catalyst has proven to be uniquely effective in the acylation reaction as, to date, it has not demonstrated promising levels of enantioselectivity in other asymmetric transformations studied in our group.

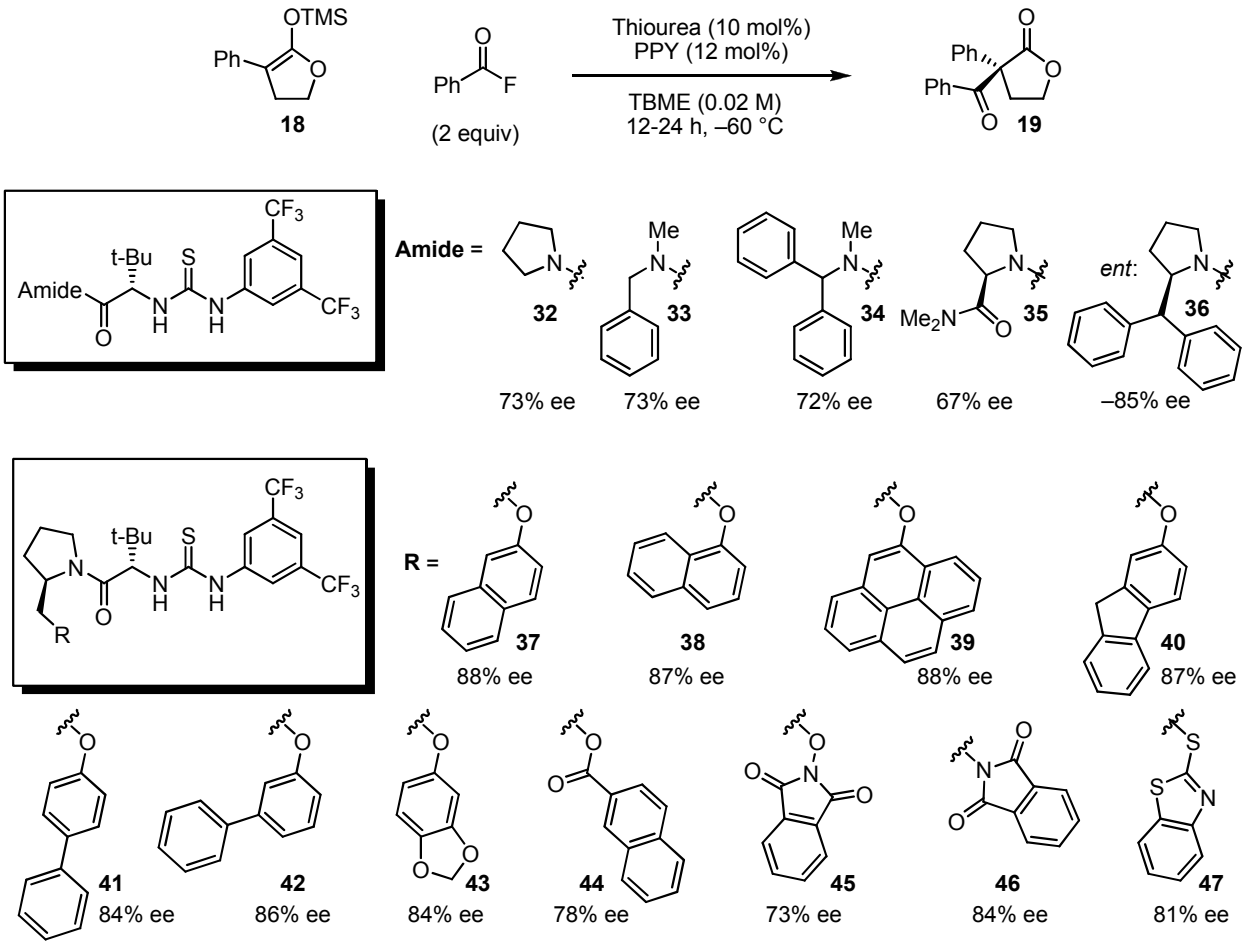

Scheme 1.12. Examination of thiourea catalyst amide substituents

Substituted phenylpyrrolidine-containing catalysts displayed a moderate dependence on the sterics and electronics of the substitutents (Scheme 1.13). A survey of expanded aromatic and heteroaromatic substituents on the pyrrolidine revelaed *N*-methylcarbazole-substituted catalyst **59** as optimal, providing the product in 92% ee. In contrast to the enantioselective, thiourea-catlayzed polycyclization reactions reported by our group,[7e] there was no clear trend between the size of the aromatic ring on the pyrrolidino fragment of the catalyst and the enantioselectivity induced in the product. Interestingly, the diastereomer of the optimal *N*-methylcarbazole catalyst (**60**) provided the opposite enantiomer of product in 84% ee, which is more selective than unsubstituted pyrrolidino thiourea catalyst **32**. These results demonstrate that having an aryl

substituent of either configuration at the 2-position of the pyrrolidine provides a beneficial effect on enantioselectivity.

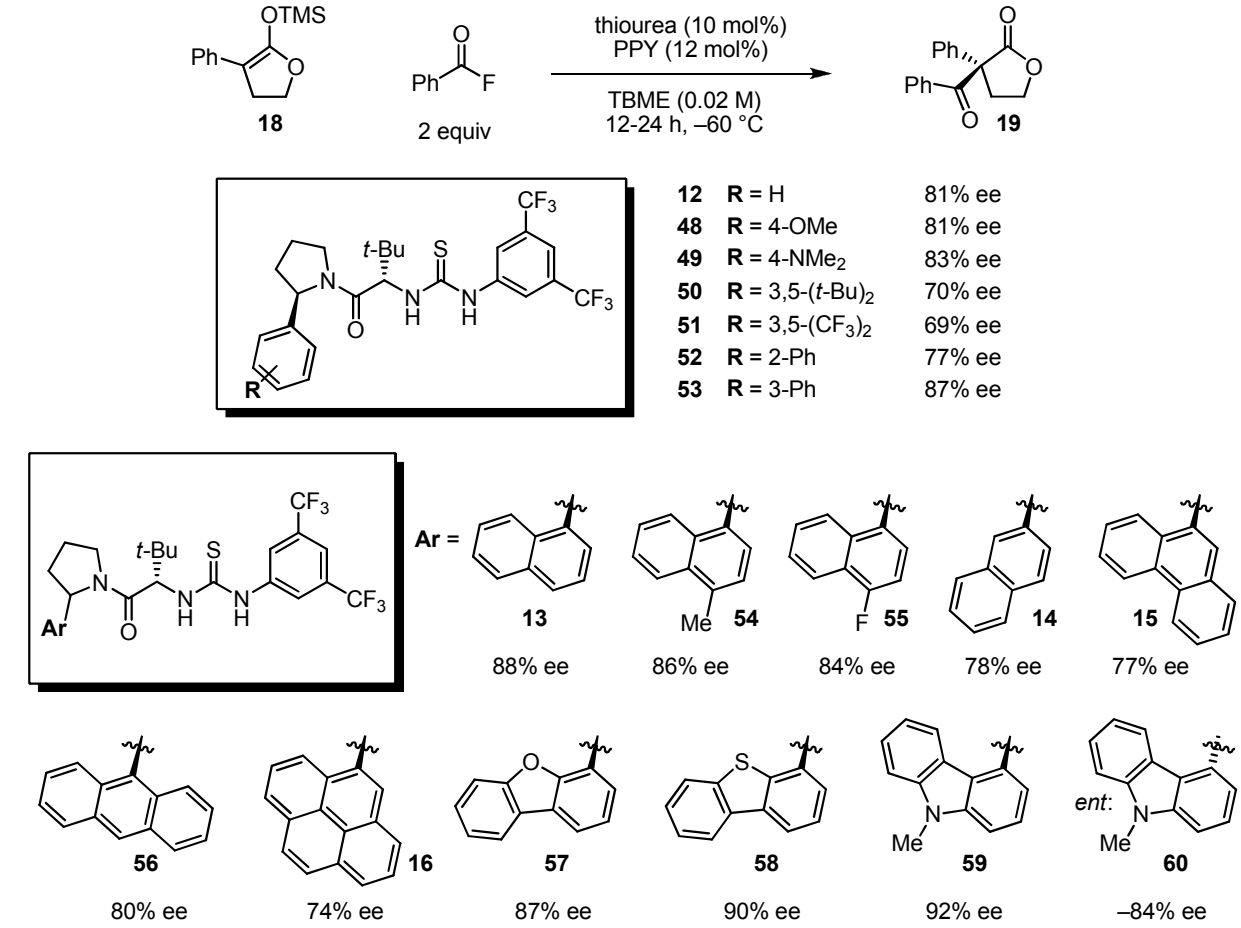

Scheme 1.13. Examination of aryl-pyrrolidino thiourea catalysts

1.2.5 Rate Dependence on Thiourea and Nucleophilic Catalysts

The loading and molar ratios of thiourea catalyst **13** and PPY were examined to determine the efficiency of the transformation (Scheme 1.14).[20] With equimolar amounts of both catalysts, it was found the catalyst loading could be dropped to as low as 1 mol% with only a slight reduction in enantioselectivity. In addition, we found an excess of PPY compared to thiourea catalyst **13** had a minimal effect on the enantioselectivity of the transformation up to as

[20] A number of the experiments discussed in this section were performed with catalyst **13** prior to the identification of optimal catalyst **59**. These catalysts are expected to perform similarly and to proceed through analogous mechanisms.

high as a 10:1 ratio of PPY to thiourea. This observation raised the possibility of maintaining useful reaction rates while using an excess of commercially-available PPY and reducing the loading of the more-valuable chiral thiourea catalyst accordingly. This strategy was utilized in the preparative-scale reaction protocol in Section 1.2.8.

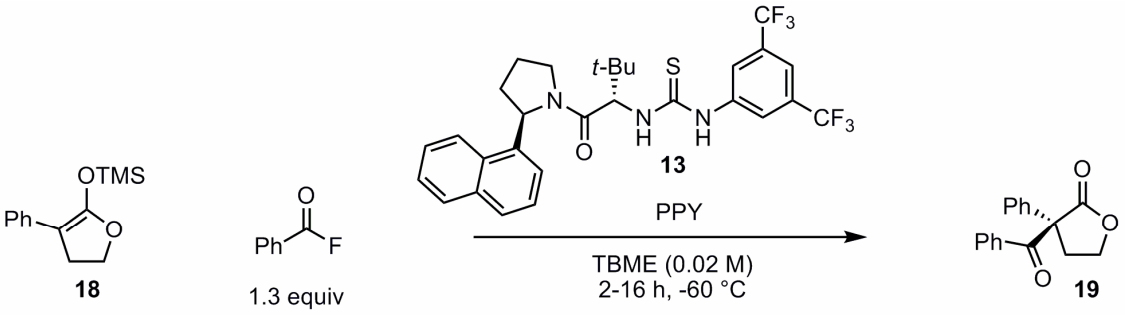

Catalyst Loading:

Thiourea / PPY	Yield	ee
20% / 20%	83%	88%
10% / 10%	84%	87%
5% / 5%	73%	86%
1% / 1%	30%	83%

Thiourea/Nucleophilic Catalyst Ratio:

Thiourea / PPY	Yield	ee
10% / 20%	71%	87%
10% / 50%	73%	85%
10% / 100%	82%	85%

Scheme 1.14. Thiourea and nucleophilic catalyst loading studies

No acylation occurs in the absence of either the thiourea catalyst or PPY (Scheme 1.15). This result is especially informative in the case where the nucleophilic catalyst is present in the absence of the hydrogen-bond donor catalyst. The trimethylsilyl group of the silyl ketene acetal is extremely labile and is expected to react with any fluoride liberated from reaction of PPY with benzoyl fluoride.[21] Since no product is observed, the key *N*-acylpyridinium/fluoride ion pair intermediate must not be generated in the absence of the thiourea catalyst. After 20 hours, the thiourea catalyst was added to the reaction containing PPY, immediately initiating a smooth

[21] Wuts, P. G. M.; Greene, T. W. *Greene's Protective Groups in Organic Synthesis*; John Wiley & Sons: New Jersey, 2006.

reaction to form the product in the same enantiomeric excess observed when both catalysts are added together. This result demonstrates the silyl ketene acetal and acyl fluoride are stable to the reaction conditions in the absence of thiourea and are simply unreactive under these conditions. This observation indicates the thiourea is playing a role not only in the enantioselectivity-determining acylation event but also in the generation of the key *N*-acylpyridinium ion pair intermediate. It is likely that the outstanding hydrogen-bond-accepting ability of the fluoride anion is important in this regard.[22]

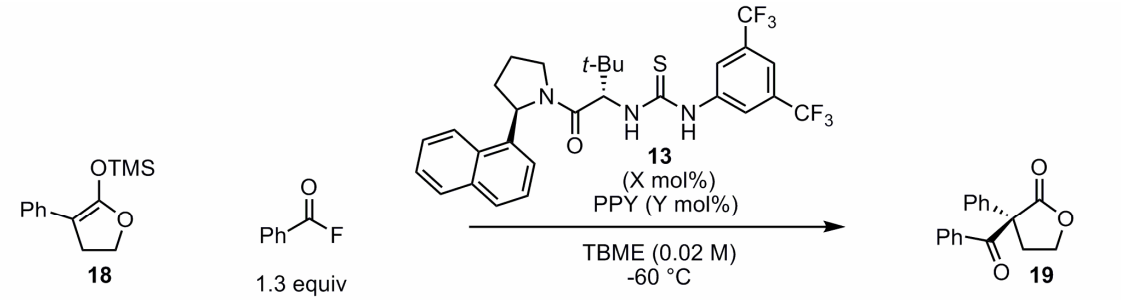

Time	Yield	ee
20 mol% catalyst, 20 mol% PPY:		
15 s	6%	-
15 min	60%	-
18 h	60%	88%
20 mol% catalyst, 0 mol% PPY		
20 h	0%	-

Addition of 10 mol% catalyst at t = 20 h

Time	Yield	ee
0 mol% catalyst, 20 mol% PPY:		
15 s	0%	-
1 h	0%	-
20 h	0%	-
20 h, 15 s	3%	-
20 h, 15 min	40%	-
20 h, 150 min	68%	87%

Scheme 1.15. Reactivity dependence on thiourea and nucleophilic catalyst

1.2.6 Effect of *N*-Acylpyridinium Counteranion on Reactivity

With evidence suggesting the thiourea is necessary in aiding formation of the *N*-acylpyridinium/fluoride ion pair, we were interested in studying the performance of acylating agents that would form ion pairs containing chloride and benzoate. We examined the rate and enantioselectivity of the acylation using benzoyl chloride or benzoic anhydride both in the

[22] (a) Hibbert, F.; Emsley, J. *Adv. Phys. Org. Chem.* **1990**, *26*, 255-379. (b) Jeffrey, G. A. *An Introduction to Hydrogen Bonding*; Oxford University Press: New York, 1997; Chapter 3.

presence and absence of thiourea catalyst (Scheme 1.16). Benzoyl chloride and benzoic anhydride are generally more reactive than benzoyl fluoride in representative pyridine-catalyzed acyl transfer reactions due to their increased propensity to form the requisite *N*-acylpyridinium electrophile while liberating chloride or benzoate, respectively. When benzoyl chloride was used as the acylating reagent with PPY as nucleophilic catalyst, no acylation product was observed either in the presence or absence of thiourea catalyst.[23] Since the *N*-acylpyridinium/chloride ion pair is expected to form under these conditions, the lack of reactivity compared with benzoyl fluoride suggests the counteranion in this transformation may be required to activate the silicon of the silyl ketene acetal.[24] By contrast, when benzoic anhydride is used as the electrophile, acylation proceeds when PPY is the only catalyst present as well as when both catalysts are used together. This outcome suggests the thiourea is not necessary to form the *N*-acylpyridinium/benzoate ion pair and that the benzoate anion generated is a strong enough Lewis base to activate the silyl ketene acetal for further reaction.

[23] For other examples where acyl fluorides react with silyl-protected nucleophiles but acyl chlorides are unreactive, see ref 10a and the following: (a) Bappert, E.; Müller, P.; Fu, G. C. *Chem. Commun.* **2006**, 2604-2606. (b) Ryan, S. J.; Candish, L.; Lupton, D. W. *J. Am. Chem. Soc.* **2011**, *133*, 4694-4697.

[24] Denmark, S. E.; Beutner, G. L. *Angew. Chem. Int. Ed.* **2008**, *47*, 1560-1638.

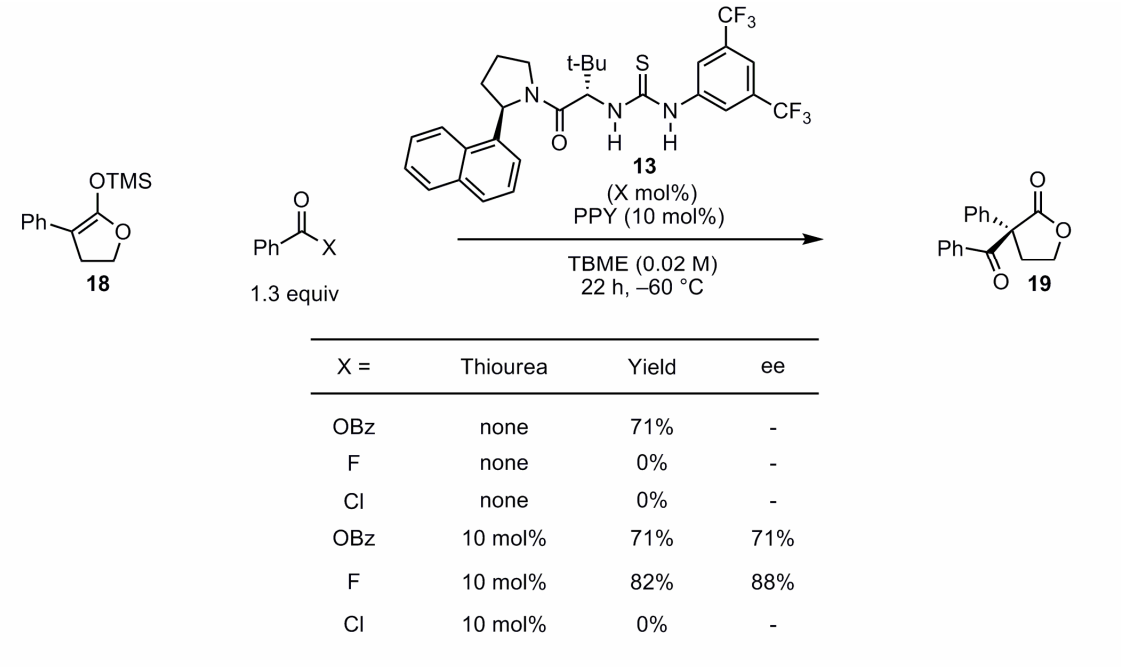

X =	Thiourea	Yield	ee
OBz	none	71%	-
F	none	0%	-
Cl	none	0%	-
OBz	10 mol%	71%	71%
F	10 mol%	82%	88%
Cl	10 mol%	0%	-

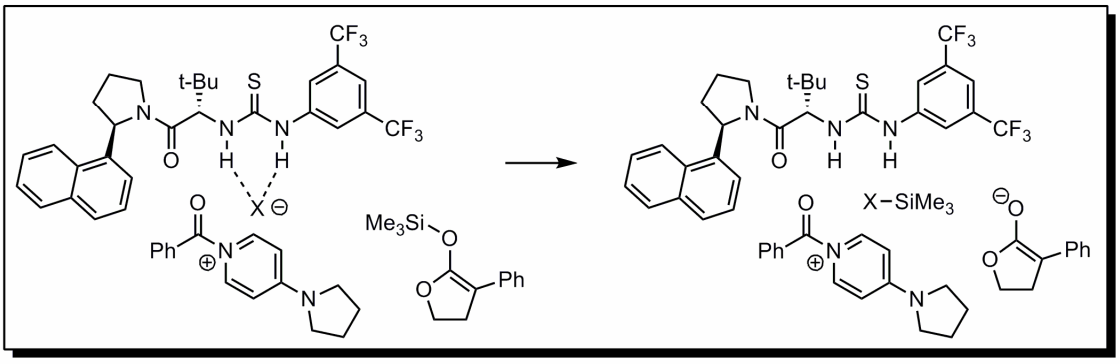

Scheme 1.16. *N*-acylpyridinium counteranion effects on reactivity

1.2.7 Examination of Silicon Group of Silyl Ketene Acetal

To evaluate the hypothesis that Lewis-base activation of the silicon group on the silyl ketene acetal is facilitating acylation, silyl ketene acetals containing different silyl protecting groups were examined. A dramatic rate dependence on the size of this group is observed, with larger silyl groups proceeding more slowly than the parent trimethylsilyl-containing substrate **18** (Scheme 1.17). This observation supports the hypothesis that activation of the silicon is required for reaction and that a Lewis-base activation mechanism[24] is operative. An alternative reaction mechanism involving rate-determining nucleophilic attack by the olefin of the silyl ketene acetal

followed by Lewis-base-promoted disilylation is not supported since this mechanism would not be expected to exhibit a strong rate dependence on the identity of the silyl group. The identity of the silyl group has a negligible effect on enantioselectivity, indicating that it plays no significant role in the organization of the stereoselectivity-determining step.[25] This result points to the existence of a thiourea-bound enolate as a key intermediate.[26]

[25] For an example of another reaction where variation of the silyl group of a silyl ketene acetal substrate does not influence enantioselectivity, see reference 15b.

[26] For another catalytic asymmetric reaction where a hydrogen-bonded enolate may be a reactive intermediate, see: Ohmatsu, K.; Kiyokawa, M.; Ooi, T. *J. Am. Chem. Soc.* **2011**, *133*, 1307-1309.

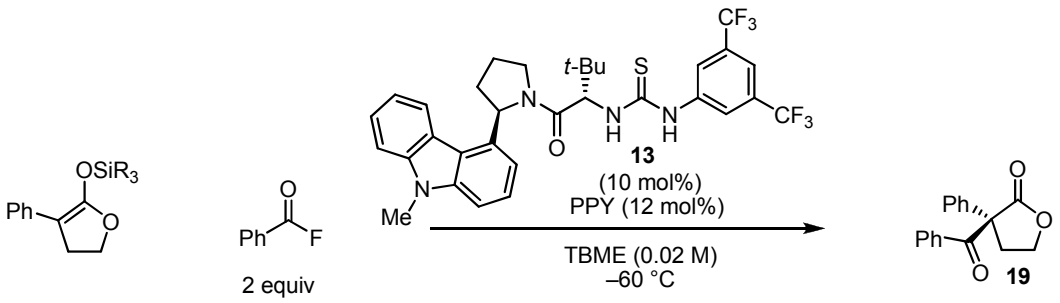

SiR_3	Yield (%) 5 min	15 min	30 min	60 min	120 min	240 min	480 min	1200 min	ee (%)
TMS (**18**)	52	83	91	-	-	-	-	-	**92**
TES (**61**)	9	22	34	55	86	92	-	-	**92**
TBS (**62**)	n.d.	n.d.	n.d.	4	8	14	24	54	**93**

[a] Reactions run on a 0.10 mmol scale. [b] Yields determined by GC analysis relative to *n*-dodecane as an internal standard. [c] Enantiomeric excess determined by HPLC analysis on commercial chiral columns.

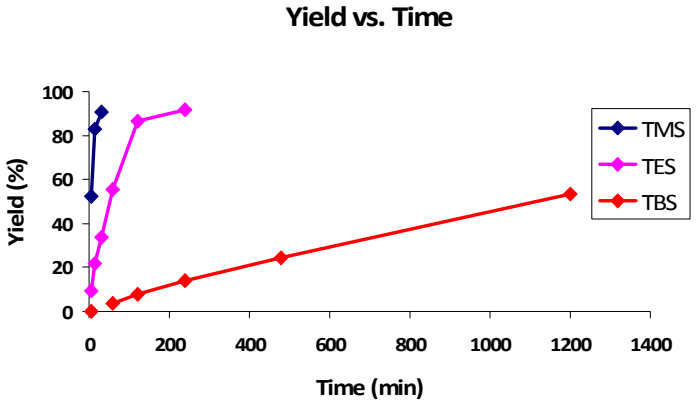

Scheme 1.17. Effect of silyl ketene acetal silyl group on reaction rate and enantioselectivity

1.2.8 Substrate Scope

To evaluate the substrate scope of the acylation reaction, a variety of benzoyl fluorides were synthesized from the corresponding benzoic acids by reaction with cyanuric fluoride, according to the method reported by Olah (Scheme 1.18).[27] Substrates containing both electron-donating and electron-withdrawing groups, as well as 2-naphthoyl fluoride, provided acylation products in high yields and enantiomeric excess (Scheme 1.19). Substitution at the *meta*- and

[27] Olah, G. A.; Nojima, M.; Kerekes, I. *Synthesis* **1973**, *8*, 487-488.

para-positions was well tolerated, however acyl fluorides containing *ortho*-substituents were completely unreactive (Scheme 1.20). This observation supports the notion of an *N*-acylpyridinium intermediate, as the rates of reactions that proceed through such species are known to be severely affected by *ortho*-substitution on the acylating agent.[28] Heteroaryl-substituted acyl fluorides **70** and **71** proceeded with moderate and poor enantioselectivity, respectively. Alkyl-substituted acyl fluoride **72** provided the acylation product in good yield and promising enantioselectivity, while alkenyl- and alkynyl-substituted acyl fluorides **73** and **74** yielded acylation products with extremely low levels of enantioinduction.

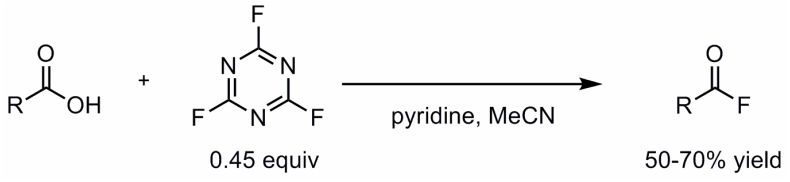

Scheme 1.18. Synthesis of acyl fluoride substrates

[28] Gold, V.; Jefferson, E. G. *J. Chem. Soc.* **1953**, 1409-1415.

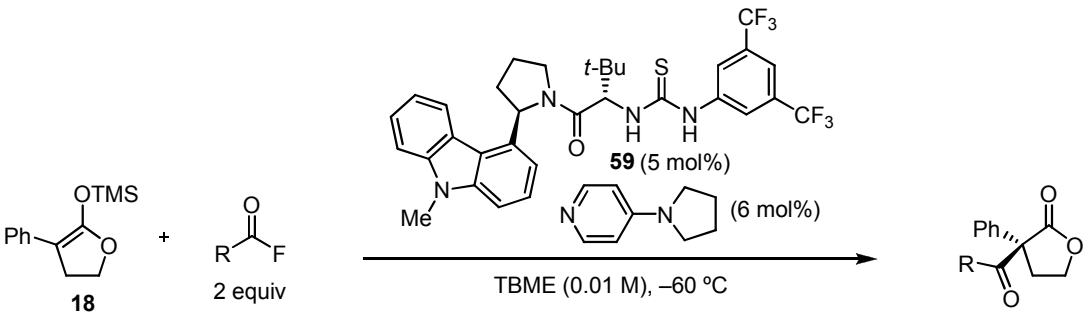

Entry[a]	Product	Time	Yield[b] (%)	ee[c] (%)
1	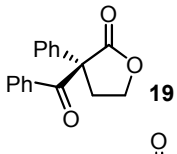 **19**	6 h	88	92
2	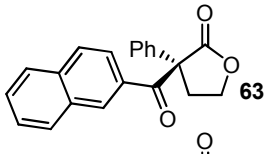 **63**	6 h	85	95
3	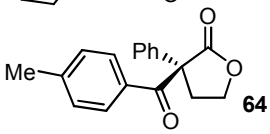 **64**	24 h	91	95
4	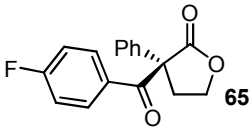 **65**	6 h	90	91
5	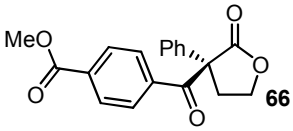 **66**	4 h	95	86
6	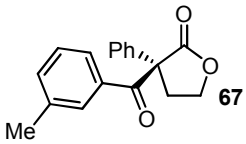 **67**	16 h	77	92
7	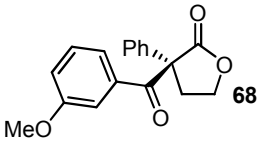 **68**	6 h	95	92
8	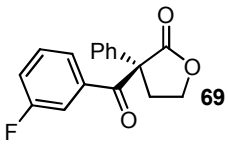 **69**	6 h	78	87

[a] Reactions run on a 0.20 mmol scale. [b] Isolated yield of purified product. [c] Enantiomeric excess determined by HPLC analysis on commercial chiral columns.

Scheme 1.19. Optimized scope in acyl fluoride

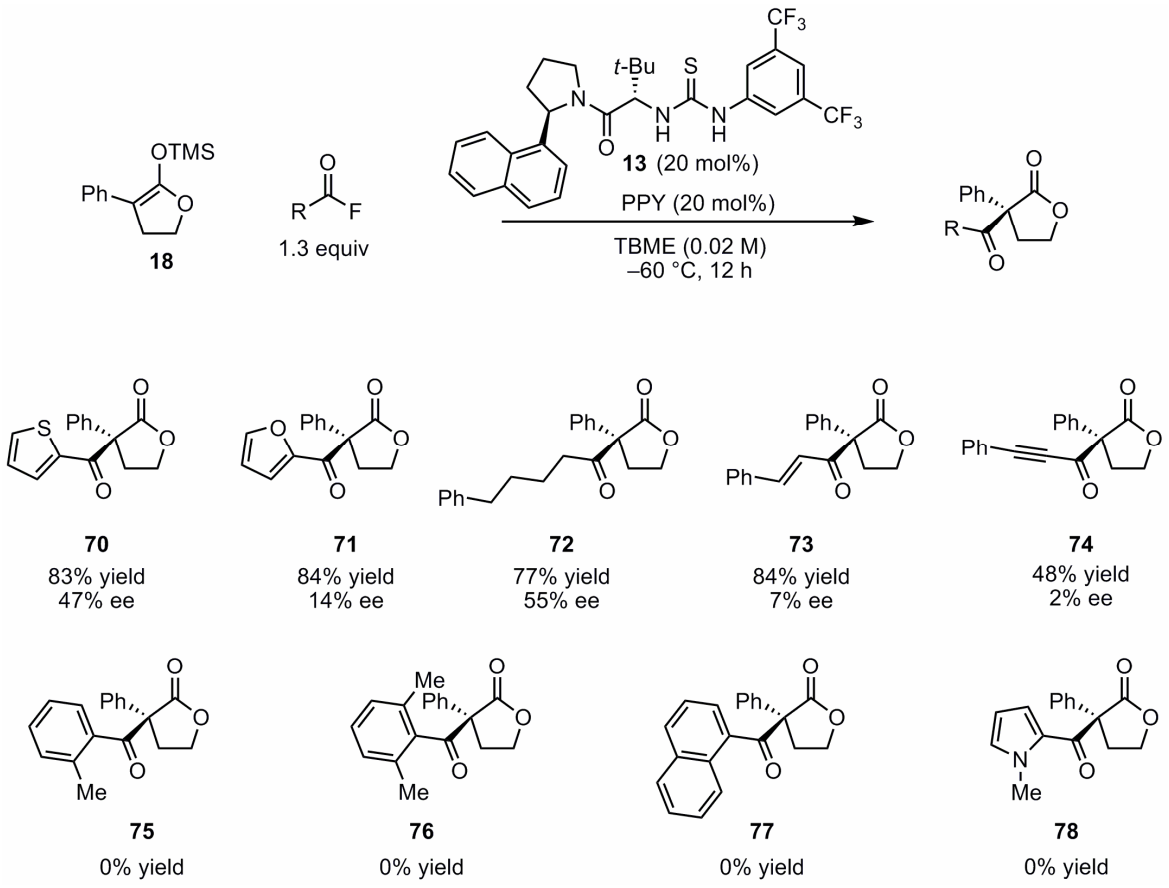

Scheme 1.20. Suboptimal acyl fluoride substrates

A number of silyl ketene acetals were synthesized from the corresponding substituted acetic acid derivatives (Scheme 1.21). Aryl-substituted silyl ketene acetals were viable substrates, with derivatives bearing electron-rich and electron-poor arene substituents, as well as heteroaromatic functionality, participating in acylation with benzoyl fluoride to provide benzoylated products in good yield and enantiomeric excess (Scheme 1.22). Alkyl-substituted, acyclic, and six-membered silyl ketene acetal analogs as well as silyl ketene thioacetal **88** provided no desired *C*-acylation product using this reaction protocol (Scheme 1.23).

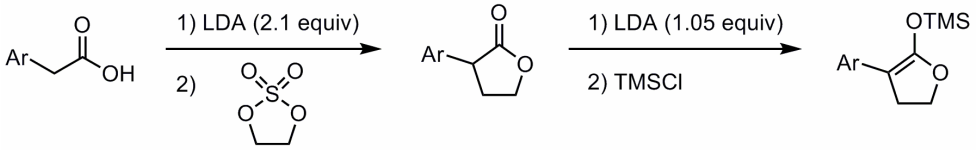

Scheme 1.21. Synthesis of silyl ketene acetal substrates

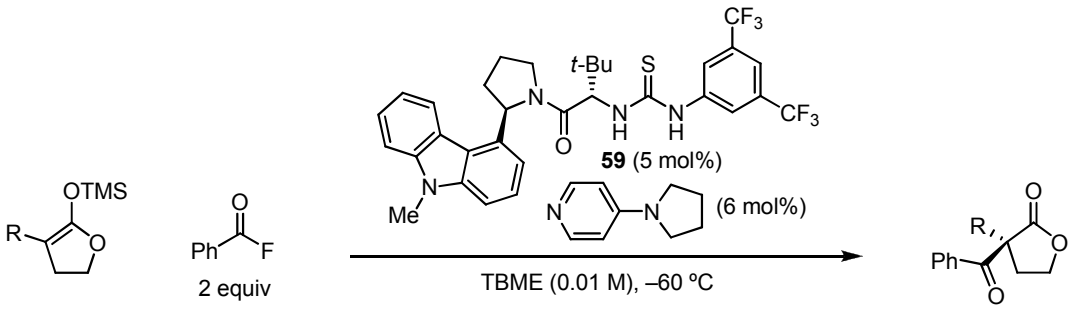

Entry[a]	Product	Time	Yield[b] (%)	ee[c] (%)
1	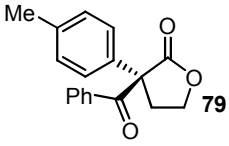 **79**	6 h	75	93
2	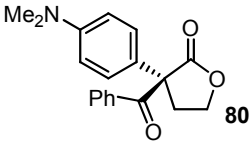 **80**	24 h	76	89
3	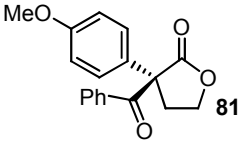 **81**	6 h	80	88
4	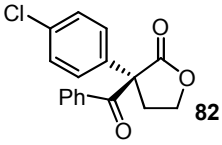 **82**	6 h	76	89
5	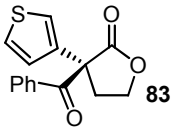 **83**	6 h	77	89

[a] Reactions run on a 0.20 mmol scale. [b] Isolated yield of purified product. [c] Enantiomeric excess determined by HPLC analysis on commercial chiral columns.

Scheme 1.22. Optimized scope in silyl ketene acetal

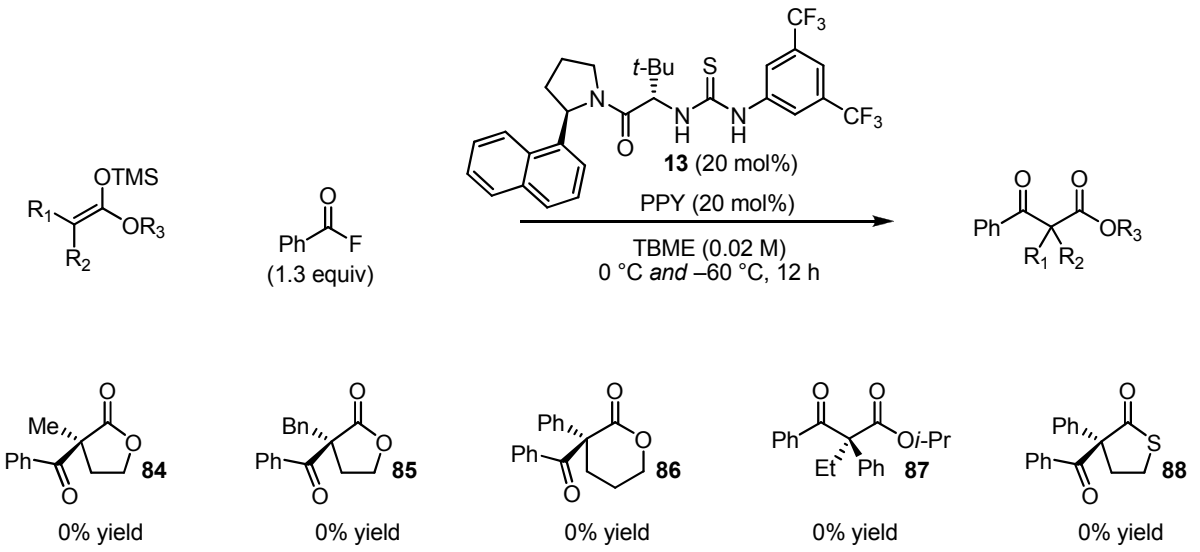

Scheme 1.23. Unreactive nucleophiles

The efficiency of this protocol was illustrated in the acylation of silyl ketene acetal **13** with 2-naphthoyl fluoride on a preparative scale using only 0.5 mol% thiourea catalyst and 20 mol% of commercially-available PPY (Scheme 1.24). The product of this reaction was purified by crystallization from the crude reaction mixture without the need for chromatography. A single recrystallization provided 1.2 grams of pure acylation product **63** in 70% overall yield and >99% ee. An X-ray crystal structure of **63** was obtained and used to assign the absolute configuration as (*R*) (Figure 1.1).[29]

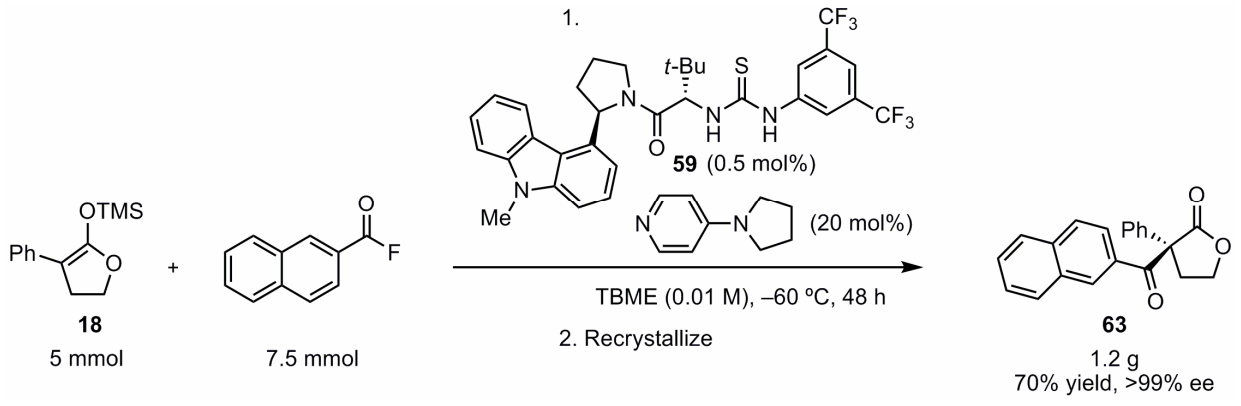

Scheme 1.24. Preparative-scale acylation of silyl ketene acetal **13** with 2-naphthoyl fluoride

[29] The absolute configuration of the other acylation products was assigned as (*R*) by analogy.

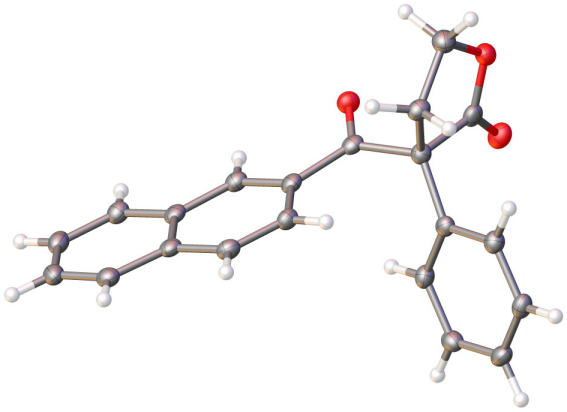

Figure 1.1. X-ray crystallographic structure of acylation product **63**

1.2.9 Kinetic Analysis

A kinetic analysis was undertaken to determine the stoichiometry of the rate-limiting transition structure and to identify catalyst resting states according to the reaction-progress kinetics method pioneered by Blackmond.[30,31] The acylation of representative silyl ketene acetal **13** with benzoyl fluoride in the presence of optimal thiourea catalyst **59** and PPY was examined under synthetically-relevant concentrations and fully homogeneous conditions in TBME at –78 ℃. The reaction progress was measured by monitoring the absorbance of benzoyl fluoride over the course of the reaction using in situ infrared spectroscopy. The absorbance versus time data were converted to concentration versus time by application of Beer's law and then to rate versus concentration by least-squares fitting of the concentration versus time data to a 7th-order polynomial followed by differentiation of the polynomial.

Kinetic data were obtained from ten independent experiments over a range of concentrations of silyl ketene acetal **13** (0.02–0.06 M), benzoyl fluoride (0.03–0.10 M), thiourea catalyst **59** (0.0005–0.004 M), and PPY (0.004–0.008 M). The data appear well-behaved,

[30] Blackmond, D. G. *Angew. Chem., Int. Ed.* **2005**, *44*, 4302-4320.

[31] For detailed mechanistic analyses that used this method, see: (a) Zuend, S. J.; Jacobsen, E. N. *J. Am. Chem. Soc.* **2007**, *129*, 15872-15883. (b) Zuend, S. J.; Jacobsen, E. N. *J. Am. Chem. Soc.* **2009**, *131*, 15358-15374. (c) Uyeda, C.; Jacobsen, E. N. *J. Am. Chem. Soc.* **2011**, *133*, 5062-5075.

indicating catalyst deactivation and product inhibition are likely not occurring to an appreciable extent. The reaction rate appears to display a straightforward first-order dependence on the initial concentration of both thiourea catalyst **59** and nucleophilic catalyst PPY (Figure 1.2). This observation indicates that, for each catalyst, the number of molecules in the rate-limiting transition structure is the same as in the catalyst resting state. The simplest interpretation of these data is that there is a single molecule of each catalyst in both the resting state and the rate-limiting transition structure. Recent work from our group has shown many thiourea and urea catalyst exist as resting-state dimers under commonly-employed reaction conditions. Due to the highly dilute reaction conditions and the presence of PPY, which is expected to be a strong hydrogen-bond acceptor,[32] we propose the resting state of the thiourea is either a free monomer or a 1:1 thiourea•PPY complex. This assumption implies a single molecule of both thiourea and PPY is present in the rate-limiting transition structure. Although we propose this scenario as most likely, we cannot preclude the possibility of a dimeric thiourea resting state and the presence of two molecules of thiourea in the rate-limiting transition structure on the basis of these data.

[32] Pyridine was shown to be a potent inhibitor of the thiourea-catalyzed ketone cyanosilylation reaction studied in reference 30a. This inhibition presumably occurs through competitive binding of the thiourea catalyst protons by the pyridine nitrogen.

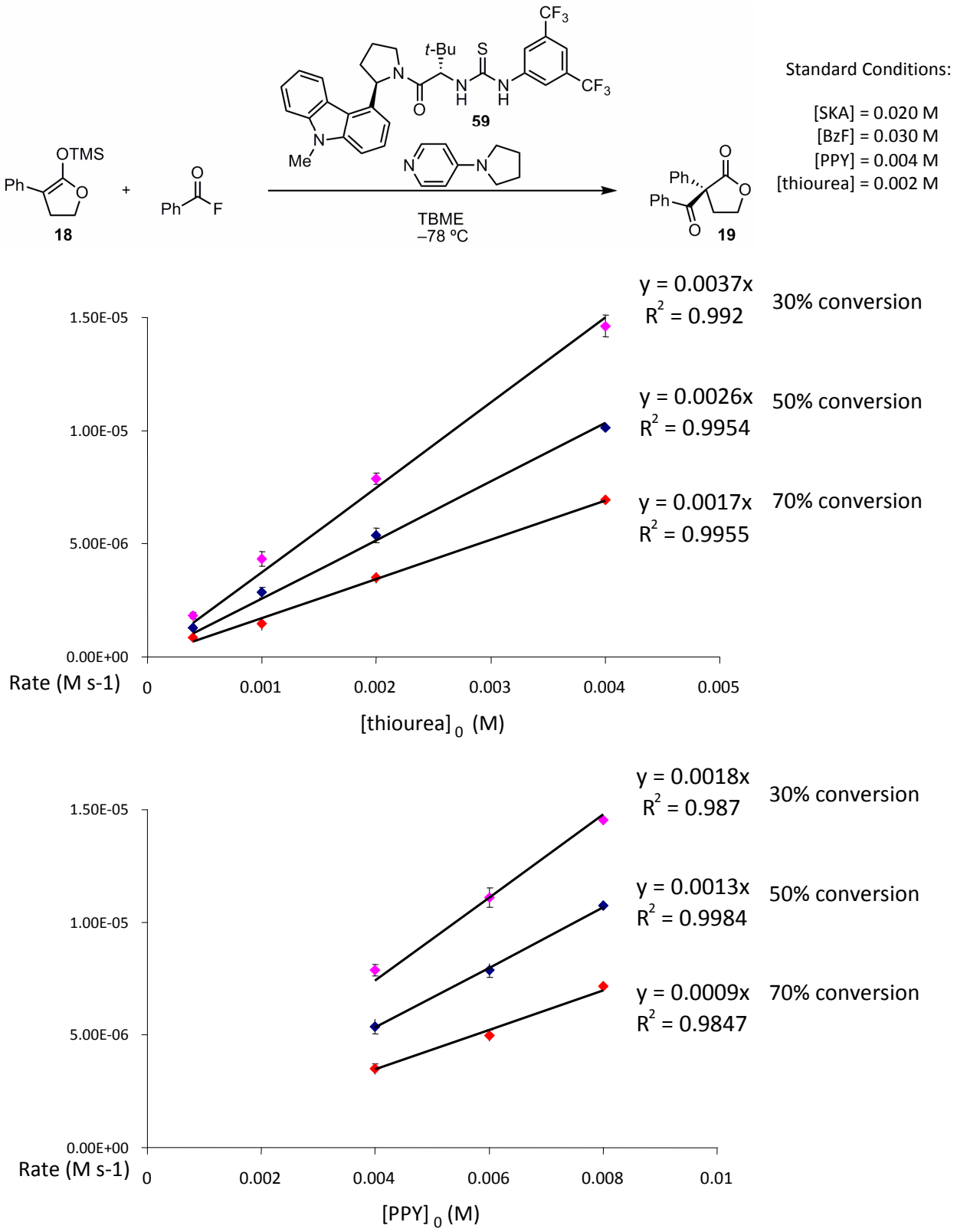

Figure 1.2. Rate versus concentration data for thiourea and nucleophilic catalyst

The reaction rate displays slightly less than first-order dependence on the initial concentration of benzoyl fluoride (Figure 1.3). This rate behavior could indicate partial kinetic saturation at elevated concentrations of acyl fluoride, potentially due to unproductive, off-cycle binding between benzoyl fluoride and thiourea **59**. The reaction rate was approximately independent of the initial concentration of silyl ketene acetal. This observation indicates the silyl ketene acetal is not present in the rate-limiting transition structure and suggests thiourea- and PPY-promoted ionization of benzoyl fluoride is rate-determining under these conditions. Given that the rate of this transformation was affected significantly by variation of the silyl group, with large silyl groups providing significantly diminished rates (see Section 1.2.7), it can be concluded that the silyl ketene acetals containing the larger TES (**61**) or TBS (**62**) groups are present in the rate-determining transition structure. Therefore, we propose a scenario in which *N*-acylpyridinium/fluoride ion pair formation is rate-limiting when the TMS-substituted silyl ketene acetal (**13**) is used as the nucleophile, however desilylation of the silyl ketene acetal is rate-limiting when the larger TES- or TBS-substituted silyl ketene acetals **61**–**62** are used.

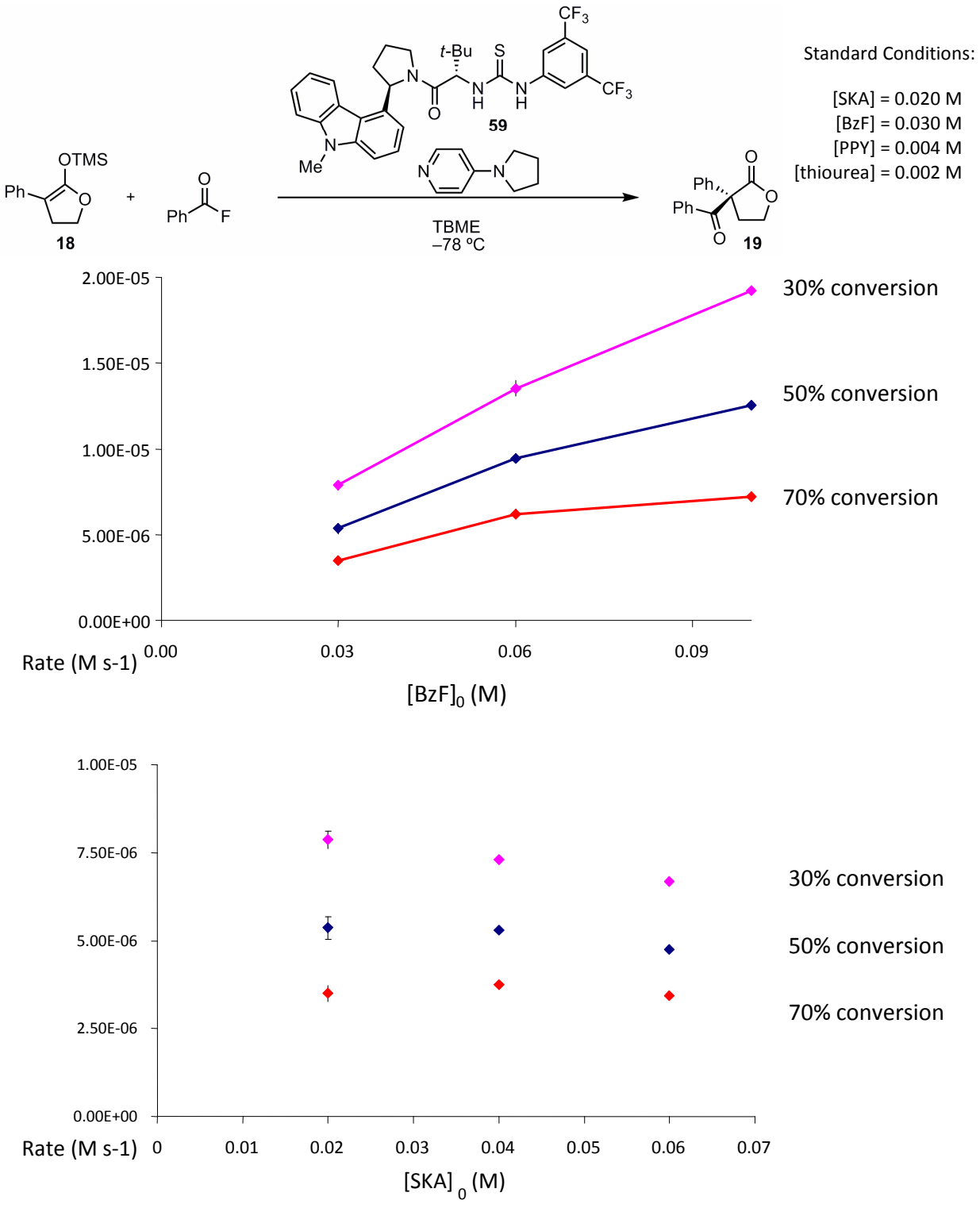

Figure 1.3. Rate-versus-concentration data for benzoyl fluoride and silyl ketene acetal

A proposed catalytic cycle that is consistent with the observations presented is provided in Figure 1.4. As noted, the thiourea catalyst activates benzoyl fluoride for reaction with PPY, presumably via initial complexation of the carbonyl group of the acyl fluoride (**A**). In the case where TMS-substituted silyl ketene acetal **13** is used, rate-determining generation of a thiourea-bound *N*-acylpyridinium/fluoride intermediate (**B**) is proposed, in which the thiourea is associated to the fluoride anion and the catalyst arene substituent is engaged in a stabilizing interaction with the *N*-acylpyridinium cation.[33] Reaction of **B** with the silyl ketene acetal likely proceeds via a pentavalent silicate intermediate[34] and is proposed to be rate-determining when silyl ketene acetals containing larger TES (**61**) or TBS (**62**) groups are used. We propose this change in rate-determining step on the basis of the observed dependence of the overall reaction rate on the identity of the silyl group. However, the independence of reaction enantioselectivity on the identity of the silyl group points to a thiourea-bound enolate such as **C** as the intermediate involved in enantiodetermining acylation.

[33] For examples of stabilizing noncovalent interactions involving pyridinium ions in asymmetric catalysis, see: (a) Kawabata, T.; Nagato, M.; Takasu, K.; Fuji, K. *J. Am. Chem. Soc.* **1997**, *119*, 3169-3170. (b) Birman, V. B.; Uffman, E. W.; Jiang, H.; Kilbane, C. J. *J. Am. Chem. Soc.* **2004**, *126*, 12226-12227. (c) Wei, Y.; Held, I.; Zipse, H. *Org. Biomol. Chem.* **2006**, *4*, 4223-4230. (d) Li, X.; Houk, K. N.; Birman, V. B. *J. Am. Chem. Soc.* **2008**, *130*, 13836-13837. (e) Hu, B.; Meng, M.; Du, W.; Fossey, J. S.; Hu, X.; Deng, W. P. *J. Am. Chem. Soc.* **2010**, *132*, 17041-17044.

[34] For discussions on hypervalent silicon species in bond-forming processes, see: (a) Rendler, S.; Oestreich, M. *Synthesis* **2005**, *11*, 1727-1747. and reference 24.

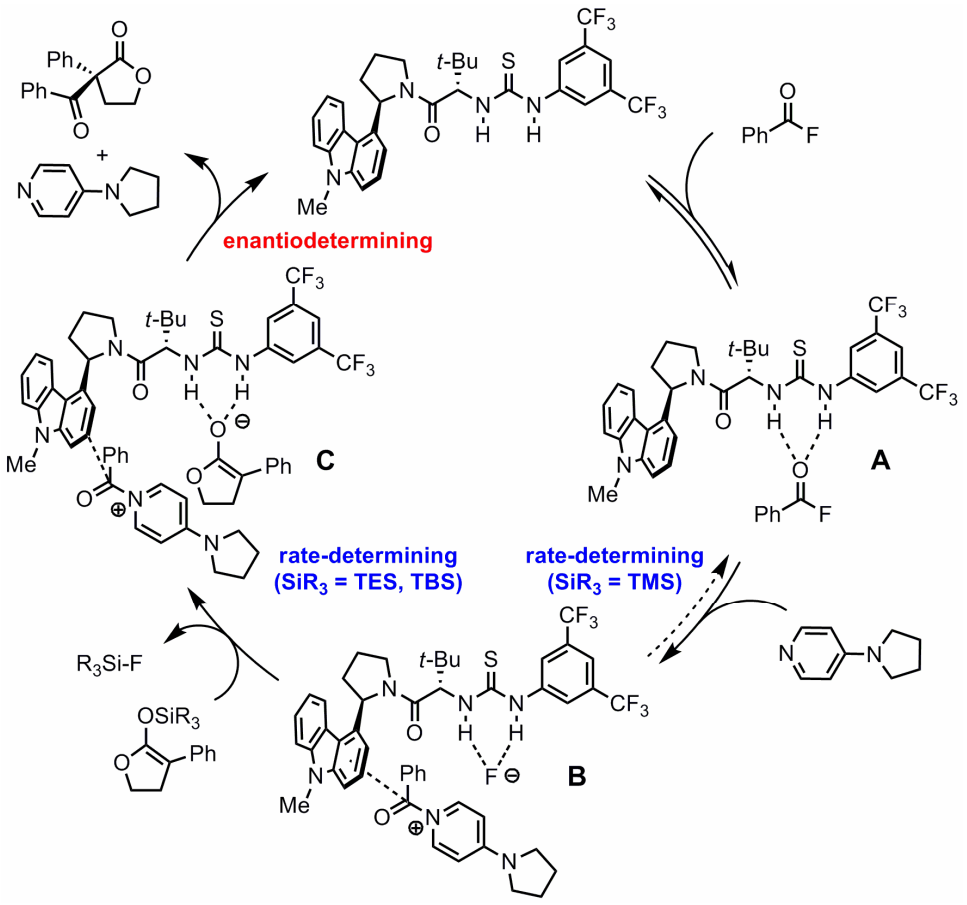

Figure 1.4. Proposed catalytic cycle for thiourea-PPY co-catalyzed acylation

1.3 Conclusions and Outlook

In conclusion, a highly enantioselective acylation of silyl ketene acetals with acyl fluorides has been developed to generate useful α,α-disubstituted butyrolactone products. The remarkable hydrogen-bond acceptor properties and silaphilicity of the fluoride anion facilitate an efficient reaction protocol with low catalyst loadings and high yields and selectivities.

Following the publication of our work, the Seidel group continued to develop the strategy of using a chiral hydrogen-bond donor catalyst with a nucleophilic catalyst to promote asymmetric reactions involving *N*-acylpyridinium ion pair intermediates. A mechanistic study was performed that demonstrated the achiral nucleophilic co-catalyst has a meaningful effect on

the enantioselectivity induced in the kinetic resolution of primary amines.[35] Synthetic methods for the catalytic enantioselective desymmetrization of *meso*-diamines[36a] and the related kinetic resolution of 1,2-diaryl-1,2-diaminoethanes[36b] were reported using this strategy, as well as the catalytic asymmetric Steglich rearrangement and enantioselective addition of *O*-acylated azlactones to isoquinolines.[36c]

1.4 Experimental

1.4.1 General Information

All reactions were performed in flame-dried vials or round-bottom flasks unless otherwise noted. The vials and flasks were fitted with virgin rubber septa, and reactions were conducted under an atmosphere of nitrogen. Stainless steel syringes and cannulae were used to transfer air- and moisture-sensitive liquids. Column chromatography was performed on a Biotage Isolera automated purification system using silica gel 60 (230-400 mesh) from EM Science. Commercial reagents were purchased from Sigma Aldrich or Lancaster and used as received with the following exceptions: acetonitrile, *tert*-butyl methyl ether, dichloromethane, 1,2-dimethoxyethane, tetrahydrofuran, and toluene were dried by passing through columns of activated alumina; triethylmine, diisopropylamine, *N*,*N*-diisopropylethylamine, and pyridine were distilled from CaH_2 at 760 torr; benzoyl fluoride and benzoyl chloride were distilled at reduced pressure; 4-pyrrolidinopyridine was washed with hexanes on a fritted funnel, and the filtrate was concentrated to provide pure product as white crystals. Proton nuclear magnetic resonance (^{1}H NMR) and carbon nuclear magnetic resonance (^{13}C NMR) spectra were recorded

[35] Mittal, N.; Sun, D. X.; Seidel, D. *Org. Lett.* **2012**, *14*, 3084-3087.

[36] (a) De, C. K.; Seidel, D. *J. Am. Chem. Soc.* **2011**, *133*, 14538-14541. (b) Mittal, N.; De, C. K.; Seidel, D. *Chem. Commun.* **2012**, *48*, 10853-10855. (c) De, C. K.; Mittal, N.; Seidel, D. *J. Am. Chem. Soc.* **2011**, *133*, 16802-16805.

on Inova-500 (500 MHz) and Inova-600 (600 MHz) spectrometers. Proton and carbon chemical shifts are reported in parts per million downfield from tetramethylsilane and are referenced to residual protium in the NMR solvent ($CHCl_3$ = δ 7.27; C_6H_6 = δ 7.16) or the carbon resonances of the NMR solvent ($CDCl_3$ = δ 77.0; C_6D_6 = δ 128.4) respectively. NMR data are represented as follows: chemical shift, multiplicity (br. = broad, s = singlet, d = doublet, t = triplet, q = quartet, m = multiplet), coupling constant in Hertz (Hz), integration. Infrared (IR) spectra were obtained using a Bruker Optics Tensor 27 FTIR spectrometer. Optical rotations were measured using a 1 mL cell with a 0.5 dm path length on a Jasco DIP 370 digital polarimeter. Mass spectroscopic (MS) data were obtained using an Agilent 6120 Single Quadrupole LC/MS instrument equipped with an ESI-APCI multimode source. High-performance liquid chromatography (HPLC) analysis was performed using an Agilent 1200 series quaternary HPLC system with commercially available ChiralPak and ChiralCel columns. Kinetics experiments were performed on a ReactIR ic10 purchased from Mettler-Toledo.

1.4.2 General Procedure for the Synthesis of Thiourea Catalysts

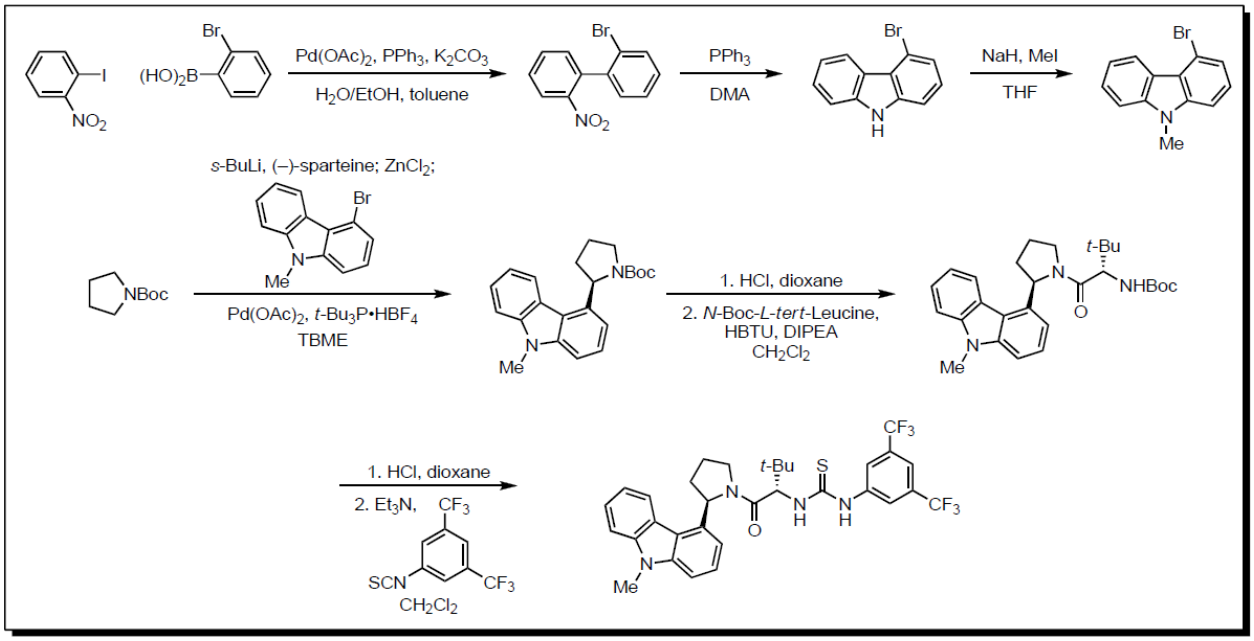

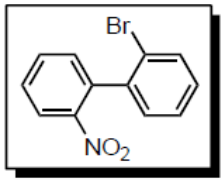

2-bromo-2'-nitrobiphenyl

A round-bottom flask was charged with a stir bar, 2-iodonitrobenzene (5.64 g, 22.6 mmol, 1 equiv), 2-bromophenylboronic acid (5.00 g, 24.9 mmol, 1.1 equiv), K_2CO_3 (6.26 g, 45.3 mmol, 2 equiv), $Pd(OAc)_2$ (254 mg, 1.1 mmol, 0.05 equiv), and PPh_3 (890 mg, 3.4 mmol, 0.15 equiv). Toluene (200 mL) was added followed by a 1:1 ethanol-water solution (40 mL). The reaction flask was equipped with a reflux condenser and heated to 100 ℃ for 18 h. Upon cooling to room temperature, the reaction solution was added to a separatory funnel, the aqueous layer was removed, and the organic layer was washed with water (50 mL). The organic layer was dried over $MgSO_4$, filtered and concentrated by rotary evaporation under reduced pressure to provide the crude residue which was purified by silica gel chromatography to give 5.20 g (83% yield) of 2-bromo-2'-nitrobiphenyl as a yellow solid. IR

(neat) 1572, 1518 (s), 1459, 1347 (s), 1002, 854, 786, 744 (s), 701, 676 cm^{-1}; ^{1}H NMR (500MHz, $CDCl_3$) δ = 8.12 (d, *J* = 7.8 Hz, 1 H), 7.70 (dt, *J* = 1.0, 7.3 Hz, 1 H), 7.66 (d, *J* = 8.3 Hz, 1 H), 7.59 (dd, *J* = 1.0, 8.3 Hz, 1 H), 7.39 (dt, *J* = 1.0, 7.3 Hz, 1 H), 7.37 (dd, *J* = 1.0, 7.8 Hz, 1 H), 7.30 - 7.25 (m, 2 H); $^{13}C\{^{1}H\}$ NMR (125MHz, $CDCl_3$) δ = 148.3, 139.2, 136.0, 132.9, 132.5, 132.3, 129.8, 129.5, 129.0, 127.4, 124.4, 122.6; MS (ESI) exact mass calculated for $[M+H]^+$ ($C_{12}H_9BrNO_2$) requires *m/z* 278.0, found *m/z* 278.0.

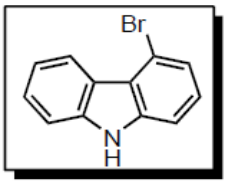

4-bromo-9*H*-carbazole

According to the procedure of Freeman,[37] a flame-dried round-bottom flask was charged with a stir bar, 2-bromo-2'-nitrobiphenyl (5.02 g, 18.1 mmol, 1 equiv), and PPh_3 (11.8 g, 45.1 mmol, 2.5 equiv). DMA (35 mL) was added, and the reaction flask was equipped with a reflux condenser and heated to 180 ℃ for 14 h. The reaction mixture was allowed to cool to room temperature and concentrated by rotary evaporation under reduced pressure to provide the crude residue which was purified by silica gel chromatography to give 2.52 g (57% yield) of 4-bromo-9*H*-carbazole as a brown solid. IR (neat) 3422, 3391, 3060, 1601, 1451, 1429, 1322, 1278, 1171 cm^{-1}; ^{1}H NMR (500MHz, $CDCl_3$) δ = 8.76 (d, *J* = 8.3 Hz, 1 H), 8.25 (br. s., 1 H), 7.49 (t, *J* = 7.3 Hz, 1 H), 7.46 - 7.40 (m, 2 H), 7.38 (d, *J* = 7.8 Hz, 1 H), 7.32 (t, *J* = 6.8 Hz, 1 H), 7.26 (t, *J* = 7.8 Hz, 1 H); $^{13}C\{^{1}H\}$ NMR (125MHz, $CDCl_3$) δ = 140.5, 139.5, 126.5, 126.3, 123.6, 122.8, 122.7, 122.1, 119.5, 116.6, 110.4, 109.4.

[37] Freeman, A. W.; Urvoy, M.; Criswell, M. E. *J. Org. Chem.* **2005**, *70*, 5014-5019.

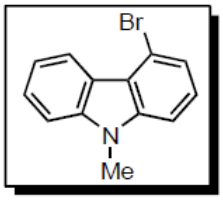

4-bromo-9-methyl-9*H*-carbazole

A flame-dried round-bottom flask was charged with a stir bar and 4-bromo-9*H*-carbazole (1.79 g, 7.3 mmol, 1 equiv). THF (40 mL) was added followed by sodium hydride (60% dispersion in mineral oil; 305 mg, 7.6 mmol, 1.05 equiv). The reaction mixture was stirred at room temperature for 30 min then cooled to 0 °C. Iodomethane (0.91 mL, 14.6 mmol, 2 equiv) was added dropwise at 0 °C. The resulting solution was allowed to warm to room temperature and stirred at room temperature for 18 h. The reaction mixture was poured onto water (50 mL), transferred to a separatory funnel, extracted with ethyl ether (3 x 50 mL), dried over $MgSO_4$, filtered and concentrated by rotary evaporation under reduced pressure to provide the crude residue which was purified by silica gel chromatography to give 1.81 g (96% yield) of 4-bromo-9-methyl-9*H*-carbazole as a tan solid. IR (neat) 3053, 2927, 1593, 1464, 1320, 1128, 1065, 744, 712, 643 cm^{-1}; ^1H NMR (500MHz, $CDCl_3$) δ = 8.79 (d, *J* = 7.8 Hz, 1 H), 7.55 (t, *J* = 7.8 Hz, 1 H), 7.44 (d, *J* = 7.8 Hz, 1 H), 7.41 (d, *J* = 7.8 Hz, 1 H), 7.38 (d, *J* = 8.3 Hz, 1 H), 7.32 (t, *J* = 7.8 Hz, 2 H), 3.87 (s, 3 H); $^{13}C\{^1H\}$ NMR (125MHz, $CDCl_3$) δ = 142.0, 141.0, 126.3, 126.0, 122.9, 122.6, 122.3, 121.4, 119.0, 116.7, 108.2, 107.3, 29.1.

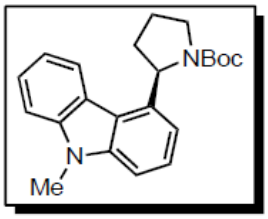

(*R*)-*tert*-butyl 2-(9-methyl-9*H*-carbazol-4-yl)pyrrolidine-1-carboxylate

According to the procedure of Campos,[38] a flame-dried round-bottom flask was charged with a stir bar, TBME (8 mL), *N*-Boc-pyrrolidine (0.63 mL, 3.6 mmol, 1.2 equiv) and (–)-sparteine (0.83 mL, 3.6 mmol, 1.2 equiv), and the resulting solution was cooled to –78 °C. To this solution was added *s*-BuLi (1.4 M in cyclohexane; 2.57 mL, 3.6 mmol, 1.2 equiv) dropwise at a rate of 150 µL/min, and the reaction mixture was stirred

[38] Campos, K. R.; Klapars, A.; Waldman, J. H.; Dormer, P.G.; Chen, C.-Y. *J. Am. Chem. Soc.* **2006**, *128*, 3538-3539.

at −78 °C for 3 h. A solution of $ZnCl_2$ (1.0 M in ethyl ether; 2.16 mL, 2.16 mmol, 0.7 equiv) was then added dropwise at a rate of 150 μL/min at −78 °C. The resulting suspension was stirred at −78 °C for 30 min and then warmed to room temperature and stirred for 30 min. 4-bromo-9-methyl-9*H*-carbazole (780 mg, 3.0 mmol, 1 equiv) was added to the reaction mixture, followed by $Pd(OAc)_2$ (34 mg, 0.15 mmol, 0.05 equiv) and *t*-Bu_3P•HBF_4 (52 mg, 0.18 mmol, 0.06 equiv) in one portion. The reaction was stirred at room temperature for 46 h and then 350 μL of NH_4OH was added to facilitate filtration. The mixture was stirred at room temperature for 1 h and then filtered over Celite and washed with TBME (60 mL). The filtrate was washed with 1 M HCl (50 mL) and water (2 x 50 mL), dried over Na_2SO_4, filtered and concentrated by rotary evaporation under reduced pressure to provide the crude residue which was purified by silica gel chromatography to give 599 mg (57% yield) of (*R*)-*tert*-butyl 2-(9-methyl-9*H*-carbazol-4-yl)pyrrolidine-1-carboxylate as a foamy, slightly-yellow oil. This material was determined to be 89% ee by HPLC analysis (ChiralPak AD-H, 10% IPA/hexanes, 1 mL/min, 254 nm, t_R(major) = 6.07 min, t_R(minor) = 7.05 min). The compound exists as a 1.9:1 mixture of amide rotamers in $CDCl_3$. IR (neat) 2973, 1689 (s), 1470, 1390 (s), 1363, 1156, 1115, 1076, 745, 723 (s) cm^{-1}; ^1H NMR (600MHz, $CDCl_3$), major rotamer resonances δ = 8.11 (d, *J* = 7.9 Hz, 1 H), 7.52 (t, *J* = 7.6 Hz, 1 H), 7.47 (d, *J* = 6.7 Hz, 1 H), 7.43 (t, *J* = 7.9 Hz, 1 H), 7.32 (d, *J* = 8.2 Hz, 1 H), 7.31 - 7.27 (m, 1 H), 7.01 (d, *J* = 7.6 Hz, 1 H), 5.84 (d, *J* = 7.3 Hz, 1 H), 3.89 (s, 3 H), 3.81 - 3.75 (m, 1 H), 3.66 (q, *J* = 10.3 Hz, 1 H), 2.63 - 2.54 (m, 1 H), 2.13 - 2.04 (m, 1 H), 1.98 - 1.84 (m, 2 H), 1.16 (s, 9 H); selected minor rotamer resonances δ = 3.86 (s, 3 H), 1.52 (s, 9 H); $^{13}C\{^1H\}$ NMR (125MHz, $CDCl_3$), major and minor resonances δ = 154.7, 154.5, 141.2, 140.9, 139.8, 138.8, 125.8, 125.3, 125.2, 125.0, 123.2, 122.9, 122.2, 120.5, 118.8, 118.7, 115.1, 114.6, 110.6, 108.4, 108.2, 107.0, 106.7, 79.2, 79.1, 59.0, 58.8, 47.3, 46.9, 34.7, 33.6, 32.7, 31.6, 29.1, 28.6, 28.2,

25.3, 23.3, 22.6, 20.7, 14.1; MS (ESI) exact mass calculated for $[M+Na]^+$ ($C_{22}H_{26}N_2NaO_2$) requires *m/z* 373.2, found *m/z* 373.2; $[\alpha]_D^{24}$ = +65.2 (c = 1.0, $CHCl_3$).

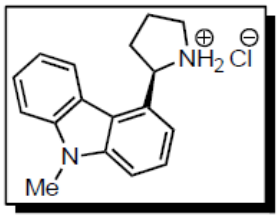

(*R*)-2-(9-methyl-9*H*-carbazol-4-yl)pyrrolidinium chloride

To (*R*)-*tert*-butyl 2-(9-methyl-9*H*-carbazol-4-yl)pyrrolidine-1-carboxylate (562 mg, 1.6 mmol, 1 equiv) in a round-bottom flask was added HCl (4.0 M in dioxane; 4 mL, 16.0 mmol, 10 equiv). The reaction mixture was stirred at room temperature for 2 h and then concentrated *in vacuo* to provide 422 mg (92% yield) of (*R*)-2-(9-methyl-9*H*-carbazol-4-yl)pyrrolidinium chloride as a tan solid that was used directly without further purification. MS (ESI) exact mass calculated for $[M+H]^+$ ($C_{17}H_{19}N_2$) requires *m/z* 251.2, found *m/z* 251.1.

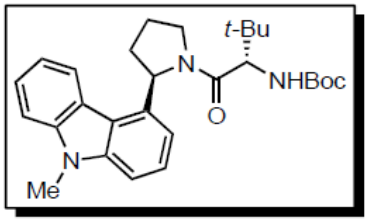

***tert*-butyl (*S*)-3,3-dimethyl-1-((*R*)-2-(9-methyl-9*H*-carbazol-4-yl)pyrrolidin-1-yl)-1-oxobutan-2-ylcarbamate**

To (*R*)-2-(9-methyl-9*H*-carbazol-4-yl)pyrrolidinium chloride (422 mg, 1.5 mmol, 1 equiv) in a round-bottom flask was added Boc-L-*tert*-leucine (442 mg, 1.9 mmol, 1.3 equiv) and HBTU (725 mg, 1.9 mmol, 1.3 equiv) followed by CH_2Cl_2 (12 mL) and *N*,*N*-diisopropylethylamine (0.77 mL, 4.4 mmol, 3 equiv). The resulting solution was stirred at room temperature for 18 h and then concentrated by rotary evaporation under reduced pressure to provide the crude residue which was purified by silica gel chromatography to give 538 mg (91% yield) of diastereomerically pure *tert*-butyl (*S*)-3,3-dimethyl-1-((*R*)-2-(9-methyl-9*H*-carbazol-4-yl)pyrrolidin-1-yl)-1-oxobutan-2-ylcarbamate as a foamy, slightly yellow oil. The compound exists as a 4.9:1 mixture of amide rotamers in $CDCl_3$. IR (neat) 2957, 2872, 1709 (s), 1644 (s),

1423, 1325, 1162, 724 cm^{-1}; ^1H NMR (500MHz, $CDCl_3$), major rotamer resonances δ = 8.10 (d, *J* = 7.8 Hz, 1 H), 7.52 - 7.45 (m, 1 H), 7.43 (d, *J* = 8.3 Hz, 1 H), 7.37 - 7.28 (m, 2 H), 7.25 - 7.22 (m, 1 H), 6.85 (d, *J* = 6.8 Hz, 1 H), 6.17 (d, *J* = 7.8 Hz, 1 H), 5.22 (d, *J* = 10.3 Hz, 1 H), 4.48 (d, *J* = 10.3 Hz, 1 H), 4.43 - 4.37 (m, 1 H), 3.86 (s, 3 H), 3.83 - 3.78 (m, 1 H), 2.54 - 2.41 (m, 1 H), 2.20 - 2.11 (m, 1 H), 2.07 - 1.96 (m, 2 H), 1.54 (s, 9 H), 1.10 (s, 9 H); selected minor rotamer resonances δ = 3.89 (s, 3 H), 1.47 (s, 9 H), 0.81 (s, 9 H); $^{13}C\{^1H\}$ NMR (125MHz, $CDCl_3$), major rotamer resonances δ = 170.7, 156.4, 141.5, 140.9, 137.2, 125.4, 125.0, 123.2, 122.0, 118.8, 114.7, 108.3, 107.0, 79.5, 58.8, 58.7, 48.4, 34.5, 32.2, 29.1, 28.4, 26.5, 23.3; MS (ESI) exact mass calculated for $[M+Na]^+$ ($C_{28}H_{37}N_3NaO_3$) requires *m/z* 486.3, found *m/z* 486.3; $[\alpha]_D^{24}$ = +12.3 (c = 0.7, $CHCl_3$).

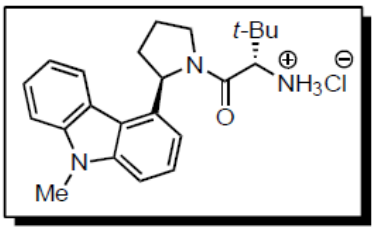

(*S*)-3,3-dimethyl-1-((*R*)-2-(9-methyl-9*H*-carbazol-4-yl)pyrrolidin-1-yl)-1-oxobutan-2-aminium chloride

To *tert*-butyl (*S*)-3,3-dimethyl-1-((*R*)-2-(9-methyl-9*H*-carbazol-4-yl)pyrrolidin-1-yl)-1-oxobutan-2-ylcarbamate (523 mg, 1.1 mmol, 1 equiv) in a round-bottom flask was added HCl (4.0 M in dioxane; 6 mL, 24.0 mmol, 22 equiv). The reaction mixture was stirred at room temperature for 12 h and then concentrated *in vacuo* to provide 451 mg (100% yield) of (*S*)-3,3-dimethyl-1-((*R*)-2-(9-methyl-9*H*-carbazol-4-yl)pyrrolidin-1-yl)-1-oxobutan-2-aminium chloride as a tan solid that was used directly without further purification. MS (ESI) exact mass calculated for $[M+H]^+$ ($C_{23}H_{30}N_3O$) requires *m/z* 364.2, found *m/z* 364.2.

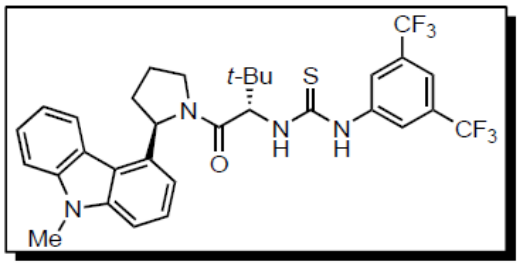

1-(3,5-bis(trifluoromethyl)phenyl)-3-((*S*)-3,3-dimethyl-1-((*R*)-2-(9-methyl-9*H*-carbazol-4-yl)pyrrolidin-1-yl)-1-oxobutan-2-yl)thiourea (59)

To (*S*)-3,3-dimethyl-1-((*R*)-2-(9-methyl-9*H*-carbazol-4-yl)pyrrolidin-1-yl)-1-oxobutan-2-aminium chloride (334 mg, 0.8 mmol, 1 equiv) in a round-bottom flask was added CH_2Cl_2 (8 mL) followed by Et_3N (0.35 mL, 2.5 mmol, 3 equiv). To the resulting solution was added 3,5-bis(trifluoromethyl)phenyl isothiocyanate (152 µL, 0.8 mmol, 1 equiv) dropwise. The reaction mixture was stirred at room temperature for 18 h and then concentrated by rotary evaporation under reduced pressure to provide the crude residue which was purified by silica gel chromatography to give 422 mg (80% yield) of 1-(3,5-bis(trifluoromethyl)phenyl)-3-((*S*)-3,3-dimethyl-1-((*R*)-2-(9-methyl-9*H*-carbazol-4-yl)pyrrolidin-1-yl)-1-oxobutan-2-yl)thiourea as a white solid. The compound exists as a 2.5:1 mixture of amide rotamers in $CDCl_3$. IR (neat) 3320, 2961, 1472, 1440, 1381, 1275 (s), 1173, 1128 (s), 724, 681 cm^{-1}; ^1H NMR (500MHz, $CDCl_3$), major rotamer resonances δ = 9.08 - 8.88 (m, 1 H), 7.95 (d, *J* = 7.8 Hz, 1 H), 7.83 (br. s., 2 H), 7.63 (br. d, *J* = 7.3 Hz, 1 H), 7.52 (s, 1 H), 7.51 - 7.34 (m, 2 H), 7.20 (t, *J* = 7.3 Hz, 1 H), 7.06 (d, *J* = 7.8 Hz, 1 H), 6.81 (d, *J* = 7.3 Hz, 1 H), 6.05 (d, *J* = 7.8 Hz, 1 H), 5.60 (d, *J* = 8.8 Hz, 1 H), 4.61 (t, *J* = 8.5 Hz, 1 H), 3.93 (dd, *J* = 9.8, 17.1 Hz, 1 H), 3.77 (s, 3 H), 2.54 - 2.39 (m, 1 H), 2.20 - 2.08 (m, 1 H), 1.97 (d, *J* = 6.3 Hz, 2 H), 1.17 (s, 9 H); selected minor rotamer resonances δ = 3.88 (s, 3 H), 0.79 (s, 9 H); $^{13}C\{^1H\}$ NMR (125MHz, $CDCl_3$), major and minor rotamer resonances δ = 181.8, 180.7, 172.5, 170.9, 141.2, 141.2, 141.0, 140.8, 139.9, 139.8, 136.8, 136.1, 131.8, 131.7, 131.5, 125.6, 125.1, 124.9, 124.6, 124.4, 124.1, 123.6, 123.3, 122.8, 121.9, 121.7, 119.2, 118.9, 118.6, 118.3, 116.9, 114.8, 108.5, 108.3, 107.7, 107.0, 63.2, 62.5, 61.0, 59.6, 48.8, 47.9, 35.8, 35.6, 33.4, 32.4, 29.1, 28.9, 27.3, 27.1, 25.3, 23.1,

20.9; MS (APCI) exact mass calculated for $[M+Na]^+$ ($C_{32}H_{32}F_6N_4NaOS$) requires *m/z* 657.2, found *m/z* 657.2; $[\alpha]_D^{24} = -70.2$ (c = 1.0, $CHCl_3$).

1.4.3 General procedures for the acylation of silyl ketene acetals

Method A (reaction optimization): A flame-dried vial equipped with a screw-top septum cap was charged with a stir bar, thiourea catalyst (8.0 μmol, 0.10 equiv), nucleophilic catalyst (9.6 μmol, 0.12 equiv) and TBME (3.2 mL). The solution was cooled to −78 °C, and the acylating agent (160 μmol, 2 equiv) was added to the reaction mixture at the same temperature. The vial was moved to a −60 °C cryogenic bath and the temperature was allowed to equilibrate for 10 min. A separate vial was charged with silyl ketene acetal (80 μmol, 1 equiv) in a glove box and equipped with a screw-top septum cap. The vial was removed from the glove box, TBME (0.8 mL) that was pre-cooled to −78 °C was added to the vial, and the resulting solution was swirled for until the silyl ketene acetal dissolved fully. The vial was then cooled to −78 °C, and the cooled silyl ketene acetal solution was added to the −60 °C reaction vessel using a syringe. The reaction mixture was aged at −60 °C for the specified reaction time and then quenched at the same temperature by the addition of water (3 mL). The quenched reaction was allowed to warm to room temperature, diluted with EtOAc (5 mL) and then added to a separatory funnel. The aqueous layer was removed, and the organic layer was washed with water (2 x 5 mL) and brine (5 mL). The organic layer was dried over Na_2SO_4, filtered and concentrated by rotary evaporation under reduced pressure to provide the crude residue. The yield of acylation product was obtained by analysis of the crude ^1H NMR spectrum using *p*-xylene as an internal standard. Purification by silica gel column chromatography then provided pure acylation product. The

enantiomeric excess of the acylation product was determined by HPLC analysis on commercial chiral columns.

Method B (substrate scope): A flame-dried round-bottom flask was charged with a stir bar and TBME (17.25 mL). Stock solutions of thiourea catalyst **59** (20 mM in TBME; 500 μL, 10 μmol, 0.05 equiv) and PPY (48 mM in TBME; 250 μL, 12 μmol 0.06 equiv) were then added to the reaction vessel using a syringe. The solution was cooled to −78 °C, and the acyl fluoride (400 μmol, 2 equiv) was added to the reaction mixture at the same temperature. The resulting solution was allowed to stir at −78 °C as the silyl ketene acetal solution was prepared. A separate pear-shaped flask was charged with silyl ketene acetal (200 μmol, 1 equiv) in a glove box and equipped with a virgin rubber septum. The flask was removed from the glove box, TBME (2 mL) was added to the flask, and the resulting solution was swirled until the silyl ketene acetal dissolved fully. The resulting silyl ketene acetal solution was then cooled to −78 °C, and the cooled solution was added to the reaction vessel using a cannula. The reaction vessel was moved to a −60 °C cryogenic bath and aged at this temperature for the specified reaction time. The reaction mixture was quenched at −60 °C by the sequential addition of three portions of water (3 x 6 mL). The quenched reaction was allowed to warm to room temperature, and then added to a separatory funnel. The aqueous layer was removed, and the organic layer was washed with water (2 x 10 mL) and brine (5 mL). The organic layer was dried over Na_2SO_4, filtered and concentrated by rotary evaporation under reduced pressure to provide the crude residue which was purified by silica gel column chromatography. The isolated yield of pure acylation product was obtained, and the enantiomeric excess was determined by HPLC analysis on commercial chiral columns.

Method C (preparative-scale reaction): A flame-dried round-bottom flask was charged with a stir bar thiourea catalyst **59** (15.9 mg, 25 μmol, 0.005 equiv), PPY (148 mg, 1.0 mmol 0.20 equiv), and TBME (480 mL). The solution was cooled to −78 °C, and 2-naphthoyl fluoride (1.31 g, 7.5 mmol, 1.5 equiv) was added to the reaction mixture in one portion at the same temperature. The resulting solution was allowed to stir at −78 °C as the silyl ketene acetal solution was prepared. A separate pear-shaped flask was charged with silyl ketene acetal (1.17 g, 5 mmol, 1 equiv) in a glove box and equipped with a virgin rubber septum. The flask was removed from the glove box, TBME (20 mL) was added to the flask, and the resulting solution was swirled until the silyl ketene acetal dissolved fully. The resulting silyl ketene acetal solution was then cooled to −78 °C, and the cooled solution was added to the reaction vessel using a cannula. The reaction vessel was moved to a −60 °C cryogenic bath and aged at this temperature for 48 h. The reaction flask was then removed from the cryogenic bath in a −78 °C bath and transferred to a fume hood. The reaction was quenched with water (200 mL) and allowed to warm to room temperature in a water bath. The quenched reaction mixture was added to a separatory funnel, the aqueous layer was removed, and the organic layer was washed with water (2 x 100 mL) and brine (100 mL). The organic layer was dried over $MgSO_4$, filtered and concentrated by rotary evaporation under reduced pressure to provide the crude residue as an off-white solid. A stir bar was added to the flask followed by 3:1 hexanes:ethyl ether (100 mL). The flask was equipped with a reflux condenser and the solution was heated to reflux. A solution of 3:1 hexanes:ethyl ether was added to the flask in 25 mL portions with rapid stirring until 450 mL of additional solution had been added (550 mL total). Complete dissolution of the solid did not occur. Stirring of the solution was stopped. The flask was capped with a plastic stopper and

allowed to cool to room temperature for 1 h. The flask was placed in a −10 °C freezer for 12 h and then moved to a −30 °C for 4 h. A crystalline solid precipitated from the solution. The mother liquor was decanted from the flask, and the remaining crystals were washed with hexanes (3 x 20 mL) to provide (1.24 g, 78% yield) of pure (*R*)-3-(2-naphthoyl)-3-phenyldihydrofuran-2(3*H*)-one (**63**) as a white solid in 92% ee. A stir bar was added to the flask followed by 4:1 hexanes:ethyl ether (200 mL). The flask was equipped with a reflux condenser and the solution was heated to reflux. A solution of 4:1 hexanes:ethyl ether was added to the flask in 25 mL portions with rapid stirring until 400 mL of additional solution had been added (600 mL total). Complete dissolution of the solid did not occur. Stirring of the solution was stopped. The flask was capped with a plastic stopper and allowed to cool to room temperature for 1 h. The flask was placed in a −10 °C freezer for 20 h and then moved to a −30 °C for 16 h. A crystalline solid precipitated from the solution. The mother liquor was decanted from the flask, and the remaining crystals were washed with hexanes (3 x 20 mL) to provide (1.10 g, 70% overall yield) of pure (*R*)-3-(2-naphthoyl)-3-phenyldihydrofuran-2(3*H*)-one (**63**) as a white solid in >99% ee.

Method D (kinetic analysis): An oven-dried reaction vessel equipped with a stir bar was attached to an in situ infrared (IR) spectroscopy probe that had been dried for 5 min with a heat gun. The vessel was capped with a rubber septum and was allowed to cool to room temperature under a nitrogen atmosphere. TBME (1.5 mL) was added followed by a stock solution of thiourea catalyst **59** (40 mM in TBME; 100 μL, 4 μmol, 0.10 equiv), and the solution was cooled to −78 °C with stirring. A background IR spectrum was collected (256 scans). Continuous data collection was started (4 spectra/min, 50 scans/spectrum). After 5 min, a stock solution of benzoyl fluoride (0.80 M in TBME; 100 μL, 80 μmol, 2 equiv) was added and the solution was

allowed to stir for 5 min. A stock solution of silyl ketene acetal **13** was added (0.16 M in TBME; 250 μL, 40 μmol, 1 equiv) and the solution was allowed to stir for 5 min. A stock solution of PPY (96 mM in TBME; 50 μL, 4.8 μmol, 0.12 equiv) was added, and the absorbance of benzoyl fluoride was monitored over the course of the reaction. The reaction mixture was quenched at −78 °C with 2 M HCl in ether (2 mL). The quenched reaction was allowed to warm to room temperature, and then added to a separatory funnel. The aqueous layer was removed, and the organic layer was washed with water (10 mL), saturated $NaHCO_3$ (10 mL), water (10 mL) and brine (5 mL). The organic layer was dried over Na_2SO_4, filtered and concentrated by rotary evaporation under reduced pressure to provide the crude residue which was purified by silica gel column chromatography. The enantiomeric excess was determined by HPLC analysis on commercial chiral columns.

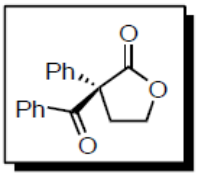

(*R*)-3-benzoyl-3-phenyldihydrofuran-2(3*H*)-one (19)

Followed method B from benzoyl fluoride and trimethyl(3-phenyl-4,5-dihydrofuran-2-yloxy)silane on 200 μmol scale for 6 h and purified using silica gel column chromatography to provide 46.7 mg (88% yield) of (*R*)-3-benzoyl-3-phenyldihydrofuran-2(3*H*)-one (**19**) as a white solid. This material was determined to be 92% ee by HPLC analysis (ChiralPak AS-H, 10% IPA/hexanes, 1 mL/min, 254 nm, t_R(major) = 11.79 min, t_R(minor) = 15.90 min). IR (neat) 1773 (s), 1662 (s), 1447, 1373, 1159, 1024, 1003, 696 cm^{-1}; ^1H NMR (500MHz, $CDCl_3$) δ = 7.88 (d, *J* = 7.8 Hz, 2 H), 7.44 (t, *J* = 7.3 Hz, 6 H), 7.38 (t, *J* = 8.3 Hz, 12 H), 7.35 - 7.28 (m, 29 H), 4.40 - 4.35 (m, 2 H), 3.47 (td, *J* = 5.3, 12.8 Hz, 1 H), 2.55 (td, *J* = 8.2, 12.9 Hz, 1 H); $^{13}C\{^1H\}$ NMR (125MHz, $CDCl_3$) δ = 193.1, 173.4, 138.2, 133.8,

133.2, 131.2, 129.4, 128.0, 128.0, 126.7, 65.9, 65.1, 36.6; MS (ESI) exact mass calculated for $[M+Na]^+$ ($C_{17}H_{14}NaO_3$) requires *m/z* 289.1, found *m/z* 289.1; $[\alpha]_D^{24}$ = +242.9 (c = 1.0, $CHCl_3$).

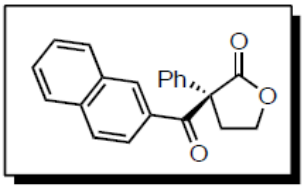

(*R*)-3-(2-naphthoyl)-3-phenyldihydrofuran-2(3*H*)-one (63)

Followed method B from 2-naphthoyl fluoride and trimethyl(3-phenyl-4,5-dihydrofuran-2-yloxy)silane on 200 μmol scale for 6 h and purified using silica gel column chromatography to provide 53.5 mg (85% yield) of (*R*)-3-(2-naphthoyl)-3-phenyldihydrofuran-2(3*H*)-one (**63**) as a white solid. This material was determined to be 95% ee by HPLC analysis (ChiralPak AS-H, 10% IPA/hexanes, 1 mL/min, 254 nm, t_R(major) = 12.69 min, t_R(minor) = 21.35 min). IR (neat) 1763 (s), 1667 (s), 1625, 1367, 1152, 1126, 1022, 760 cm^{-1}; ^1H NMR (600MHz, $CDCl_3$) δ = 8.47 (s, 1 H), 7.94 (dd, *J* = 1.8, 8.8 Hz, 1 H), 7.77 (d, *J* = 8.8 Hz, 2 H), 7.72 (d, *J* = 8.5 Hz, 1 H), 7.55 (t, *J* = 7.9 Hz, 1 H), 7.46 (t, *J* = 7.3 Hz, 1 H), 7.41 - 7.35 (m, 4 H), 7.33 - 7.29 (m, 1 H), 4.46 - 4.36 (m, 2 H), 3.54 (ddd, *J* = 4.4, 6.2, 10.5 Hz, 1 H), 2.60 (td, *J* = 8.2, 12.9 Hz, 1 H); $^{13}C\{^1H\}$ NMR (125MHz, $CDCl_3$) δ = 193.0, 173.5, 138.5, 135.3, 134.2, 132.0, 131.1, 130.0, 129.4, 128.8, 128.0, 127.6, 127.5, 126.8, 126.5, 126.0, 66.0, 65.2, 36.8; MS (ESI) exact mass calculated for $[M+Na]^+$ ($C_{21}H_{16}NaO_3$) requires *m/z* 339.1, found *m/z* 339.0; $[\alpha]_D^{24}$ = +254.4 (c = 1.0, $CHCl_3$).

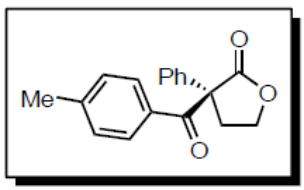

(*R*)-3-(4-methylbenzoyl)-3-phenyldihydrofuran-2(3*H*)-one (64)

Followed method B from 4-methylbenzoyl fluoride and trimethyl(3-phenyl-4,5-dihydrofuran-2-yloxy)silane on 200 μmol scale for 24 h and purified using silica gel column chromatography to provide 51.2 mg (91% yield) of (*R*)-3-(4-methylbenzoyl)-3-phenyldihydrofuran-2(3*H*)-one (**64**) as a white solid. This material was

determined to be 95% ee by HPLC analysis (ChiralPak AS-H, 10% IPA/hexanes, 1 mL/min, 254 nm, t_R(major) = 11.52 min, t_R(minor) = 15.98 min). IR (neat) 1770 (s), 1662 (s), 1604, 1371, 1162, 1026, 1003, 938, 829 cm^{-1}; ^1H NMR (600MHz, $CDCl_3$) δ = 7.79 (d, *J* = 8.2 Hz, 2 H), 7.40 - 7.35 (m, 2 H), 7.34 - 7.29 (m, 3 H), 7.08 (d, *J* = 8.2 Hz, 2 H), 4.39 - 4.33 (m, 2 H), 3.46 (td, *J* = 5.2, 13.0 Hz, 1 H), 2.53 (td, *J* = 8.2, 12.9 Hz, 1 H), 2.31 (s, 3 H); $^{13}C\{^1H\}$ NMR (125MHz, $CDCl_3$) δ = 192.5, 173.5, 144.2, 138.5, 131.4, 131.2, 129.3, 128.7, 127.9, 126.7, 65.9, 65.0, 36.6, 21.6; MS (ESI) exact mass calculated for $[M+Na]^+$ ($C_{18}H_{16}NaO_3$) requires *m/z* 303.1, found *m/z* 303.1; $[\alpha]_D^{24}$ = +240.3 (c = 1.0, $CHCl_3$).

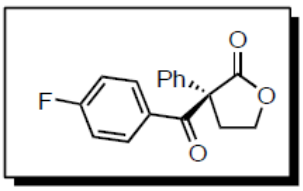

(*R*)-3-(4-fluorobenzoyl)-3-phenyldihydrofuran-2(3*H*)-one (65)

Followed method B from 4-fluorobenzoyl fluoride and trimethyl(3-phenyl-4,5-dihydrofuran-2-yloxy)silane on 200 μmol scale for 6 h and purified using silica gel column chromatography to provide 51.3 mg (90% yield) of (*R*)-3-(4-fluorobenzoyl)-3-phenyldihydrofuran-2(3*H*)-one (**65**) as a pale yellow oil. This material was determined to be 91% ee by HPLC analysis (ChiralPak AS-H, 10% IPA/hexanes, 1 mL/min, 254 nm, t_R(major) = 10.71 min, t_R(minor) = 12.76 min). IR (neat) 1770 (s), 1674 (s), 1597, 1505, 1448, 1372, 1237, 1152 (s), 1025, 749, 698 cm^{-1}; ^1H NMR (500MHz, $CDCl_3$) δ = 7.95 (dd, *J* = 5.4, 8.8 Hz, 2 H), 7.41 - 7.35 (m, 2 H), 7.35 - 7.30 (m, 1 H), 7.30 - 7.26 (m, 2 H), 6.95 (t, *J* = 8.8 Hz, 2 H), 4.42 - 4.33 (m, 2 H), 3.50 (ddd, *J* = 4.9, 6.3, 13.2 Hz, 1 H), 2.47 (td, *J* = 8.2, 12.9 Hz, 1 H); $^{13}C\{^1H\}$ NMR (125MHz, $CDCl_3$) δ = 191.3, 173.3, 165.5 (d, J_{C-F} = 256.3 Hz), 138.4, 134.2 (d, J_{C-F} = 10.1 Hz), 130.1 (d, J_{C-F} = 2.7 Hz), 129.5, 128.0, 126.6, 115.1 (d, J_{C-F} = 22.0 Hz), 66.1, 65.1, 36.9; MS (ESI) exact mass calculated for $[M+Na]^+$ ($C_{17}H_{13}FNaO_3$) requires *m/z* 307.1, found *m/z* 307.0; $[\alpha]_D^{24}$ = +304.1 (c = 1.0, $CHCl_3$).

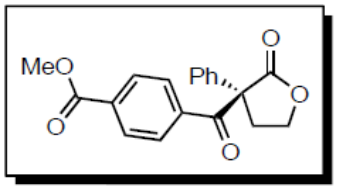

(*R*)-methyl 4-(2-oxo-3-phenyltetrahydrofuran-3-carbonyl)benzoate (66)

Followed method B from methyl 4-(fluorocarbonyl)benzoate and trimethyl(3-phenyl-4,5-dihydrofuran-2-yloxy)silane on 200 μmol scale for 4 h and purified using silica gel column chromatography to provide 61.7 mg (95% yield) of (*R*)-methyl 4-(2-oxo-3-phenyltetrahydrofuran-3-carbonyl)benzoate (**66**) as a white solid. This material was determined to be 86% ee by HPLC analysis (ChiralPak AS-H, 10% IPA/hexanes, 1 mL/min, 210 nm, t_R(major) = 20.15 min, t_R(minor) = 29.42 min). IR (neat) 1777 (s), 1715 (s), 1674 (s), 1435, 1289, 1167, 1108, 1034, 761, 702 cm^{-1}; ^1H NMR (600MHz, $CDCl_3$) δ = 7.93 (s, 4 H), 7.40 - 7.34 (m, 2 H), 7.33 (d, *J* = 7.0 Hz, 1 H), 7.30 - 7.28 (m, 2 H), 4.44 - 4.34 (m, 2 H), 3.89 (s, 3 H), 3.49 (ddd, *J* = 4.8, 6.7, 13.0 Hz, 1 H), 2.52 (td, *J* = 7.7, 13.1 Hz, 1 H); $^{13}C\{^1H\}$ NMR (125MHz, $CDCl_3$) δ = 192.9, 173.0, 166.0, 137.8, 137.4, 133.5, 131.0, 129.5, 129.0, 128.2, 126.7, 65.9, 65.3, 52.3, 36.5; MS (ESI) exact mass calculated for $[M+Na]^+$ ($C_{19}H_{16}NaO_5$) requires *m/z* 347.1, found *m/z* 347.0; $[\alpha]_D^{23}$ = +239.2 (c = 1.0, $CHCl_3$).

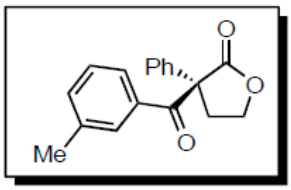

(*R*)-3-(3-methylbenzoyl)-3-phenyldihydrofuran-2(3*H*)-one (67)

Followed method B from 3-methylbenzoyl fluoride and trimethyl(3-phenyl-4,5-dihydrofuran-2-yloxy)silane on 200 μmol scale for 16 h and purified using silica gel column chromatography to provide 43.3 mg (77% yield) of (*R*)-3-(3-methylbenzoyl)-3-phenyldihydrofuran-2(3*H*)-one (**67**) as a white solid. This material was determined to be 92% ee by HPLC analysis (ChiralPak AS-H, 10% IPA/hexanes, 1 mL/min, 254 nm, t_R(major) = 9.93 min, t_R(minor) = 14.53 min). IR (neat) 1776 (s), 1661 (s), 1600, 1446,

1376, 1151, 1022, 951, 698 cm^{-1}; ^{1}H NMR (500MHz, $CDCl_3$) δ = 7.73 (s, 1 H), 7.62 (d, *J* = 7.8 Hz, 1 H), 7.41 - 7.30 (m, 5 H), 7.26 - 7.23 (m, 1 H), 7.14 (t, *J* = 7.8 Hz, 1 H), 4.39 - 4.34 (m, 2 H), 3.44 (td, *J* = 5.3, 12.8 Hz, 1 H), 2.57 (td, *J* = 8.2, 12.9 Hz, 1 H), 2.29 (s, 3 H); $^{13}C\{^{1}H\}$ NMR (125MHz, $CDCl_3$) δ = 193.4, 173.4, 138.2, 137.8, 134.0, 133.8, 131.4, 129.3, 128.7, 127.9, 127.7, 126.7, 65.8, 65.0, 36.5, 21.2; MS (ESI) exact mass calculated for $[M+Na]^+$ ($C_{18}H_{16}NaO_3$) requires *m/z* 303.1, found *m/z* 303.1; $[\alpha]_D^{24}$ = +268.0 (c = 1.0, $CHCl_3$).

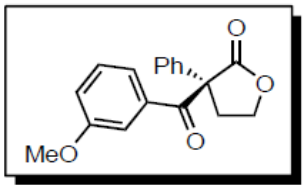

(*R*)-3-(3-methoxybenzoyl)-3-phenyldihydrofuran-2(3*H*)-one (68)

Followed method B from 3-methoxybenzoyl fluoride and trimethyl(3-phenyl-4,5-dihydrofuran-2-yloxy)silane on 200 μmol scale for 6 h and purified using silica gel column chromatography to provide 56.2 mg (95% yield) of (*R*)-3-(3-methoxybenzoyl)-3-phenyldihydrofuran-2(3*H*)-one (**68**) as a pale yellow oil. This material was determined to be 92% ee by HPLC analysis (ChiralPak AD-H, 10% IPA/hexanes, 1 mL/min, 254 nm, t_R(minor) = 9.57 min, t_R(major) = 11.78 min). IR (neat) 1767 (s), 1674 (s), 1575, 1444, 1365, 1259, 1206, 1150, 1047, 1022, 697 cm^{-1}; ^{1}H NMR (600MHz, $CDCl_3$) δ = 7.48 - 7.43 (m, 2 H), 7.40 - 7.35 (m, 2 H), 7.35 - 7.29 (m, 3 H), 7.18 (t, *J* = 7.9 Hz, 1 H), 6.98 (dd, *J* = 2.3, 8.2 Hz, 1 H), 4.41 - 4.35 (m, 2 H), 3.69 (s, 3 H), 3.46 (td, *J* = 5.1, 12.9 Hz, 1 H), 2.56 (td, *J* = 8.2, 12.9 Hz, 1 H); $^{13}C\{^{1}H\}$ NMR (125MHz, $CDCl_3$) δ = 192.9, 173.3, 159.0, 138.3, 135.0, 129.3, 128.9, 128.0, 126.7, 123.8, 120.2, 115.2, 65.9, 65.1, 55.2, 36.6; MS (ESI) exact mass calculated for $[M+Na]^+$ ($C_{18}H_{16}NaO_4$) requires *m/z* 319.1, found *m/z* 319.1; $[\alpha]_D^{24}$ = +225.6 (c = 1.0, $CHCl_3$).

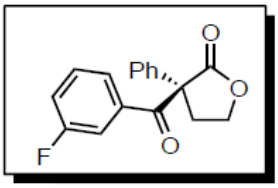

(*R*)-3-(3-fluorobenzoyl)-3-phenyldihydrofuran-2(3*H*)-one (69)

Followed method B from 3-fluorobenzoyl fluoride and trimethyl(3-phenyl-4,5-dihydrofuran-2-yloxy)silane on 200 μmol scale for 6 h and purified using silica gel column chromatography to provide 44.2 mg (78% yield) of (*R*)-3-(3-fluorobenzoyl)-3-phenyldihydrofuran-2(3*H*)-one (**69**) as an off-white solid. This material was determined to be 87% ee by HPLC analysis (ChiralPak AS-H, 10% IPA/hexanes, 1 mL/min, 254 nm, t_R(major) = 10.82 min, t_R(minor) = 13.63 min). IR (neat) 1777 (s), 1667 (s), 1586, 1439, 1373, 1262, 1152, 1021, 742, 699 cm^{-1}; ^1H NMR (500MHz, $CDCl_3$) δ = 7.65 (d, *J* = 7.8 Hz, 1 H), 7.60 (d, *J* = 9.8 Hz, 1 H), 7.42 - 7.36 (m, 2 H), 7.35 - 7.28 (m, 3 H), 7.26 - 7.20 (m, 1 H), 7.17 - 7.10 (m, 1 H), 4.43 - 4.32 (m, 2 H), 3.51 - 3.43 (m, 1 H), 2.51 (td, *J* = 7.8, 13.2 Hz, 1 H); $^{13}C\{^1H\}$ NMR (125MHz, $CDCl_3$) δ = 192.0, 173.1, 162.1 (d, J_{C-F} = 247.2 Hz), 137.9, 135.9 (d, J_{C-F} = 6.4 Hz), 129.5, 128.2, 127.2, 126.7, 120.2 (d, J_{C-F} = 21.1 Hz), 117.7 (d, J_{C-F} = 22.9 Hz), 66.0, 65.2, 36.7; MS (ESI) exact mass calculated for $[M+Na]^+$ ($C_{17}H_{13}FNaO_3$) requires *m/z* 307.1, found *m/z* 307.1; $[\alpha]_D^{24}$ = +274.2 (c = 1.0, $CHCl_3$).

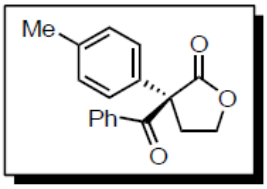

(*R*)-3-benzoyl-3-*p*-tolyldihydrofuran-2(3*H*)-one (79)

Followed method B from benzoyl fluoride and trimethyl(3-*p*-tolyl-4,5-dihydrofuran-2-yloxy)silane on 200 μmol scale for 6 h and purified using silica gel column chromatography to provide 42.0 mg (75% yield) of (*R*)-3-benzoyl-3-*p*-tolyldihydrofuran-2(3*H*)-one (**79**) as a white solid. This material was determined to be 93% ee by HPLC analysis (ChiralPak AS-H, 2% IPA/hexanes, 1 mL/min, 254 nm, t_R(major) = 30.08 min, t_R(minor) = 40.16 min). IR (neat) 1770 (s), 1671 (s), 1448, 1371, 1151, 1026, 940, 690 cm^{-1}; ^1H NMR (500MHz, $CDCl_3$) δ = 7.89 (d, *J* = 7.3 Hz, 2 H), 7.44 (t, *J* = 7.3 Hz, 1 H), 7.29 (d, *J* = 7.8

Hz, 2 H), 7.20 (d, *J* = 8.3 Hz, 2 H), 7.17 (d, *J* = 8.3 Hz, 2 H), 4.38 - 4.32 (m, 2 H), 3.43 (td, *J* = 5.4, 12.7 Hz, 1 H), 2.53 (td, *J* = 8.2, 12.9 Hz, 1 H), 2.34 (s, 3 H); $^{13}C\{^{1}H\}$ NMR (125MHz, $CDCl_3$) δ = 193.3, 173.6, 137.8, 135.1, 133.9, 133.1, 131.2, 130.0, 127.9, 126.6, 65.9, 64.8, 36.6, 21.0; MS (ESI) exact mass calculated for $[M+Na]^+$ ($C_{18}H_{16}NaO_3$) requires *m/z* 303.1, found *m/z* 303.1; $[\alpha]_D^{25}$ = +234.0 (c = 0.4, $CHCl_3$).

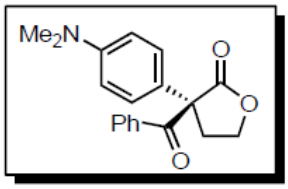

(*R*)-3-benzoyl-3-(4-(dimethylamino)phenyl)dihydrofuran-2(3*H*)-one (80)

Followed method B from benzoyl fluoride and *N*,*N*-dimethyl-4-(2-(trimethylsilyloxy)-4,5-dihydrofuran-3-yl)aniline on 200 μmol scale for 24 h and purified using silica gel column chromatography to provide 46.9 mg (76% yield) of (*R*)-3-benzoyl-3-(4-(dimethylamino)phenyl)dihydrofuran-2(3*H*)-one (**80**) as a yellow solid. This material was determined to be 89% ee by HPLC analysis (ChiralPak AS-H, 10% IPA/hexanes, 1 mL/min, 254 nm, t_R(minor) = 19.01 min, t_R(major) = 25.53 min). IR (neat) 1770 (s), 1672 (s), 1612, 1519, 1447, 1160, 1024, 800, 710, 689 cm^{-1}; ^{1}H NMR (500MHz, $CDCl_3$) δ = 7.90 (d, *J* = 7.3 Hz, 2 H), 7.42 (t, *J* = 7.1 Hz, 1 H), 7.29 (d, *J* = 7.8 Hz, 2 H), 7.17 (d, *J* = 8.8 Hz, 2 H), 6.69 (d, *J* = 8.8 Hz, 2 H), 4.38 - 4.28 (m, 2 H), 3.37 (td, *J* = 5.9, 12.7 Hz, 1 H), 2.95 (s, 6 H), 2.55 (td, *J* = 7.8, 12.7 Hz, 1 H); $^{13}C\{^{1}H\}$ NMR (125MHz, $CDCl_3$) δ = 193.9, 174.0, 149.9, 134.2, 132.9, 131.2, 127.9, 127.5, 124.9, 112.8, 65.7, 64.3, 40.2, 36.3; MS (ESI) exact mass calculated for $[M+Na]^+$ ($C_{19}H_{19}NNaO_3$) requires *m/z* 332.1, found *m/z* 332.1; $[\alpha]_D^{23}$ = +172.8 (c = 0.8, $CHCl_3$).

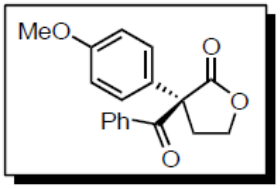

(*R*)-3-benzoyl-3-(4-methoxyphenyl)dihydrofuran-2(3*H*)-one (81)

Followed method B from benzoyl fluoride and (3-(4-methoxyphenyl)-4,5-dihydrofuran-2-yloxy)trimethylsilane on 200 μmol scale for 6 h and purified using silica gel column chromatography to provide 47.4 mg (80% yield) of (*R*)-3-benzoyl-3-(4-methoxyphenyl)dihydrofuran-2(3*H*)-one (**81**) as a colorless oil. This material was determined to be 88% ee by HPLC analysis (ChiralCel OD-H, 10% IPA/hexanes, 1 mL/min, 254 nm, t_R(major) = 14.60 min, t_R(minor) = 22.54 min). IR (neat) 1778 (s), 1668 (s), 1512, 1252, 1180, 1152, 1027, 1002, 832, 798, 691 cm^{-1}; ^1H NMR (600MHz, $CDCl_3$) δ = 7.88 (d, *J* = 7.6 Hz, 2 H), 7.44 (t, *J* = 7.3 Hz, 1 H), 7.29 (t, *J* = 7.9 Hz, 2 H), 7.25 (d, *J* = 8.8 Hz, 2 H), 6.90 (d, *J* = 8.8 Hz, 2 H), 4.40 - 4.31 (m, 2 H), 3.80 (s, 3 H), 3.45 - 3.36 (m, 1 H), 2.55 (td, *J* = 8.0, 13.0 Hz, 1 H); $^{13}C\{^1H\}$ NMR (125MHz, $CDCl_3$) δ = 193.4, 173.7, 159.2, 133.9, 133.1, 131.2, 129.9, 128.9, 128.0, 114.7, 65.8, 64.4, 55.2, 36.4; MS (ESI) exact mass calculated for $[M+Na]^+$ ($C_{18}H_{16}NaO_4$) requires *m/z* 319.1, found *m/z* 319.1; $[\alpha]_D^{25}$ = +193.3 (c = 1.1, $CHCl_3$).

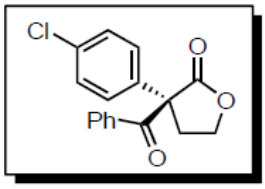

(*R*)-3-benzoyl-3-(4-chlorophenyl)dihydrofuran-2(3*H*)-one (82)

Followed method B from benzoyl fluoride and (3-(4-chlorophenyl)-4,5-dihydrofuran-2-yloxy)trimethylsilane on 200 μmol scale for 6 h and purified using silica gel column chromatography to provide 45.7 mg (76% yield) of (*R*)-3-benzoyl-3-(4-chlorophenyl)dihydrofuran-2(3*H*)-one (**82**) as a white solid. This material was determined to be 89% ee by HPLC analysis (ChiralPak AD-H, 10% IPA/hexanes, 1 mL/min, 254 nm, t_R(minor) = 9.39 min, t_R(major) = 10.47 min). IR (neat) 1776 (s), 1667 (s), 1159, 1094, 1027, 1002, 942, 795, 742, 710, 686 cm^{-1}; ^1H NMR (500MHz, $CDCl_3$) δ = 7.86 (d, *J* = 7.8 Hz, 2 H), 7.44 (t, *J* = 7.3 Hz, 1 H), 7.33 (d, *J* = 8.3 Hz, 2 H), 7.29 (d, *J* = 7.8 Hz, 2 H), 7.25 (d, *J* = 6.8

Hz, 2 H), 4.39 - 4.32 (m, 2 H), 3.42 (td, *J* = 4.9, 12.7 Hz, 1 H), 2.50 (td, *J* = 8.7, 12.9 Hz, 1 H); $^{13}C\{^{1}H\}$ NMR (125MHz, $CDCl_3$) δ = 192.6, 173.1, 136.7, 134.1, 133.5, 133.4, 131.2, 129.6, 128.2, 128.1, 66.0, 64.5, 36.6; MS (ESI) exact mass calculated for $[M+Na]^+$ ($C_{17}H_{13}ClNaO_3$) requires *m/z* 323.0, found *m/z* 323.0; $[\alpha]_D^{23}$ = +179.7 (c = 1.0, $CHCl_3$).

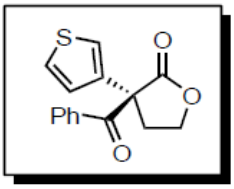

(*R*)-3-benzoyl-3-(thiophen-3-yl)dihydrofuran-2(3*H*)-one (83)

Followed method B from benzoyl fluoride and trimethyl(3-(thiophen-3-yl)-4,5-dihydrofuran-2-yloxy)silane on 200 μmol scale for 6 h and purified using silica gel column chromatography to provide 42.0 mg (77% yield) of (*R*)-3-benzoyl-3-(thiophen-3-yl)dihydrofuran-2(3*H*)-one (**83**) as a white solid. This material was determined to be 89% ee by HPLC analysis (ChiralPak AS-H, 10% IPA/hexanes, 1 mL/min, 254 nm, t_R(major) = 16.51 min, t_R(minor) = 21.04 min). IR (neat) 1768 (s), 1665 (s), 1447, 1374, 1168, 1028, 792, 767, 686 cm^{-1}; ^{1}H NMR (600MHz, $CDCl_3$) δ = 7.91 (d, *J* = 7.3 Hz, 2 H), 7.49 - 7.44 (m, 1 H), 7.37 - 7.29 (m, 4 H), 6.98 (dd, *J* = 1.2, 5.0 Hz, 1 H), 4.44 - 4.33 (m, 2 H), 3.43 (ddd, *J* = 3.5, 6.2, 12.9 Hz, 1 H), 2.59 (td, *J* = 8.6, 13.0 Hz, 1 H); $^{13}C\{^{1}H\}$ NMR (125MHz, $CDCl_3$) δ = 192.8, 173.5, 137.8, 134.1, 133.2, 130.7, 128.1, 127.2, 126.3, 122.4, 66.1, 61.8, 36.0; MS (ESI) exact mass calculated for $[M+Na]^+$ ($C_{15}H_{12}NaO_3S$) requires *m/z* 295.0, found *m/z* 295.0; $[\alpha]_D^{23}$ = +183.2 (c = 1.0, $CHCl_3$).

1.4.4 General procedure for the synthesis of silyl ketene acetals

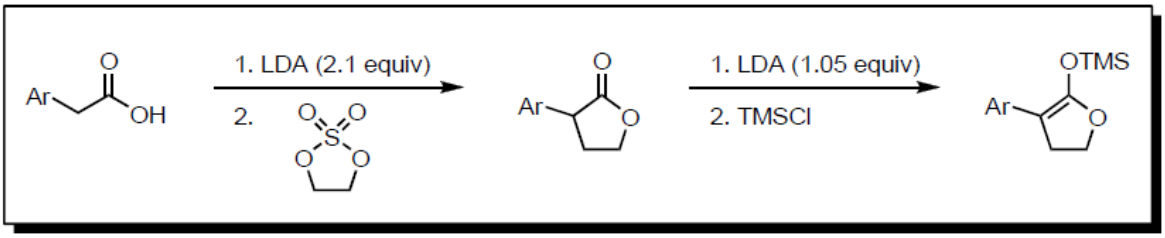

Lactone Synthesis:[39] To a −78 °C solution of diisopropylamine (5.93 mL, 42.0 mmol, 2.1 equiv) in THF (12 mL) was added a solution of *n*-BuLi (2.5 M in hexanes; 16.8 mL, 42.0 mmol, 2.1 equiv) using a syringe. The mixture was stirred at −78 °C for 10 min, warmed to 0 °C for 5 min, and cooled to −78 °C for 10 min. A solution of arylacetic acid (20.0 mmol, 1 equiv) in THF (12 mL) was added to the LDA solution at −78 °C using a cannula. The reaction mixture was stirred at −78 °C for 20 min, warmed to room temperature, and stirred at this temperature for 45 min. A solution of 1,3,2-dioxathiolane-2,2-dioxide (2.48 g, 20.0 mmol, 1 equiv) in THF (12 mL) was added to the reaction using a syringe. DME (10 mL) was added to the reaction mixture, and the resulting solution was refluxed for 16 h. The reaction mixture was allowed to cool to room temperature and water (20 mL) was added. The resulting solution was transfered to a separatory funnel, and the mixture was extracted with CH_2Cl_2 (3 x 100 mL). The combined organic layers were washed with saturated aqueous $NaHCO_3$ (2 x 100 mL) and brine (1 x 50 mL), dried over Na_2SO_4, filtered and concentrated by rotary evaporation under reduced pressure to provide the crude residue, which was purified by silica gel column chromatography to obtain the lactone product.

[39] Mermeria, A. H.; Fu, G. C. *J. Am. Chem. Soc.* **2003**, *125*, 4050-4051.

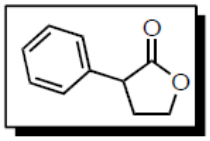

3-phenyldihydrofuran-2(3*H*)-one

Followed general procedure from phenylacetic acid on 20.0 mmol scale and purified using silica gel column chromatography to provide 2.16 g (67% yield) of 3-phenyldihydrofuran-2(3*H*)-one as a pale-yellow oil. IR (neat) 2912, 1763 (s), 1498, 1454, 1372, 1146, 1023, 752, 698 cm^{-1}; ^{1}H NMR (500MHz, $CDCl_3$) δ = 7.39 (t, *J* = 7.8 Hz, 2 H), 7.35 - 7.28 (m, 3 H), 4.50 (dt, *J* = 3.2, 8.7 Hz, 1 H), 4.37 (dt, *J* = 7.3, 9.3 Hz, 1 H), 3.83 (t, *J* = 9.5 Hz, 1 H), 2.79 - 2.68 (m, 1 H), 2.46 (qd, *J* = 9.2, 12.5 Hz, 1 H); $^{13}C\{^{1}H\}$ NMR (125MHz, $CDCl_3$) δ = 177.3, 136.6, 128.8, 127.8, 127.6, 66.4, 45.4, 31.5; MS (ESI) exact mass calculated for $[M+Na]^+$ ($C_{10}H_{10}NaO_2$) requires *m/z* 185.1, found *m/z* 185.1.

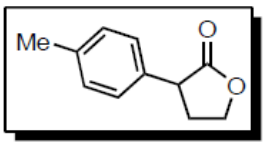

3-*p*-tolyldihydrofuran-2(3*H*)-one

Followed general procedure from *p*-tolylacetic acid on 20.0 mmol scale and purified using silica gel column chromatography to provide 1.82 g (52% yield) of 3-*p*-tolyldihydrofuran-2(3*H*)-one as a white solid. IR (neat) 2905, 1768 (s), 1521, 1321, 1148, 1021, 920, 804, 694 cm^{-1}; ^{1}H NMR (500MHz, $CDCl_3$) δ = 7.21 - 7.17 (m, 4 H), 4.47 (dt, *J* = 3.4, 8.8 Hz, 1 H), 4.35 (dt, *J* = 6.8, 9.3 Hz, 1 H), 3.78 (t, *J* = 9.5 Hz, 1 H), 2.75 - 2.65 (m, 1 H), 2.49 - 2.38 (m, 1 H), 2.36 (s, 3 H); $^{13}C\{^{1}H\}$ NMR (125MHz, $CDCl_3$) δ = 177.5, 137.3, 133.6, 129.5, 127.7, 66.4, 45.1, 31.5, 21.0; MS (ESI) exact mass calculated for $[M+Na]^+$ ($C_{11}H_{12}NaO_2$) requires *m/z* 199.1, found *m/z* 199.1.

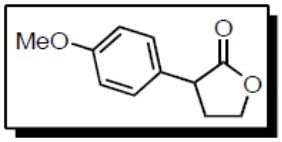

3-(4-methoxyphenyl)dihydrofuran-2(3*H*)-one

Followed general procedure from 4-methoxyphenylacetic acid on 20.0 mmol scale and purified using silica gel column chromatography to provide 2.59 g (67% yield)

of 3-(4-methoxyphenyl)dihydrofuran-2(3*H*)-one as a yellow oil. IR (neat) 2912, 2360, 1765 (s), 1514, 1247, 1147, 1024, 831, 805, 734 cm^{-1}; ^{1}H NMR (600MHz, $CDCl_3$) δ = 7.22 (d, *J* = 8.8 Hz, 2 H), 6.91 (d, *J* = 8.8 Hz, 2 H), 4.47 (dt, *J* = 3.2, 8.8 Hz, 1 H), 4.38 - 4.31 (m, 1 H), 3.81 (s, 3 H), 3.77 (d, *J* = 9.7 Hz, 1 H), 2.74 - 2.65 (m, 1 H), 2.47 - 2.37 (m, 1 H); $^{13}C\{^{1}H\}$ NMR (125MHz, $CDCl_3$) δ = 177.6, 159.0, 128.9, 128.6, 114.3, 66.4, 55.3, 44.7, 31.6; MS (ESI) exact mass calculated for $[M+Na]^+$ ($C_{11}H_{12}NaO_3$) requires *m/z* 215.1, found *m/z* 215.1.

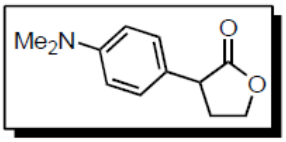

3-(4-(dimethylamino)phenyl)dihydrofuran-2(3*H*)-one

Followed general procedure from 4-(dimethylamino)phenylacetic acid on 20.0 mmol scale and purified using silica gel column chromatography to provide 2.74 g (67% yield) of 3-(4-(dimethylamino)phenyl)dihydrofuran-2(3*H*)-one as a flaky, off-white solid. IR (neat) 2921, 2803, 1757 (s), 1615, 1524, 1351, 1145, 1015, 824, 795, 691 cm^{-1}; ^{1}H NMR (600MHz, $CDCl_3$) δ = 7.16 (d, *J* = 8.5 Hz, 2 H), 6.74 (d, *J* = 8.8 Hz, 2 H), 4.46 (dt, *J* = 3.2, 8.5 Hz, 1 H), 4.36 - 4.29 (m, 1 H), 3.73 (t, *J* = 9.5 Hz, 1 H), 2.95 (s, 6 H), 2.71 - 2.63 (m, 1 H), 2.46 - 2.36 (m, 1 H); $^{13}C\{^{1}H\}$ NMR (125MHz, $CDCl_3$) δ = 178.0, 150.0, 128.4, 124.1, 112.8, 66.4, 44.5, 40.5, 31.5; MS (ESI) exact mass calculated for $[M+Na]^+$ ($C_{12}H_{15}NNaO_2$) requires *m/z* 228.1, found *m/z* 228.1.

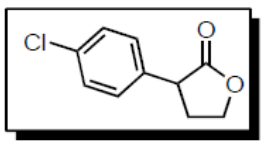

3-(4-chlorophenyl)dihydrofuran-2(3*H*)-one

Followed general procedure from 4-chlorophenylacetic acid on 20.0 mmol scale and purified using silica gel column chromatography to provide 2.23 g (57% yield) of 3-(4-chlorophenyl)dihydrofuran-2(3*H*)-one as a flaky, off-white solid. IR (neat) 2906, 1769 (s), 1494, 1372, 1220, 1156, 1086, 1018, 827, 801, 723 cm^{-1}; ^{1}H NMR (500MHz, $CDCl_3$) δ = 7.36 (d, *J* =

8.8 Hz, 23 H), 7.25 (d, *J* = 8.3 Hz, 2 H), 4.49 (dt, *J* = 2.9, 8.8 Hz, 1 H), 4.36 (dt, *J* = 6.8, 9.3 Hz, 1 H), 3.80 (t, *J* = 9.8 Hz, 1 H), 2.73 (dddd, *J* = 2.9, 6.2, 9.2, 12.4 Hz, 1 H), 2.48 - 2.37 (m, 1 H); $^{13}C\{^{1}H\}$ NMR (125MHz, $CDCl_3$) δ = 176.8, 134.9, 133.6, 129.3, 129.1, 66.4, 44.8, 31.4; MS (ESI) exact mass calculated for $[M+Na]^+$ ($C_{10}H_9ClNaO_2$) requires *m/z* 219.0, found *m/z* 219.0.

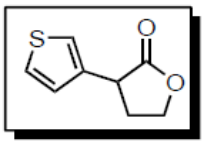

3-(thiophen-3-yl)dihydrofuran-2(3*H*)-one

Followed general procedure from 3-thiopheneacetic acid on 20.0 mmol scale and purified using silica gel column chromatography to provide 1.51 g (45% yield) of 3-(thiophen-3-yl)dihydrofuran-2(3*H*)-one as a yellow oil. IR (neat) 3104, 2911, 1761 (s), 1371, 1148 (s), 1023, 949, 840, 781 cm^{-1}; ^{1}H NMR (600MHz, $CDCl_3$) δ = 7.35 (dd, *J* = 2.9, 5.0 Hz, 1 H), 7.26 - 7.23 (m, 1 H), 7.10 (dd, *J* = 0.9, 5.0 Hz, 1 H), 4.45 (dt, *J* = 3.5, 8.5 Hz, 1 H), 4.34 (dt, *J* = 6.7, 9.1 Hz, 1 H), 3.90 (t, *J* = 9.4 Hz, 1 H), 2.76 - 2.68 (m, 1 H), 2.45 (qd, *J* = 9.2, 12.7 Hz, 1 H); $^{13}C\{^{1}H\}$ NMR (125MHz, $CDCl_3$) δ = 176.7, 136.1, 126.8, 126.4, 122.1, 66.5, 40.7, 30.6; MS (ESI) exact mass calculated for $[M+Na]^+$ ($C_8H_8NaO_2S$) requires *m/z* 191.0, found *m/z* 191.0.

Silyl Ketene Acetal Synthesis: To a 2 M solution of diisopropylamine (1.05 equiv) in THF at −78 °C was added a solution of *n*-BuLi (2.5 M in hexanes; 1.05 equiv) using a syringe. The mixture was stirred at −78 °C for 10 min, warmed to 0 °C for 5 min, and cooled to −78 °C for 10 min. A 2 M solution of lactone (1 equiv) in THF was added to the LDA solution at −78 °C using a cannula. The reaction mixture was stirred at −78 °C for 1 h, and then chlorotrimethylsilane (1.05 equiv) was added at the same temperature. The solution was warmed to room temperature and stirred for 3 h. Stirring of the solution was stopped, allowing the solid present in the reaction mixture to settle to the bottom of the reaction flask. The solution was removed from the flask

using a syringe and added to a flame-dried round-bottom flask containing a stir bar under a nitrogen atmosphere. The solvent was removed under reduced pressure to provide the crude residue. The flask containing the crude residue was fitted to a flame-dried fractional distillation apparatus under a nitrogen atmosphere, and distillation under reduced pressure provided the silyl ketene acetal product which was stored in a glove box freezer at –30 ℃.

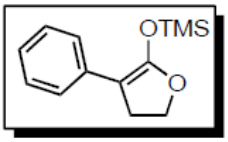

trimethyl(3-phenyl-4,5-dihydrofuran-2-yloxy)silane

Followed general procedure from 3-phenyldihydrofuran-2(3*H*)-one on 6.9 mmol scale and purified by distillation to provide 1.04 g (65% yield) of trimethyl(3-phenyl-4,5-dihydrofuran-2-yloxy)silane as a white solid. IR (neat) 1657, 1598, 1382, 1247 (s), 1120, 984, 842 (s), 753 (s), 692 cm^{-1}; ^{1}H NMR (500MHz, C_6D_6) δ = 7.60 (d, *J* = 7.8 Hz, 2 H), 7.34 (t, *J* = 7.8 Hz, 2 H), 7.05 (t, *J* = 7.3 Hz, 1 H), 3.87 (t, *J* = 9.0 Hz, 2 H), 2.59 (t, *J* = 8.8 Hz, 2 H), 0.24 (s, 9 H); $^{13}C\{^{1}H\}$ NMR (125MHz, C_6D_6) δ = 155.8, 136.9, 128.8, 124.7, 123.9, 83.2, 66.8, 30.8, 0.7.

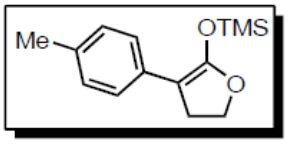

trimethyl(3-*p*-tolyl-4,5-dihydrofuran-2-yloxy)silane

Followed general procedure from 3-*p*-tolyldihydrofuran-2(3*H*)-one on 8.8 mmol scale and purified by distillation to provide 1.19 g (54% yield) of trimethyl(3-*p*-tolyl-4,5-dihydrofuran-2-yloxy)silane as a white solid. IR (neat) 1671, 1375, 1248 (s), 1149, 1097, 994, 847 (s), 811 (s), 761 cm^{-1}; ^{1}H NMR (500MHz, C_6D_6) δ = 7.55 (d, *J* = 7.8 Hz, 2 H), 7.17 (d, *J* = 7.8 Hz, 2 H), 3.89 (t, *J* = 9.0 Hz, 2 H), 2.63 (t, *J* = 8.8 Hz, 2 H), 2.21 (s, 3 H), 0.25 (s, 9 H); $^{13}C\{^{1}H\}$ NMR (125MHz, C_6D_6) δ = 155.2, 133.9, 132.9, 129.6, 124.8, 83.2, 67.0, 30.9, 21.8, 0.7.

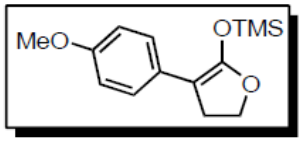

(3-(4-methoxyphenyl)-4,5-dihydrofuran-2-yloxy)trimethylsilane

Followed general procedure from 3-(4-methoxyphenyl)dihydrofuran-2(3*H*)-one on 6.6 mmol scale and purified by distillation to provide 1.09 g (62% yield) of (3-(4-methoxyphenyl)-4,5-dihydrofuran-2-yloxy)trimethylsilane as an off-white solid. IR (neat) 1668, 1514, 1243 (s), 1179, 1093, 988, 843 (s), 820 (s), 761 cm^{-1}; ^{1}H NMR (500MHz, C_6D_6) δ = 7.54 (d, *J* = 8.8 Hz, 2 H), 6.98 (d, *J* = 8.8 Hz, 2 H), 3.91 (t, *J* = 8.8 Hz, 2 H), 3.39 (s, 3 H), 2.62 (t, *J* = 8.8 Hz, 2 H), 0.26 (s, 9 H); $^{13}C\{^{1}H\}$ NMR (125MHz, C_6D_6) δ = 157.4, 154.3, 129.5, 125.8, 114.6, 83.1, 66.6, 55.2, 31.1, 0.8.

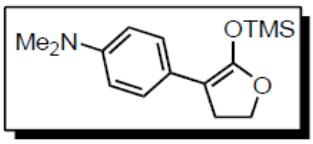

***N*,*N*-dimethyl-4-(2-(trimethylsilyloxy)-4,5-dihydrofuran-3-yl)aniline**

Followed general procedure from 3-(4-(dimethylamino)phenyl)dihydrofuran-2(3*H*)-one on 9.4 mmol scale and purified by distillation to provide 555 mg (21% yield) of *N*,*N*-dimethyl-4-(2-(trimethylsilyloxy)-4,5-dihydrofuran-3-yl)aniline as a pale-yellow solid. IR (neat) 1681, 1522, 1361, 1244 (s), 1092, 1010, 989, 843 (s), 806 (s), 757 cm^{-1}; ^{1}H NMR (600MHz, C_6D_6) δ = 7.57 (d, *J* = 8.8 Hz, 2 H), 6.80 (d, *J* = 8.8 Hz, 2 H), 3.96 (t, *J* = 8.8 Hz, 2 H), 2.71 (t, *J* = 8.8 Hz, 2 H), 2.61 (s, 6 H), 0.29 (s, 9 H); $^{13}C\{^{1}H\}$ NMR (125MHz, C_6D_6) δ = 153.7, 148.2, 128.7, 125.8, 114.0, 83.2, 66.6, 41.1, 31.4, 0.8.

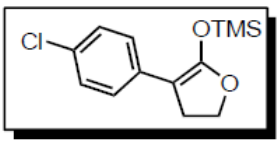

(3-(4-chlorophenyl)-4,5-dihydrofuran-2-yloxy)trimethylsilane

Followed general procedure from 3-(4-chlorophenyl)dihydrofuran-2(3*H*)-one on 10.1 mmol scale and purified by distillation to provide 1.72 g (63% yield) of (3-(4-chlorophenyl)-4,5-dihydrofuran-2-yloxy)trimethylsilane as a white solid. IR (neat) 1657, 1494,

1374, 1245 (s), 1085, 990, 846 (s), 818 (s), 758 cm^{-1}; ^{1}H NMR (500MHz, C_6D_6) δ = 7.31 (d, *J* = 6.8 Hz, 2 H), 7.28 (d, *J* = 6.8 Hz, 2 H), 3.82 (t, *J* = 8.8 Hz, 2 H), 2.43 (t, *J* = 8.8 Hz, 2 H), 0.20 (s, 9 H); $^{13}C\{^{1}H\}$ NMR (125MHz, C_6D_6) δ = 156.1, 135.3, 129.1, 129.0, 125.8, 82.4, 66.9, 30.5, 0.6.

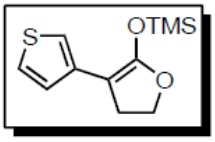

trimethyl(3-(thiophen-3-yl)-4,5-dihydrofuran-2-yloxy)silane

Followed general procedure from 3-(thiophen-3-yl)dihydrofuran-2(3*H*)-one on 11.7 mmol scale and purified by distillation to provide 913 mg (33% yield) of trimethyl(3-(thiophen-3-yl)-4,5-dihydrofuran-2-yloxy)silane as an off-white solid. IR (neat) 1679, 1325, 1248 (s), 1098, 1018, 886, 842 (s), 766 (s), 625 cm^{-1}; ^{1}H NMR (600MHz, C_6D_6) δ = 7.52 (d, *J* = 5.3 Hz, 1 H), 7.07 (dd, *J* = 3.1, 4.8 Hz, 1 H), 6.68 - 6.64 (m, 1 H), 3.90 (t, *J* = 8.9 Hz, 2 H), 2.54 (t, *J* = 8.8 Hz, 2 H), 0.22 (s, 9 H); $^{13}C\{^{1}H\}$ NMR (125MHz, C_6D_6) δ = 154.8, 137.5, 126.0, 125.4, 114.5, 81.2, 67.1, 31.1, 0.7.

1.4.5 General procedure for the synthesis of acyl fluorides[40]

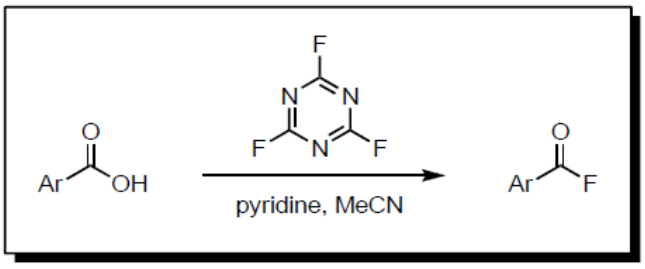

[40] Olah, G. A.; Nojima, M.; Kerekes, I. *Synthesis* **1973**, *8*, 487-488.

A flame-dried round-bottom flask was charged with a stir bar and carboxylic acid (1 equiv). Acetonitrile (25 mL) was added followed by pyridine (1 equiv). The solution was stirred at room temperature, and acetonitrile (5-75 mL) was added until a homogeneous solution formed. A 1 M solution of cyanuric fluoride (0.45 equiv; 1.35 equiv fluorine) in acetonitrile was added to the reaction mixture using a cannula and the mixture was allowed to stir at room temperature for 16 h. The reaction mixture was poured onto ice water (50 mL) and diluted with ethyl ether (50 mL). The mixture was added to a separatory funnel, the aqueous layer was removed, and the organic layer was washed with water (2 x 20 mL) and brine (20 mL). The organic layer was dried over $MgSO_4$, filtered and concentrated by rotary evaporation under reduced pressure to provide the crude residue, which was purified by silica gel chromatography to obtain the acyl fluoride product.

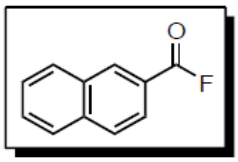

2-naphthoyl fluoride

Followed general procedure from 2-naphthoic acid on 10.0 mmol scale with the following exception: the addition of acetonitrile (100 mL) to 2-naphthoic acid and pyridine yielded a heterogeneous solution (complete dissolution did not occur) to which cyanuric fluoride was added. The general procedure was followed as described from this point. Purification using silica gel column chromatography to provide 1.10 g (63% yield) of 2-naphthoyl fluoride as a fluffy white solid. IR (neat) 1795 (s), 1596, 1262, 1184, 1129, 1042, 1010, 830, 761 cm^{-1}; ^1H NMR (600MHz, $CDCl_3$) δ = 8.66 (s, 1 H), 8.04 - 7.99 (m, 2 H), 7.97 (d, J = 8.5 Hz, 1 H), 7.94 (d, J = 8.2 Hz, 1 H), 7.70 (t, J = 7.5 Hz, 1 H), 7.62 (t, J = 7.3 Hz, 1 H); $^{13}C\{^1H\}$ NMR (125MHz, $CDCl_3$) δ = 157.6 (d, $J_{C\text{-}F}$ = 343.6 Hz), 136.4, 133.9 (d, $J_{C\text{-}F}$ = 3.1 Hz),

132.2, 129.6, 129.6, 129.0, 127.9, 127.3, 125.5 (d, $J_{C\text{-}F}$ = 4.3 Hz), 121.9 (d, $J_{C\text{-}F}$ = 61.0 Hz). MS (EI) exact mass calculated for $[M]^{+\bullet}$ ($C_{11}H_7FO$) requires *m/z* 174.0, found *m/z* 174.3.

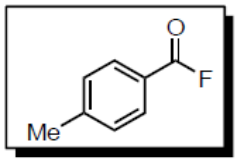

4-methylbenzoyl fluoride

Followed general procedure from 4-methylbenzoic acid on 20.0 mmol scale and purified using silica gel column chromatography to provide 1.81 g (65% yield) of 4-methylbenzoyl fluoride as a colorless oil that freezes slightly below room temperature. IR (neat) 1803 (s), 1610, 1244, 1180, 1032, 1010, 836, 740 cm^{-1}; ^1H NMR (500MHz, $CDCl_3$) δ = 7.94 (d, *J* = 7.8 Hz, 2 H), 7.33 (d, *J* = 7.8 Hz, 2 H), 2.47 (s, 3 H); $^{13}C\{^1H\}$ NMR (125MHz, $CDCl_3$) δ = 157.5 (d, $J_{C\text{-}F}$ = 342.3 Hz), 146.6, 131.4 (d, $J_{C\text{-}F}$ = 3.7 Hz), 129.7, 122.1 (d, $J_{C\text{-}F}$ = 61.4 Hz), 21.8; MS (EI) exact mass calculated for $[M]^{+\bullet}$ (C_8H_7FO) requires *m/z* 138.1, found *m/z* 138.3.

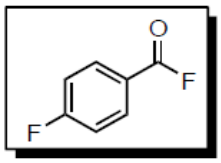

4-fluorobenzoyl fluoride

Followed general procedure from 4-fluorobenzoic acid on 20.0 mmol scale and purified using a short plug of silica gel to provide 334 mg (12% yield) of 4-fluorobenzoyl fluoride as a pale-yellow oil. Note: This compound decomposes slightly on silica gel. IR (neat) 1807 (s), 1600, 1508, 1240, 1157, 1024, 1009, 853, 756 cm^{-1}; ^1H NMR (500MHz, $CDCl_3$) δ = 8.08 (dd, *J* = 4.9, 8.3 Hz, 2 H), 7.22 (dd, *J* = 8.3, 8.5 Hz, 2 H); $^{13}C\{^1H\}$ (125MHz, $CDCl_3$) δ = 167.1 (d, $J_{C\text{-}F}$ = 259.1 Hz), 156.4 (d, $J_{C\text{-}F}$ = 343.3 Hz), 134.2 (dd, $J_{C\text{-}F}$ = 3.7, 10.1 Hz), 121.2 (d, $J_{C\text{-}F}$ = 61.3 Hz), 116.5 (d, $J_{C\text{-}F}$ = 22.0 Hz); MS (EI) exact mass calculated for $[M]^{+\bullet}$ ($C_7H_4F_2O$) requires *m/z* 142.0, found *m/z* 142.3.

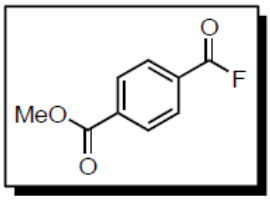

methyl 4-(fluorocarbonyl)benzoate

Followed general procedure from 4-(methoxycarbonyl)benzoic acid on 10.0 mmol scale and purified using silica gel column chromatography to provide 920 mg (51% yield) of methyl 4-(fluorocarbonyl)benzoate as a fluffy white solid. IR (neat) 1807 (s), 1715 (s), 1257, 1230, 1104, 1025, 1002, 713, 672 cm^{-1}; ^{1}H NMR (500MHz, $CDCl_3$) δ = 8.20 (d, J = 8.3 Hz, 2 H), 8.13 (d, J = 8.3 Hz, 2 H), 3.99 (s, 3 H); $^{13}C\{^{1}H\}$ NMR (125MHz, $CDCl_3$) δ = 165.6, 156.5 (d, $J_{C\text{-}F}$ = 345.5 Hz), 136.0, 131.3 (d, $J_{C\text{-}F}$ = 3.7 Hz), 130.0, 128.6 (d, $J_{C\text{-}F}$ = 61.0 Hz), 52.7. MS (EI) exact mass calculated for $[M]^{+\bullet}$ ($C_9H_7FO_3$) requires *m/z* 182.0, found *m/z* 182.3.

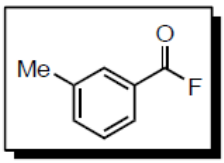

3-methylbenzoyl fluoride

Followed general procedure from 3-methylbenzoic acid on 10.0 mmol scale and purified using silica gel column chromatography to provide 776 mg (56% yield) of 3-methylbenzoyl fluoride as a colorless liquid. IR (neat) 1805 (s), 1591, 1268, 1174, 1056, 1028, 883, 730 cm^{-1}; ^{1}H NMR (500MHz, $CDCl_3$) δ = 7.90 - 7.83 (m, 2 H), 7.52 (d, J = 7.3 Hz, 1 H), 7.44 (t, J = 7.8 Hz, 1 H), 2.44 (s, 3 H); $^{13}C\{^{1}H\}$ NMR (125MHz, $CDCl_3$) δ = 157.6 (d, $J_{C\text{-}F}$ = 344.4 Hz), 139.0, 136.1, 131.9 (d, $J_{C\text{-}F}$ = 3.7 Hz), 128.9, 128.6 (d, 3.7 Hz), 124.8 (d, $J_{C\text{-}F}$ = 60.3 Hz), 21.2; MS (EI) exact mass calculated for $[M]^{+\bullet}$ (C_8H_7FO) requires *m/z* 138.1, found *m/z* 138.4.

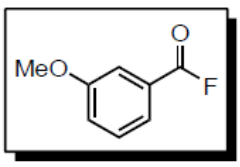

3-methoxybenzoyl fluoride

Followed general procedure from 3-methoxybenzoic acid on 10.0 mmol scale and purified using silica gel column chromatography to provide 620

mg (40% yield) of 3-methoxybenzoyl fluoride as a colorless liquid. IR (neat) 1806 (s), 1489, 1271, 1208, 1179, 1021, 869, 740 cm^{-1}; ^{1}H NMR (500MHz, $CDCl_3$) δ = 7.65 (d, J = 7.3 Hz, 1 H), 7.54 (s, 1 H), 7.44 (t, J = 8.1 Hz, 1 H), 7.25 (dd, J = 2.0, 8.3 Hz, 1 H), 3.88 (s, 3 H); $^{13}C\{^{1}H\}$ NMR (125MHz, $CDCl_3$) δ = 159.9, 157.3 (d, $J_{C\text{-}F}$ = 343.3 Hz), 130.0, 126.0 (d, $J_{C\text{-}F}$ = 62.3 Hz), 123.8 (d, $J_{C\text{-}F}$ = 3.7 Hz), 122.0, 115.5 (d, $J_{C\text{-}F}$ = 3.7 Hz), 55.5; MS (EI) exact mass calculated for $[M]^{+\bullet}$ ($C_8H_7FO_2$) requires *m/z* 154.0, found *m/z* 154.3.

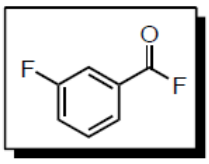

3-fluorobenzoyl fluoride

Followed general procedure from 3-fluorobenzoic acid on 20.0 mmol scale and purified using a short plug of silica gel to provide 1.57 g (55% yield) of 3-fluorobenzoyl fluoride as a colorless liquid. IR (neat) 1811 (s), 1594, 1486, 1446, 1267, 1179, 1023, 885, 739 cm^{-1}; ^{1}H NMR (500MHz, $CDCl_3$) δ = 7.87 (d, J = 7.8 Hz, 1 H), 7.74 (d, J = 8.8 Hz, 1 H), 7.53 (q, J = 6.3 Hz, 1 H), 7.43 (dt, J = 2.0, 8.3 Hz, 1 H); $^{13}C\{^{1}H\}$ NMR (125MHz, $CDCl_3$) δ = 162.6 (d, $J_{C\text{-}F}$ = 249.0 Hz), 156.2 (dd, $J_{C\text{-}F}$ = 2.7, 344.2 Hz), 130.8 (d, $J_{C\text{-}F}$ = 8.2 Hz), 127.2 (d, $J_{C\text{-}F}$ = 2.7 Hz), 127.0 (dd, $J_{C\text{-}F}$ = 7.3, 63.2 Hz), 122.6 (d, $J_{C\text{-}F}$ = 21.1 Hz), 118.1 (dd, $J_{C\text{-}F}$ = 4.6, 23.8 Hz); MS (EI) exact mass calculated for $[M]^{+\bullet}$ ($C_7H_4F_2O$) requires *m/z* 142.0, found *m/z* 142.3.

1.4.6 X-ray Crystallographic Report

with Shao-Liang Zheng

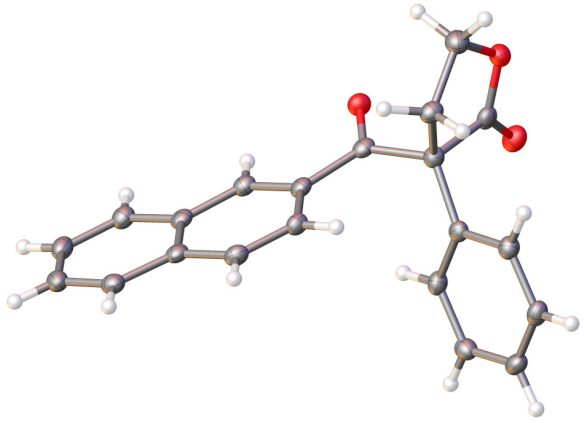

X-Ray Crystallography: A crystal mounted on a diffractometer was collected data at 100 K. The intensities of the reflections were collected by means of a Bruker APEX II DUO CCD diffractometer ($Cu_{K\alpha}$ radiation, λ=1.54178 Å), and equipped with an Oxford Cryosystems nitrogen flow apparatus. The collection method involved 1.0° scans in ω at 30°, 55°, 80° and 105° in 2θ. Data integration down to 0.84 Å resolution was carried out using SAINT V7.46 A (Bruker diffractometer, 2009) with reflection spot size optimisation. Absorption corrections were made with the program SADABS (Bruker diffractometer, 2009). The structure was solved by the direct methods procedure and refined by least-squares methods again F^2 using SHELXS-97 and SHELXL-97 (Sheldrick, 2008). Non-hydrogen atoms were refined anisotropically, and hydrogen atoms were allowed to ride on the respective atoms. Crystal data as well as details of data collection and refinement are summarized in Table 1.1 and geometric parameters are shown in Table 1.2. The Ortep plots produced with SHELXL-97 program, and the other drawings were produced with Accelrys DS Visualizer 2.0 (Accelrys, 2007).

Table 1.1 Experimental details

	JAB-B-175A
Crystal data	
Chemical formula	$C_{21}H_{16}O_3$
M_r	316.34
Crystal system, space group	Monoclinic, $P2_1$
Temperature (K)	100
a, b, c (Å)	5.7685 (3), 10.6003 (5), 12.1274 (6)
□ (°)	94.518 (2)
V (Å^3)	739.26 (6)
Z	2
Radiation type	Cu K□
□ (mm^{-1})	0.76
Crystal size (mm)	0.28 × 0.24 × 0.18
Data collection	
Diffractometer	CCD area detector diffractometer
Absorption correction	Multi-scan *SADABS*
T_{min}, T_{max}	0.815, 0.875
No. of measured, independent and observed [I > 2□(I)] reflections	17872, 2400, 2387

R_{int}	0.030
Refinement	
$R[F^2 > 2\sigma(F^2)]$, $wR(F^2)$, S	0.022, 0.056, 1.05
No. of reflections	2400
No. of parameters	218
No. of restraints	1
H-atom treatment	H-atom parameters constrained
$\Delta\rho_{max}$, $\Delta\rho_{min}$ (e Å^{-3})	0.13, -0.12
Absolute structure	Flack H D (1983), Acta Cryst. A39, 876-881
Flack parameter	-0.07 (14)

Computer programs: *APEX2* v2009.3.0 (Bruker-AXS, 2009), *SAINT* 7.46A (Bruker-AXS, 2009), *SHELXS97* (Sheldrick, 2008), *SHELXL97* (Sheldrick, 2008), Bruker *SHELXTL*.

Table 1.2. Geometric parameters (Å, º)

O1—C11	1.2200 (15)	C10—C11	1.4939 (17)
O2—C19	1.2020 (15)	C11—C12	1.5420 (17)
O3—C19	1.3354 (15)	C12—C13	1.5237 (17)
O3—C20	1.4565 (16)	C12—C19	1.5451 (17)
C1—C10	1.3737 (17)	C12—C21	1.5463 (17)
C1—C2	1.4129 (17)	C13—C14	1.3939 (17)
C1—H1	0.9500	C13—C18	1.3954 (17)

C2—C3	1.4152 (18)	C14—C15	1.3898 (19)
C2—C7	1.4274 (17)	C14—H14	0.9500
C3—C4	1.3695 (19)	C15—C16	1.3849 (18)
C3—H3	0.9500	C15—H15	0.9500
C4—C5	1.4138 (18)	C16—C17	1.3861 (19)
C4—H4	0.9500	C16—H16	0.9500
C5—C6	1.3692 (19)	C17—C18	1.3838 (18)
C5—H5	0.9500	C17—H17	0.9500
C6—C7	1.4174 (18)	C18—H18	0.9500
C6—H6	0.9500	C20—C21	1.5186 (19)
C7—C8	1.4175 (18)	C20—H20B	0.9900
C8—C9	1.3677 (18)	C20—H20A	0.9900
C8—H8	0.9500	C21—H21B	0.9900
C9—C10	1.4256 (16)	C21—H21A	0.9900
C9—H9	0.9500		
C19—O3—C20	111.12 (10)	C13—C12—C21	116.52 (10)
C10—C1—C2	121.59 (11)	C11—C12—C21	106.93 (10)
C10—C1—H1	119.2	C19—C12—C21	102.18 (10)
C2—C1—H1	119.2	C14—C13—C18	118.17 (11)
C1—C2—C3	121.71 (11)	C14—C13—C12	121.00 (11)
C1—C2—C7	118.96 (11)	C18—C13—C12	120.45 (11)

C3—C2—C7	119.32 (11)	C15—C14—C13	121.05 (11)
C4—C3—C2	120.58 (12)	C15—C14—H14	119.5
C4—C3—H3	119.7	C13—C14—H14	119.5
C2—C3—H3	119.7	C16—C15—C14	120.04 (11)
C3—C4—C5	120.11 (12)	C16—C15—H15	120.0
C3—C4—H4	119.9	C14—C15—H15	120.0
C5—C4—H4	119.9	C15—C16—C17	119.43 (12)
C6—C5—C4	120.78 (12)	C15—C16—H16	120.3
C6—C5—H5	119.6	C17—C16—H16	120.3
C4—C5—H5	119.6	C18—C17—C16	120.54 (12)
C5—C6—C7	120.48 (12)	C18—C17—H17	119.7
C5—C6—H6	119.8	C16—C17—H17	119.7
C7—C6—H6	119.8	C17—C18—C13	120.77 (12)
C6—C7—C8	122.82 (11)	C17—C18—H18	119.6
C6—C7—C2	118.72 (11)	C13—C18—H18	119.6
C8—C7—C2	118.46 (11)	O2—C19—O3	122.48 (12)
C9—C8—C7	121.36 (11)	O2—C19—C12	126.81 (12)
C9—C8—H8	119.3	O3—C19—C12	110.70 (10)
C7—C8—H8	119.3	O3—C20—C21	106.05 (10)
C8—C9—C10	120.30 (11)	O3—C20—H20B	110.5
C8—C9—H9	119.8	C21—C20—H20B	110.5
C10—C9—H9	119.8	O3—C20—H20A	110.5

C1—C10—C9	119.26 (11)	C21—C20—H20A	110.5
C1—C10—C11	117.38 (10)	H20B—C20—H20A	108.7
C9—C10—C11	123.31 (11)	C20—C21—C12	103.63 (10)
O1—C11—C10	120.29 (11)	C20—C21—H21B	111.0
O1—C11—C12	118.18 (11)	C12—C21—H21B	111.0
C10—C11—C12	121.42 (10)	C20—C21—H21A	111.0
C13—C12—C11	115.83 (10)	C12—C21—H21A	111.0
C13—C12—C19	108.52 (10)	H21B—C21—H21A	109.0
C11—C12—C19	105.47 (10)		
C10—C1—C2—C3	-179.58 (11)	C10—C11—C12—C21	-81.19 (13)
C10—C1—C2—C7	1.75 (17)	C11—C12—C13—C14	26.68 (16)
C1—C2—C3—C4	-177.77 (11)	C19—C12—C13—C14	-91.65 (13)
C7—C2—C3—C4	0.90 (17)	C21—C12—C13—C14	153.77 (11)
C2—C3—C4—C5	0.38 (18)	C11—C12—C13—C18	-160.56 (11)
C3—C4—C5—C6	-0.99 (19)	C19—C12—C13—C18	81.11 (13)
C4—C5—C6—C7	0.28 (19)	C21—C12—C13—C18	-33.47 (17)
C5—C6—C7—C8	-179.47 (12)	C18—C13—C14—C15	-0.02 (18)
C5—C6—C7—C2	0.99 (17)	C12—C13—C14—C15	172.90 (11)
C1—C2—C7—C6	177.13 (11)	C13—C14—C15—C16	-0.64 (19)
C3—C2—C7—C6	-1.57 (16)	C14—C15—C16—C17	1.08 (19)
C1—C2—C7—C8	-2.42 (16)	C15—C16—C17—C18	-0.86 (19)

C3—C2—C7—C8	178.88 (11)	C16—C17—C18—C13	0.20 (19)
C6—C7—C8—C9	-178.72 (12)	C14—C13—C18—C17	0.24 (18)
C2—C7—C8—C9	0.81 (17)	C12—C13—C18—C17	-172.72 (11)
C7—C8—C9—C10	1.53 (18)	C20—O3—C19—O2	177.38 (12)
C2—C1—C10—C9	0.57 (17)	C20—O3—C19—C12	-3.33 (14)
C2—C1—C10—C11	-177.13 (11)	C13—C12—C19—O2	43.10 (17)
C8—C9—C10—C1	-2.23 (17)	C11—C12—C19—O2	-81.61 (15)
C8—C9—C10—C11	175.32 (11)	C21—C12—C19—O2	166.75 (12)
C1—C10—C11—O1	15.25 (16)	C13—C12—C19—O3	-136.15 (10)
C9—C10—C11—O1	-162.35 (12)	C11—C12—C19—O3	99.14 (11)
C1—C10—C11—C12	-168.56 (11)	C21—C12—C19—O3	-12.50 (13)
C9—C10—C11—C12	13.84 (17)	C19—O3—C20—C21	18.31 (14)
O1—C11—C12—C13	-133.17 (12)	O3—C20—C21—C12	-25.00 (13)
C10—C11—C12—C13	50.56 (15)	C13—C12—C21—C20	140.28 (11)
O1—C11—C12—C19	-13.17 (14)	C11—C12—C21—C20	-88.35 (12)
C10—C11—C12—C19	170.56 (10)	C19—C12—C21—C20	22.19 (12)
O1—C11—C12—C21	95.08 (13)		

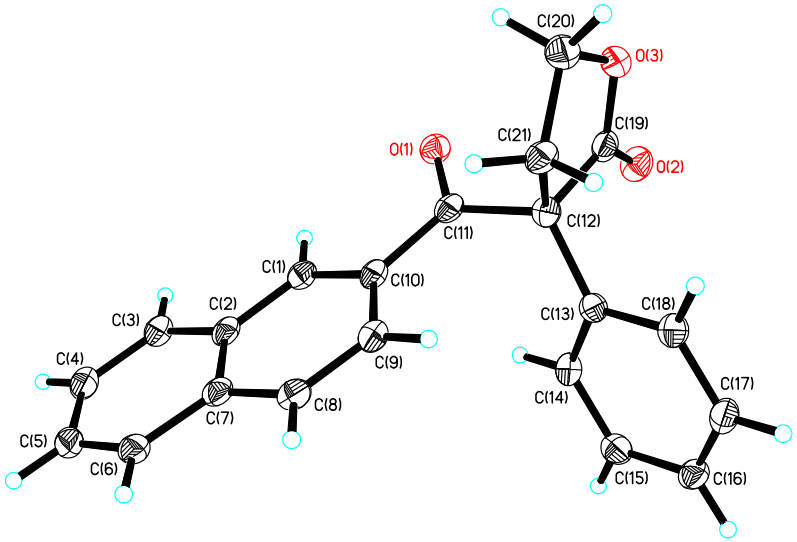

Figure 1.5 Perspective views showing 50%.

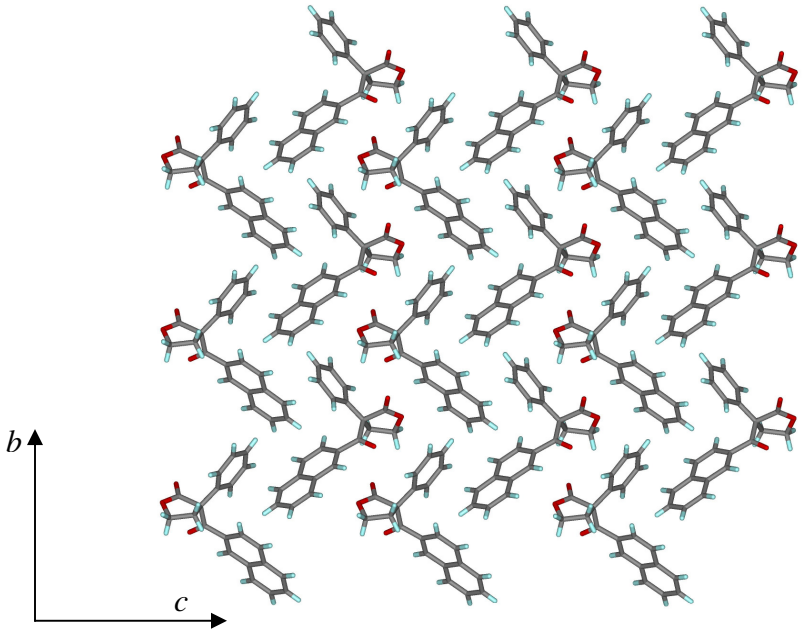

Figure 1.6 Three-dimensional supramolecular architecture viewed along the *a*-axis direction.

Chapter Two

Development of a Practical Method for the Synthesis of Highly Enantioenriched *trans*-1,2-Amino Alcohols

2.1 Introduction

2.1.1 Preparation of Enantioenriched *trans*-1,2-Amino Alcohols

Enantioenriched *trans*-1,2-amino alcohols are useful building blocks for the preparation of complex molecules and chiral catalysts as well as ligands and auxiliaries for asymmetric synthesis.[1] Three major approaches to access these compounds consist of: (1) ring-opening of *meso*-epoxides with a chiral amine and subsequent separation of the resulting diastereomers,[2] (2) resolution of racemic compounds or related precursors,[3] and (3) catalytic enantioselective opening of *meso*-epoxides with nucleophilic nitrogen species (Scheme 2.1).[4] Among these

[1] (a) Ager, D. J.; Prakash, I.; Schaad, D. R. *Chem. Rev.* **1996**, *96*, 835-876. (b) Fache, F.; Schulz, E.; Tommasino, M. L.; Lemaire, M. *Chem. Rev.* **2000**, *100*, 2159-2231. (c) Bergmeier, S. C. *Tetrahedron* **2000**, *56*, 2561-2576. (d) Anaya de Parrodi, C.; Juaristi, E. *Synlett* **2006**, 2699-2715.

[2] Overman, L. E.; Sugai, S. *J. Org. Chem.* **1985**, *50*, 4154-4155.

[3] (a) Schiffers, I.; Rantanen, T.; Schmidt, F.; Bergmans, W.; Zani, L.; Bolm, C. *J. Org. Chem.* **2006**, *71*, 2320-2331. (b) Schiffers, I.; Bolm, C. *Org. Synth.* **2008**, *85*, 106-117.

approaches, catalytic asymmetric methods are most efficient because of the opportunity to convert all of the substrate to the desired enantiomer of product and the use of substoichiometric amounts of a chiral catalyst.

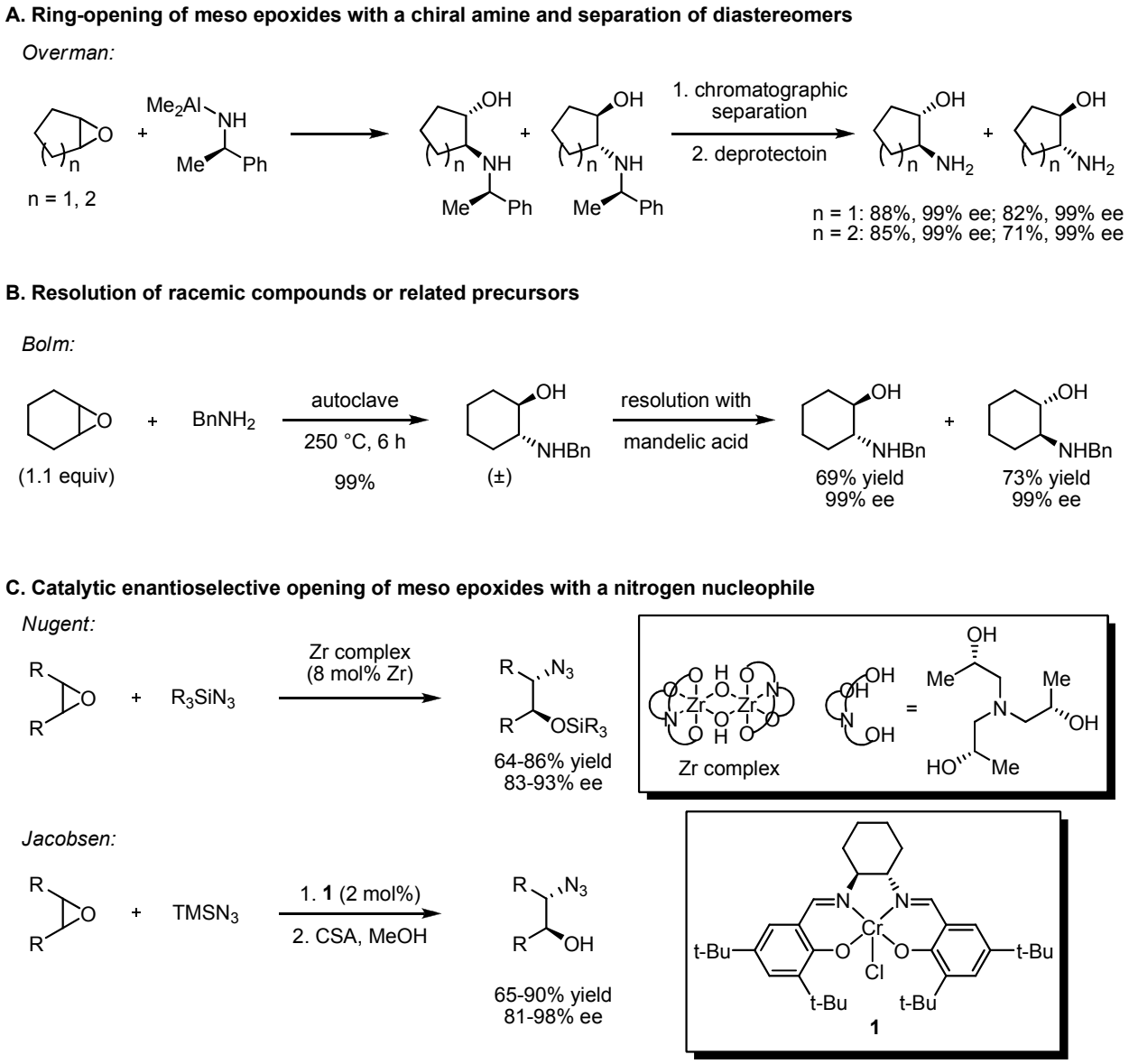

Scheme 2.1. Synthetic approaches to enantioenriched *trans*-1,2-amino alcohols

Catalytic asymmetric approaches to synthesize *trans*-1,2-amino alcohols have been developed in the context of the addition of hydrazoic acid to *meso*-epoxides.[4] Specifically,

[4] (a) Nugent, W. A. *J. Am. Chem. Soc.* **1992**, *114*, 2768-2769. (b) Martínez, L. E.; Leighton, J. L.; Carsten, D. H.; Jacobsen, E. N. *J. Am. Chem. Soc.* **1995**, *117*, 5897-5898.

Nugent reported a Zr-catalyzed azidosilylation of *meso*-epoxides, generating chiral amino alcohol precursors in good yield and enantioselectivity, and our group reported the use of (salen)Cr(III) complexes to catalyze the same transformation (Scheme 2.1C). Although these approaches to synthesize *trans*-1,2-amino alcohols are efficient, their application on a preparative scale has been limited. A chief concern in known methods is the use of hydrazoic acid as an ammonia equivalent since use of this reagent is potentially dangerous and requires special safety measures. Catalytic asymmetric addition of an alternative nitrogen nucleophile would constitute a straightforward and useful approach toward this desired class of molecules.

2.1.2 (salen)Co(III)-catalyzed Asymmetric Ring Openings with Carbamates

Bartoli has demonstrated that carbamates can be employed successfully in (salen)Co(III)-catalyzed kinetic resolutions of terminal epoxides using monomeric (salen)Co(II) complex **2**, which is oxidized to (salen)Co(III) in situ.[5] A variety of alkyl-, alkenyl-, and aryl-substituted terminal epoxides are resolved with consistently excellent selectivity of >99% enantiomeric excess and s-factors ranging from 540-3000 (Scheme 2.2). In addition, a range of substituted carbamates are shown to be competent nucleophiles for the transformation, enabling the synthesis of products with different protecting groups. In a subsequent publication, Bartoli demonstrated that the carbamate addition products can be converted to 5-substituted oxazolidinones through an intramolecular, base-promoted cyclization. Despite these reports, there are no known examples of enantioselective carbamate additions to *meso*-epoxides, which are intrinsically less reactive than terminal epoxides in (salen)Co(III)-catalyzed reactions.

[5] (a) Bartoli, G.; Bosco, M.; Carlone, A.; Locatelli, M.; Melchiorre, P.; Sambri, L. *Org. Lett.* **2004**, *6*, 3973-3975. (b) Bartoli, G.; Bosco, M.; Carlone, A.; Locatelli, M.; Melchiorre, P.; Sambri, L. *Org. Lett.* **2005**, *7*, 1983-1985.

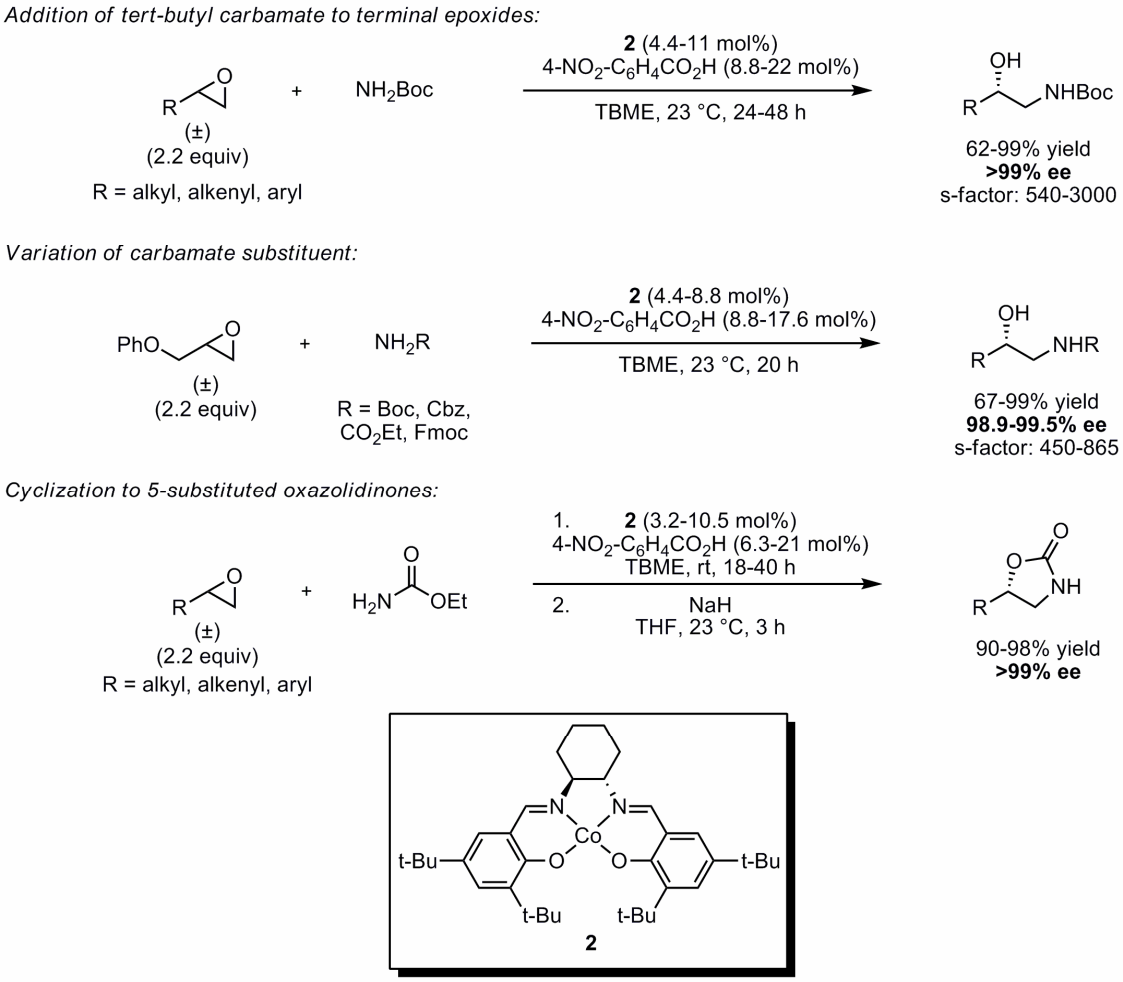

Scheme 2.2. (salen)Co(III)-catalyzed kinetic resolution of terminal epoxides with carbamates

2.1.3 Mechanism of (salen)metal-catalyzed Asymmetric Ring Openings

Bimetallic mechanisms have been established for (salen)metal-catalyzed nucleophilic ring-opening of both terminal and *meso*-epoxides.[6,7] In this mechanistic scenario, ring opening proceeds through activation of both the nucleophile and electrophile by separate catalyst molecules. This mechanistic proposal is supported by: (1) a second-order rate dependence on catalyst concentration, (2) kinetic studies that show the reaction proceeds fastest at a 1:1 molar

[6] Konsler, R. G.; Karl, J.; Jacobsen, E. N. *J. Am. Chem. Soc.* **1998**, *120*, 10780-10781.

[7] Nielsen, L. P. C.; Stevenson, C. P.; Blackmond, D. G.; Jacobsen, E. N. *J. Am. Chem. Soc.* **2004**, *126*, 1360-1362.

ratio of nucleophilic and Lewis-acidic catalyst, and (3) the observance of a positive nonlinear effect with monomeric catalyst that disappears when dimeric catalysts are used under high-dilution. Detailed analysis of the hydrolytic kinetic resolution of terminal epoxides has elucidated the representative mechanism for (salen)Co(III)-catalyzed asymmetric ring-opening reactions shown in Scheme 2.3.[8] Addition of the (salen)Co–X counteranion into a molecule of epoxide was shown to be irreversible when X = Cl, OAc and reversible when X = OTs. Protonolysis of the alkoxide addition product with a molecule of water and complexation of the resulting hydroxide with the cationic (salen)Co(III) provides the nucleophilic (salen)Co–OH species. A separate molecule of (salen)Co–X serves as a Lewis acid to activate a molecule of epoxide for addition by (salen)Co–OH in a bimolecular transition state. The addition product is then protonolyzed from the cobalt center by a molecule of water, regenerating the free Lewis-acidic (salen)Co–X species and another molecule of (salen)Co–OH.

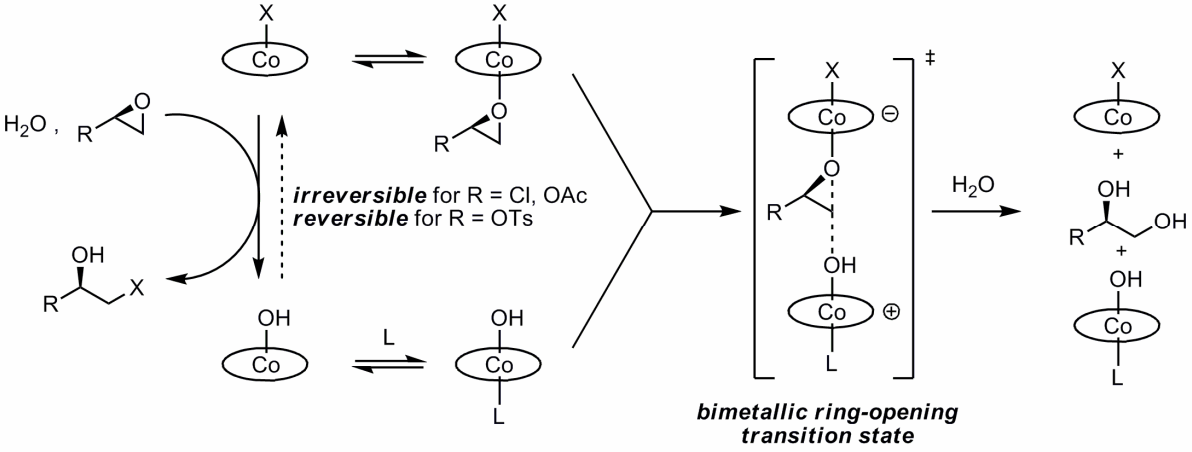

Scheme 2.3. Mechanism of (salen)Co(III)-catalyzed hydrolytic kinetic resolution of epoxides

[8] For detailed mechanistic investigations of (salen)Co(III)-catalyzed ring opening reactions, see reference 6b and: Nielsen, L. P. C.; Zuend, S. J.; Ford, D. D.; Jacobsen, E. N. *J. Org. Chem.* **2012**, *77*, 2486-2495.

2.1.4 Development of Multimeric (salen)Co(III) Catalysts

To facilitate cooperativity between the metal centers, a variety of polymer-supported, dendrimeric, and cyclic oligomeric (salen)Co(III) and (salen)Cr(III) complexes have been developed (Figure 2.1).[6,9] These multimeric complexes have been shown to display striking improvements in both rate and selectivity in relation to their monomeric equivalents.[10] Cyclic oligomeric catalysts are particularly attractive multimeric species due to their inherent symmetry. Inefficiencies in the synthesis of other classes of multimeric catalysts were encountered due to the requirement for unsymmetrical Schiff base substitution on the diamine backbone of the ligand precursors (Scheme 2.4A). The desired differentially-substituted ligands are formed as part of a statistical mixture with the corresponding symmetrically-substituted species following condensation of two different salicylaldehydes with *trans*-1,2-diaminocyclohexane. To overcome this synthetic problem, a linking strategy was developed that used a single salicylaldehyde precursor to generate a symmetrical Schiff base that was then linked to form the cyclic oligomeric ligand (Scheme 2.4B).

[9] (a) Annis, D. A.; Jacobsen, E. N. *J. Am. Chem. Soc.* **1999**, *121*, 4147-4154. (b) Breinbauer, R.; Jacobsen, E. N. *Angew. Chem., Int. Ed.* **2000**, *39*, 3604-3607. (c) Ready, J. M.; Jacobsen, E. N. *J. Am. Chem. Soc.* **2001**, *123*, 2687-2688. (d) Ready, J. M.; Jacobsen, E. N.; *Angew. Chem., Int. Ed.* **2002**, *41*, 1374-1377. (e) White, D. E.; Jacobsen, E. N. *Tetrahedron: Asymmetry* **2003**, *14*, 3633-3638. (f) White, D. E. Ph.D. Thesis, Harvard University, Cambridge, Massachusetts, 2005. (g) Zheng, X.; Jones, C. W.; Weck, M. *J. Am. Chem. Soc.* **2007**, *129*, 1105-1112. (h) Madhavan, N.; Jones, C. W.; Weck, M. *Acc. Chem. Res.* **2008**, *41*, 1153-1165. (i) Thomas, R. M.; Widger, P. C. B.; Ahmed, S. M.; Jeske, R. C.; Hirahata, W.; Lobkovsky, E. B.; Coates, G. W. *J. Am. Chem. Soc.* **2010**, *132*, 16520-16525. (j) Haak, R. M.; Wezenberg, S. J.; Kleij, A. W. *Chem. Commun.* **2010**, *46*, 2713-2723.

[10] For an example in the context of enantioselective intramolecular openings of oxetanes, see: Loy, R. N.; Jacobsen, E. N. *J. Am. Chem. Soc.* **2009**, *131*, 2786-2787.

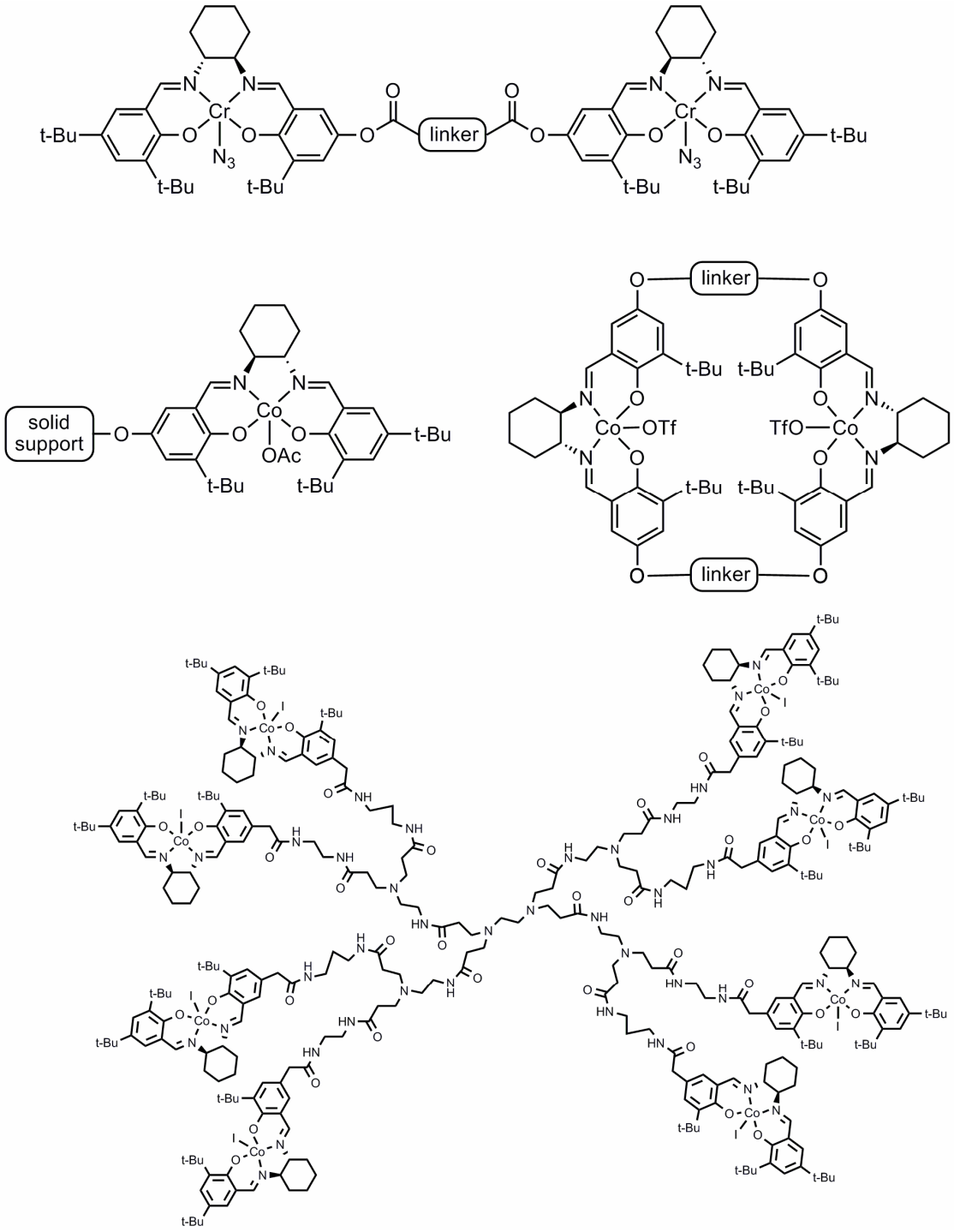

Figure 2.1. Linking strategies for multimeric (salen)Co(III) complexes

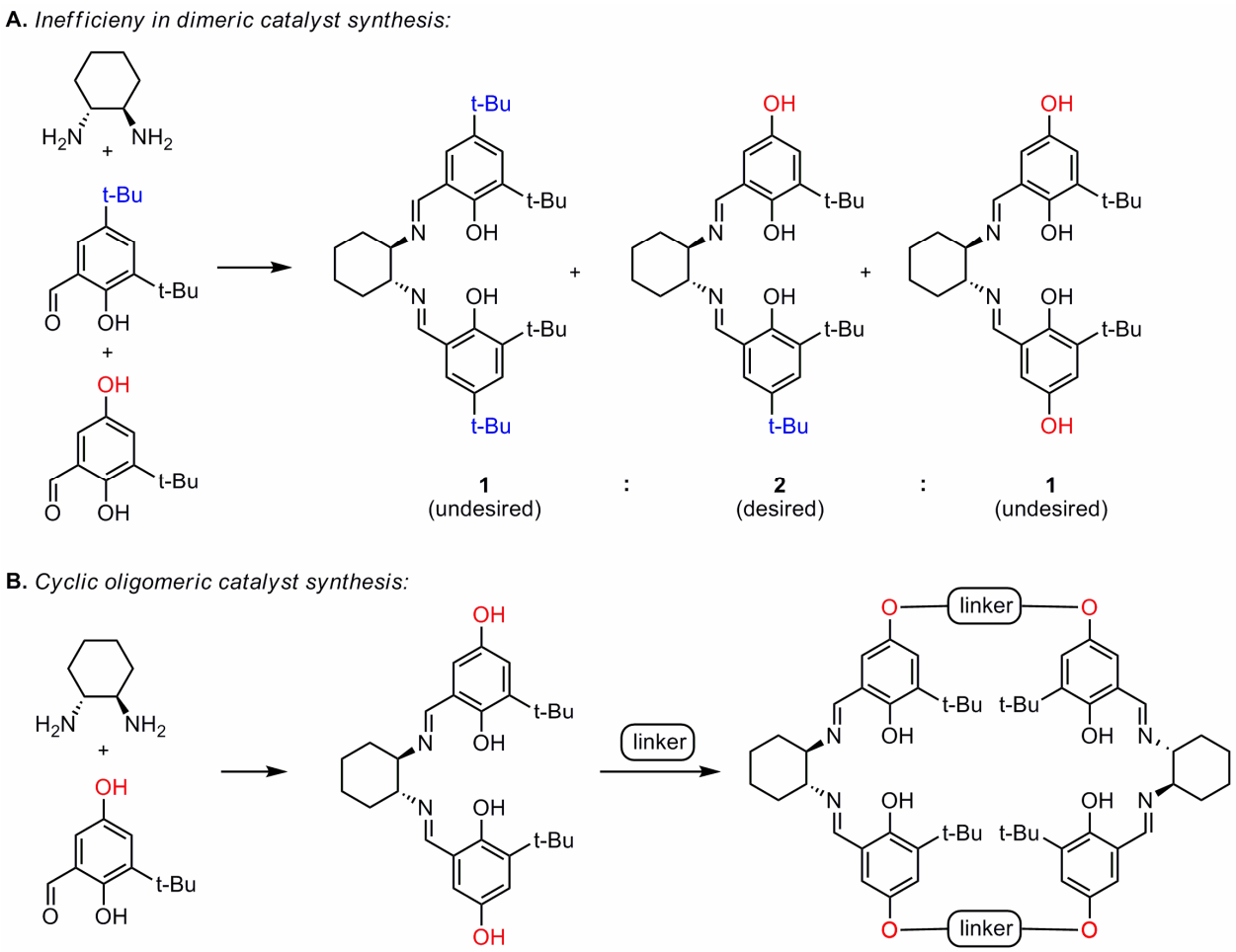

Scheme 2.4. Practical considerations in multimeric (salen)Co(III) complex synthesis

Three distinct generations of oligomeric (salen)Co(III) catalysts were developed within our group, each time with the goals of improving catalyst synthesis and effectiveness in asymmetric transformations (Figure 2.2).[11] The first-generation cyclic oligomeric catalyst (**3**) incorporated an α-chloro substituent on the linker, leading to a more Lewis-acidic metal center. Improvements in reactivity and selectivity were observed when compared with previous multimeric catalysts in a representative set of asymmetric ring-opening reactions. Although effective, this catalyst was not ideal due to a low-yielding synthesis of the α,α'-dichloropimelate

[11] For a comprehensive summary of the development and study of cyclic oligomeric (salen)Co(III) complexes, see reference 9f.

linker that also required a chromatographic purification step. In addition, analysis of **3** was difficult due to the presence of multiple sterogenic centers on the linker, causing the catalyst to be synthesized as a mixture of many diastereomers. An improved second-generation cyclic oligomeric catalyst (**4**) incorporated a highly electron-withdrawing counterion on the cobalt metal center, allowing for the removal of the chlorine substituents on the linker. This change led to a catalyst with improved performance and also simplified the synthesis of the catalyst, obviating the need for a chromatographic purification step. However, these catalysts displayed poor solubility presumably due to the large dipole between the hydrophobic linker and the polar metal center. This lack of solubility rendered the purification of these catalysts difficult and necessitated the use of solvating agents in many catalytic ring-opening reactions.

A third-generation cyclic oligomeric catalyst (**5**) incorporated an oxygen atom in the linker, reducing the overall dipole in the molecule and providing a complex with vastly improved solubility. This catalyst provided dramatic improvements in the rate and selectivity of representative asymmetric ring-opening reactions. Furthermore, a scaleable, chromatography-free synthesis of this complex was developed, enabling multi-gram quantities of **5** to be accessed in a single synthetic sequence. This highly effective catalyst has been used in the development of new methodology[10] and in complex molecule total synthesis (Scheme 2.5)[12] and remains among the premier (salen)Co(III) complexes developed to date.

[12] For applications of catalyst **5** in total synthesis, see: (a) Chae, J.; Buchwald, S. L. *J. Org. Chem.* **2004**, *69*, 3336-3339. (b) Snider, B. B.; Zhou, J. *Org. Lett.* **2006**, *8*, 1283-1286. (c) Adachi, M.; Zhang, Y.; Leimkuhler, C.; Sun, B.; LaTour, J. V.; Kahne, D. E. *J. Am. Chem. Soc.* **2006**, *128*, 14012-14013. (d) McGowan, M. A.; Stevenson, C. P.; Schiffler, M. A.; Jacobsen, E. N. *Angew. Chem., Int. Ed.* **2010**, *49*, 6147-6150. (e) Rajapaksa, N. S.; McGowan, M. A.; Rienzo, M.; Jacobsen, E. N. *Org. Lett.* **2013**, *15*, 706-709.

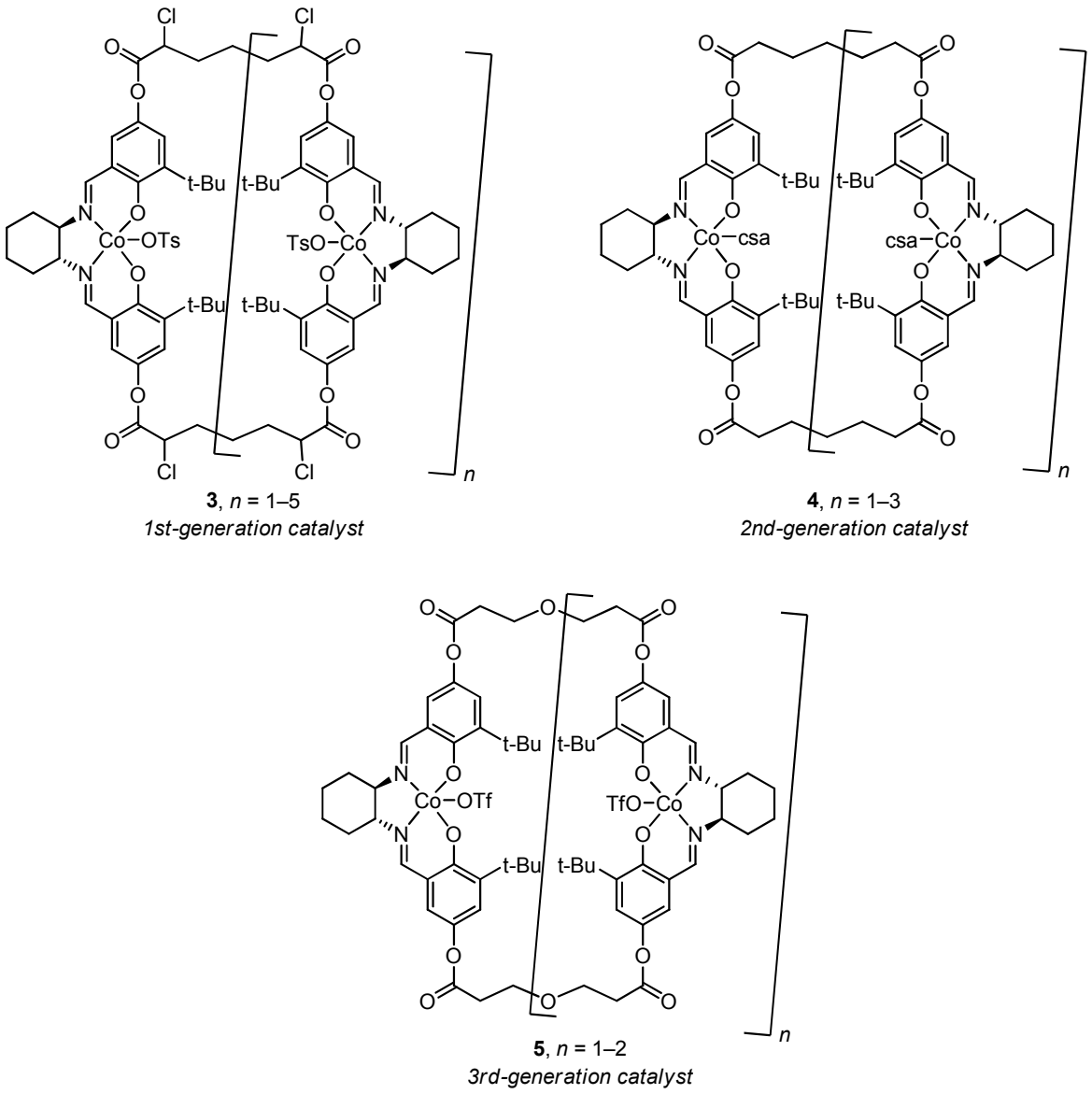

Figure 2.2. 1st-, 2nd-, and 3rd-generation cyclic oligomeric (salen)Co(III) complexes

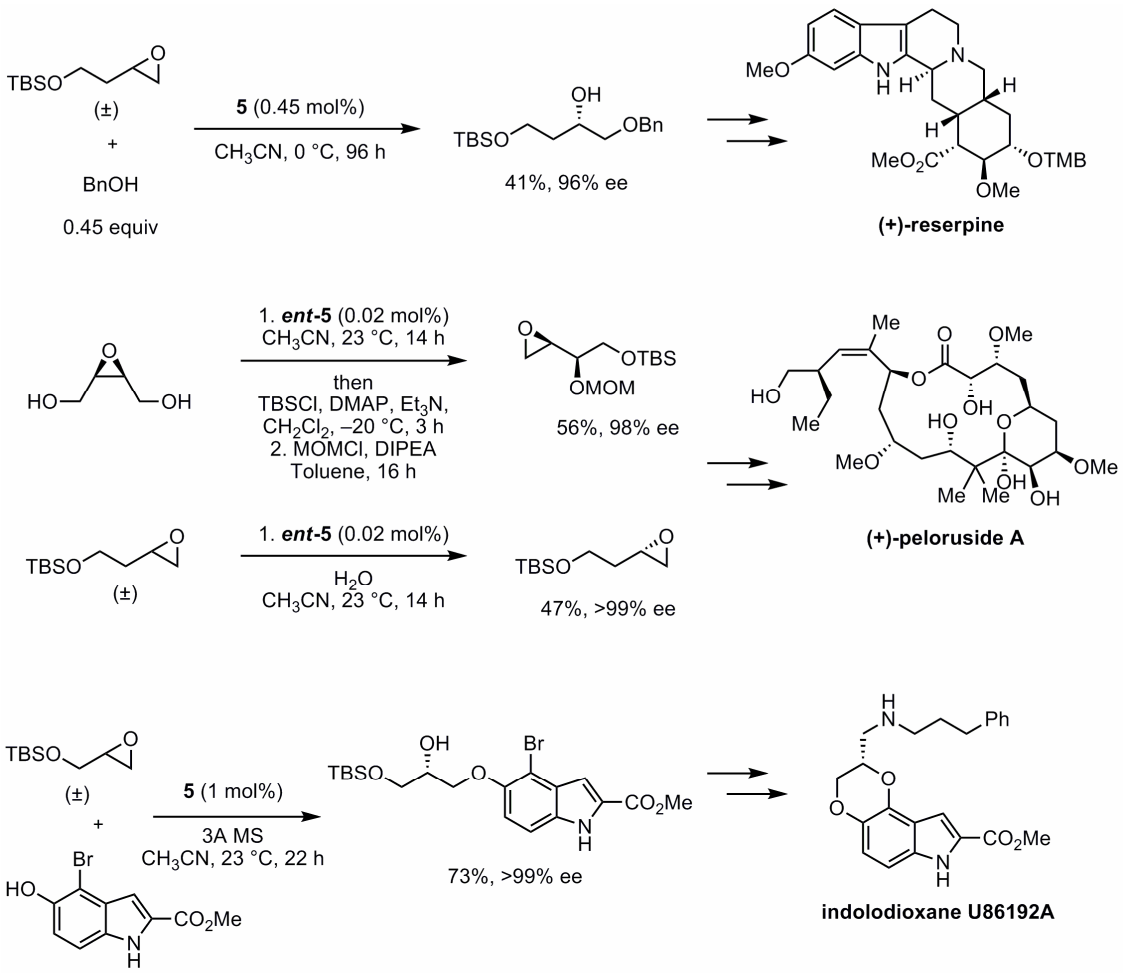

Scheme 2.5. Use of (salen)Co(III) complex **5** in complex molecule total synthesis

In preliminary studies from our group, David White found that oligomeric (salen)Co–OTf complex **5** provides a marked improvement in reactivity in the kinetic resolution of 1,2-epoxyhexane with *tert*-butyl carbamate (Scheme 2.6).[7f] For example, only 0.2 mol% of **5** was needed to effectively catalyze this reaction whereas, under similar conditions, 4.4 mol% of a related monomeric (salen)Co(III) (**2**) was required.[5a] Having established that **5** is highly effective for promoting asymmetric ring-opening reactions using carbamate nucleophiles, we sought to use this catalyst to facilitate carbamate addition to inherently less-reactive *meso*-epoxides.

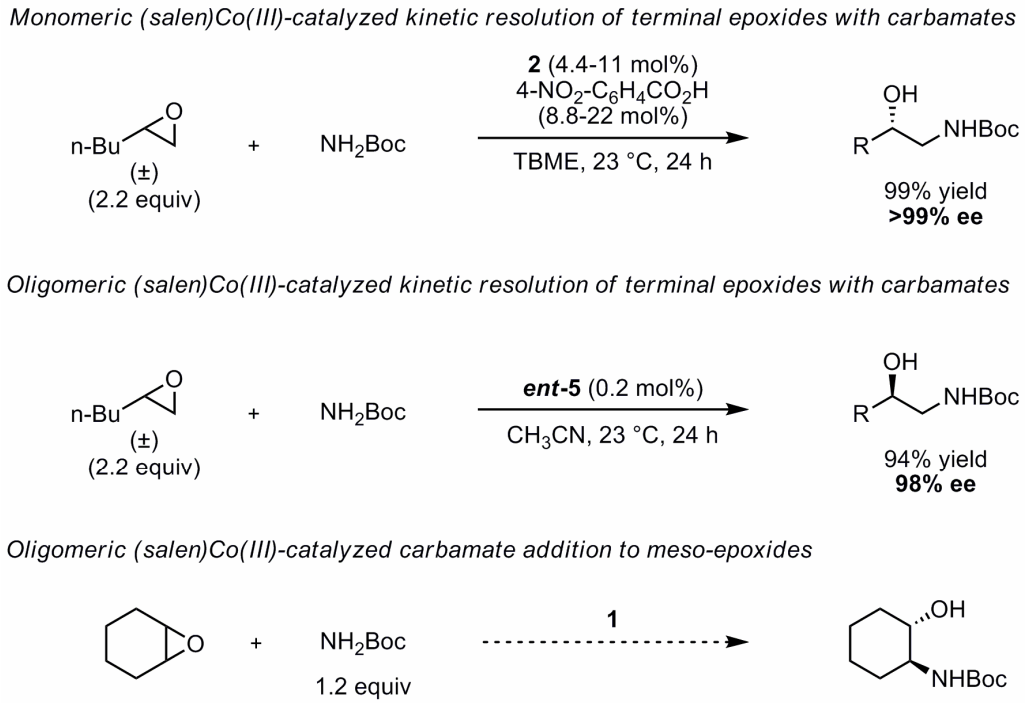

Scheme 2.6. Comparison of monomeric and oligomeric catalysts in carbamate additions

2.2 Results and Discussion

2.2.1 Lead Result and Reaction Optimization

The addition of carbamates to cyclohexene oxide was selected as a model reaction, and it was found that phenyl carbamate was particularly effective as a nucleophilic reacting partner. Clean addition to cyclohexene oxide with subsequent intramolecular cyclization occurred to afford *trans*-1,2-substituted oxazolidinone **6** (Scheme 2.7). The cyclization appears to be relatively rapid, as the initial addition intermediate is not detectable. An examination of reaction solvent identified a variety of solvents as similarly effective, with acetonitrile providing optimal results.[13] Reaction rate was increased significantly at higher concentration and temperature, with a corresponding slight drop in enantioselectivity. While both monomeric and oligomeric

[13] Effective solvents examined include acetonitrile, *tert*-butyl methyl ether, dichloromethane, toluene, and ethyl ether. The use of *N*,*N*-dimethylformamide as solvent resulted in a complete loss of reactivity.

(salen)Co–OTf complexes were found to catalyze this transformation, results were far superior with oligomeric catalyst **5**. The best balance of rate and enantioselectivity was achieved in reactions carried out at 50 ℃ in acetonitrile at high concentration, with oxazolidinone **6** obtained in 91% yield and 95% ee after 24 h.

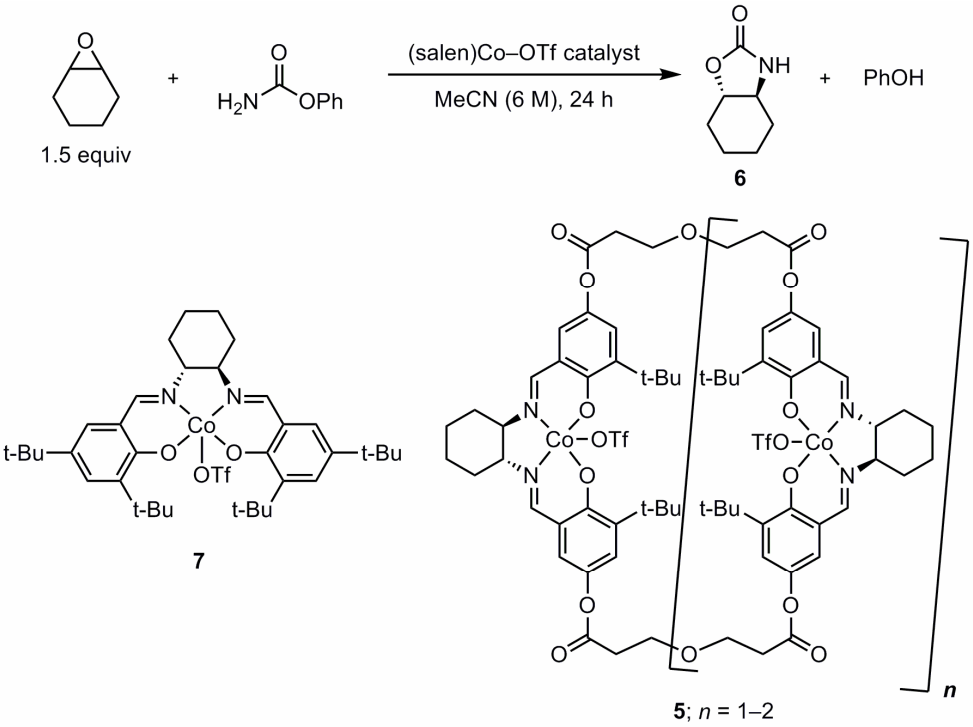

entry[a]	catalyst (mol %)	temperature	carbamate (R =)	yield[b] (%)	ee[c] (%)
1	**7** (5)	23	Ph	3	n.d.
2	**7** (5)	50	Ph	33	21
3	**5** (1)	23	Ph	21	97
4	**5** (1)	50	Ph	91	95

[a] Reactions run on a 0.5 mmol scale. [b] Yield determined by ^{1}H NMR analysis relative to *p*-xylene as an internal standard. [c] Enantiomeric excess determined by GC analysis on commercial chiral columns.

Scheme 2.7. Optimization of phenyl carbamate addition to cyclohexene oxide

Aryl carbamates are uniquely effective nucleophiles in this transformation, as *tert*-butyl carbamate, methyl carbamate, benzyl carbamate, *S*-phenyl thiocarbamate, acetamide,

trichloroacetamide, and trifluoroacetamide all proved unreactive. In addition, a correlation between reaction rate and the electronics of a series of substituted aryl carbamates was observed, with electron-deficient carbamates proceeding most rapidly (Scheme 2.8). These results point to the electronics of the nucleophile as crucially important for reaction rate, with acidity potentially being a determining factor. Electron-deficient aryl carbamates were found to decompose at appreciable rates under synthetically-relevant conditions, especially at elevated temperatures. As a result of its increased stability and commercial availability, phenyl carbamate was chosen as the optimal nucleophile for the substrate scope evaluation despite the superior rates observed with electron-deficient aryl carbamates.

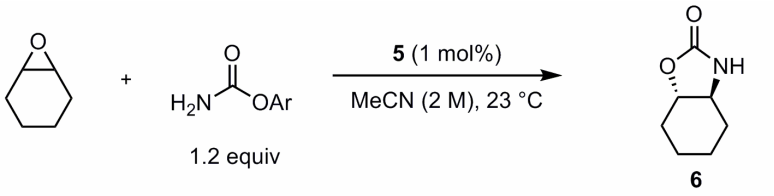

entry[a]	carbamate (Ar =)	yield[b] (%) 1 h	12 h	23 h
1	*p*-NO_2Ph	18	62	88
2	*m*-MeOPh	13	44	60
3	*p*-ClPh	8	33	46
4	Ph	4	20	30
5	*p*-MeOPh	3	11	16

[a] Reactions run on a 0.4 mmol scale. [b] Yield determined by GC analysis relative to bromobenzene as an internal standard.

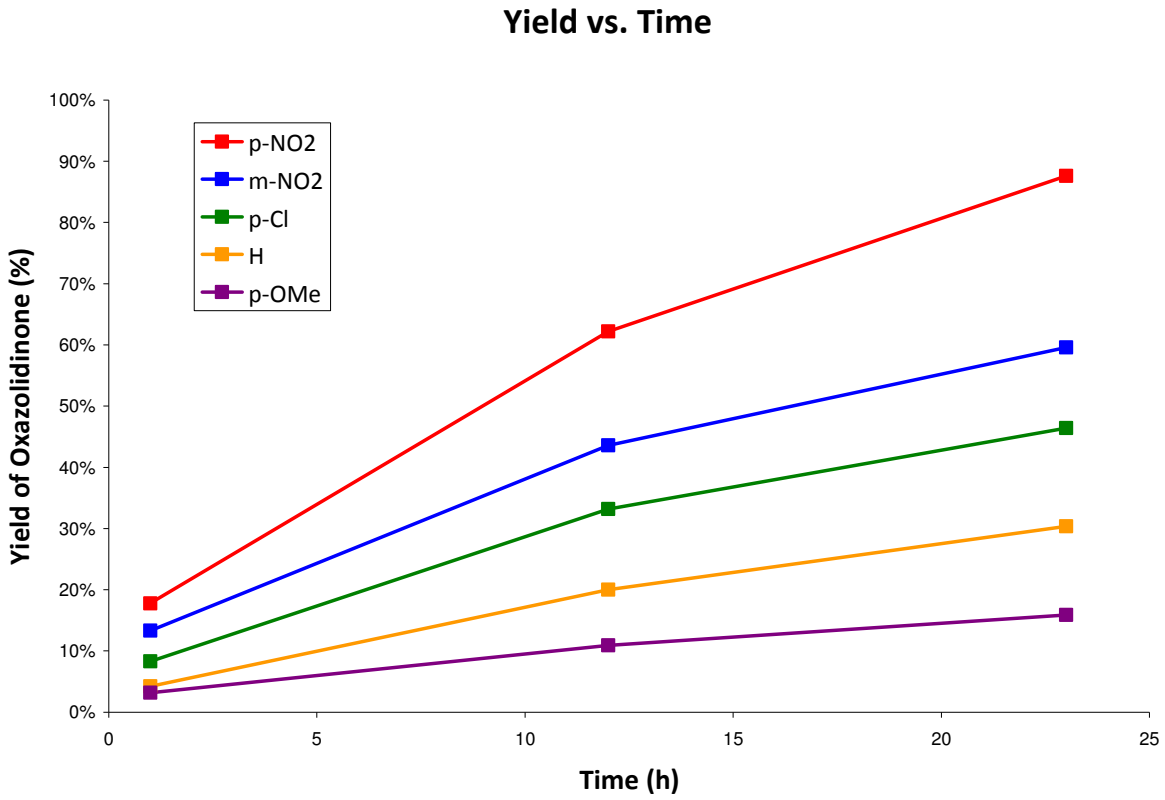

Scheme 2.8. Reaction rates of electronically-substituted carbamates

2.2.2 Substrate Scope

The addition of phenyl carbamate to a variety of *meso*-epoxides was evaluated under the optimized reaction conditions. Epoxides with unsaturation in the ring were viable substrates but proceeded with slightly lower rates than cyclohexene oxide (Scheme 2.9). Addition to cyclopentene oxide derivatives proceeds with excellent enantioselectivity, however the products from these reactions do not undergo intramolecular cyclization, presumably due to the unfavorable strain in *trans*-fused 5–5 oxazolidinone ring systems.[14] Instead intermolecular condensation of the addition products occurs to form carbamate-bridged oligomers (Scheme 2.10). In an attempt to prevent product oligomerization, phenyl *N*-(trimethylsilyl)carbamate was used as the nucleophilic species with the goal of silyl protecting the alkoxide resulting from carbamate addition to the epoxide. The use of this reagent resulted in increased levels of oligomerization, suggesting that silylation of the resulting alkoxide is slower than condensation of the addition products. Ultimately it was found that the mixture of monomeric and oligomeric products can be deprotected by treatment with base to liberate the desired *trans*-1,2-amino alcohol in high yield. Acyclic *cis*-2,3-epoxybutane underwent phenyl carbamate addition to generate **12**, although the reactivity and selectivity were poor compared with five- and six-membered ring substrates (Scheme 2.11). No conversion of epoxide was observed under the standard reaction conditions with *cis*-stilbene oxide, nitrogen-containing five-membered ring epoxides, cycloheptene oxide, cyclooctene oxide, or 2,3-epoxynorbornane.

[14] (a) Chang, S.; McNally, D.; Shary-Tehrany, S.; Hickey, M. J.; Boyd, R. H. *J. Am. Chem. Soc.* **1970**, *92*, 3109-3118. (b) Allinger, N. L.; Tribble, M. T.; Miller, M. A.; Wertz, D. H. *J. Am. Chem. Soc.* **1971**, *93*, 1637-1648.

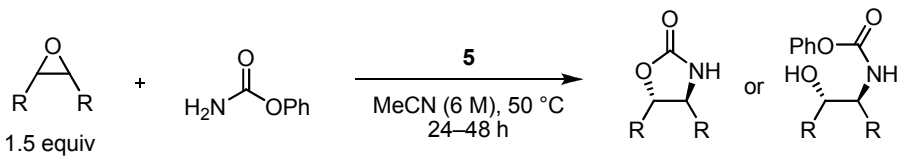

entry[a]	substrate	product	catalyst loading (mol%)	time (h)	yield[b] (%)	ee[c] (%)
1	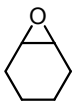	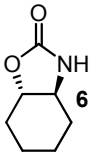 **6**	1	24	94	96
2	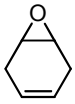	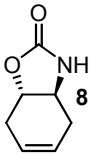 **8**	2	48	84	96
3	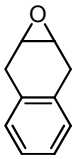	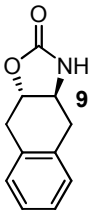 **9**	2	48	63	95
4		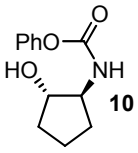 **10**	1	24	66	>99
5		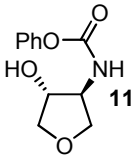 **11**	1	24	49	>99

[a] Reactions run on a 1.0 mmol scale. [b] Isolated yield of purified product. [c] Enantiomeric excess determined by GC or HPLC analysis on commercial chiral columns.

Scheme 2.9. Substrate scope of carbamate addition to *meso*-epoxides

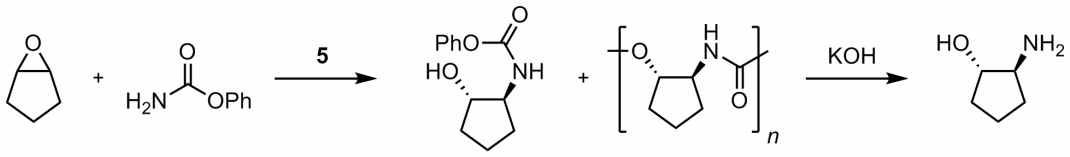

Scheme 2.10. Deprotection of monomeric and oligomeric five-membered ring addition products

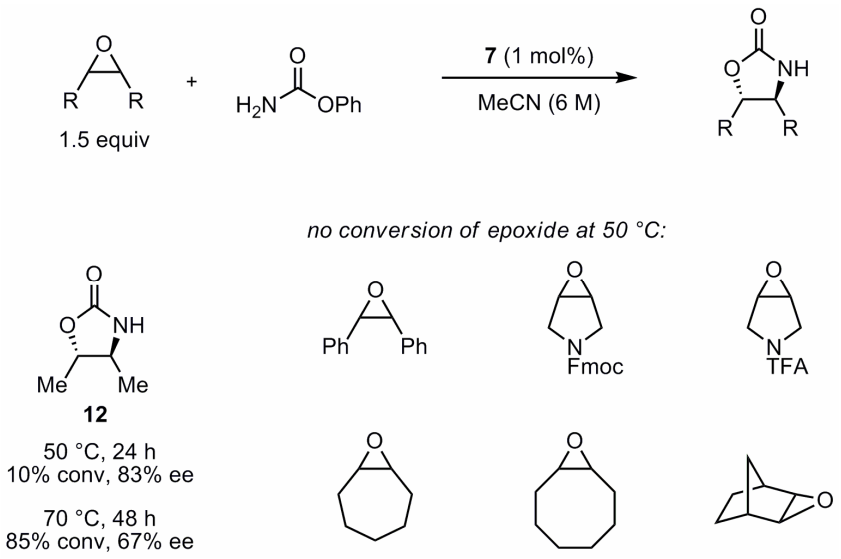

Scheme 2.11. Poorly-reactive *meso*-epoxide substrates

The synthetic utility of the carbamate addition protocol is illustrated in the preparation of *trans*-2-aminocyclohexanol hydrochloride and *trans*-2-aminocyclopentanol hydrochloride on a 0.1 mol scale using 0.5 and 1 mol% of catalyst, respectively (Scheme 2.12).[15] Following the catalytic reaction, each reaction mixture was subjected to basic deprotection conditions and recrystallized from toluene. Due to ease of storage and characterization, each amino alcohol was converted to the corresponding hydrochloride salt, providing 11.1 grams of **13** in >99% ee and 8.0 grams of **14** in >99% ee. These 2-aminocycloalkanols are versatile precursors for organic synthesis and can readily be transformed into a variety of related chiral building blocks (Scheme 2.13).[3,16]

[15] For classical resolution approaches to these compounds, see reference 3a. For an alternative method to synthesize these compounds, see reference 2.

[16] Schaus, S. E.; Larrow, J. F.; Jacobsen, E. N. *J. Org. Chem.* **1997**, *62*, 4197-4199.

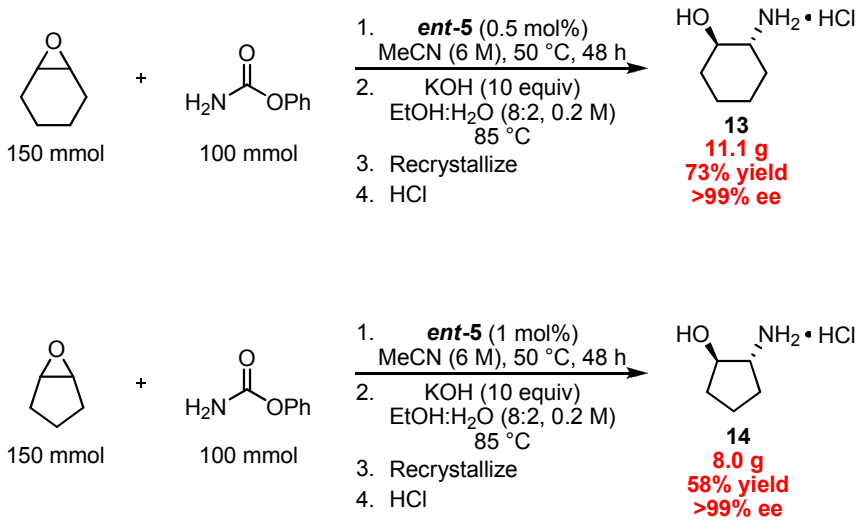

Scheme 2.12. Preparative-scale synthesis of 2-aminocycloalkanol hydrochlorides

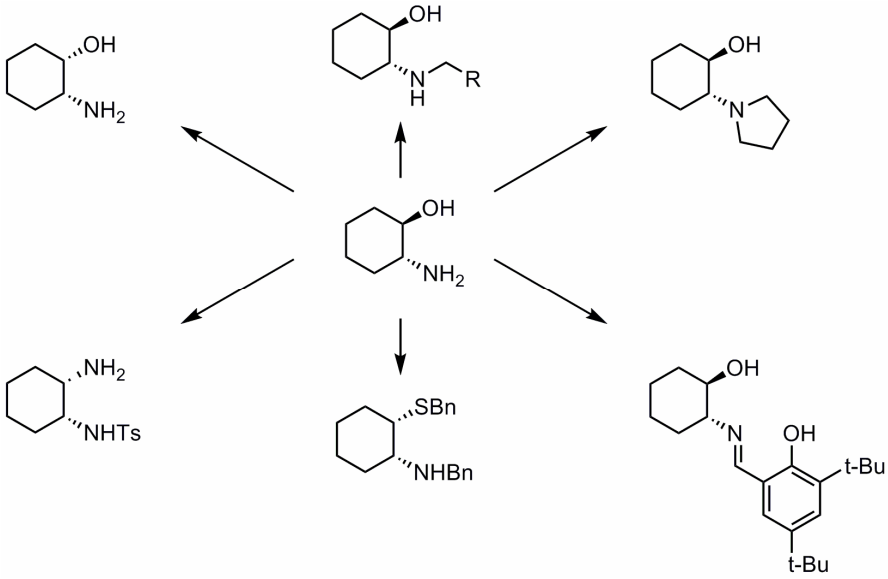

Scheme 2.13. Representative synthetic manipulations of cyclic *trans*-1,2-amino alcohols

2.3 Conclusions and Outlook

We have developed an efficient protocol for the catalytic enantioselective synthesis of protected *trans*-1,2-amino alcohols in high yield and enantiomeric excess. Crucial to this development was the use of oligomeric salen(Co)–OTf complex **5** as the catalyst and aryl carbamate nucleophiles. This method is amenable to large-scale synthesis due to the low catalyst

loadings and high concentrations used, its operational simplicity, and the use of inexpensive, commercially-available starting materials. The synthetic utility of this protocol was demonstrated in the synthesis of two representative amino alcohol building blocks, **13** and **14** in enantiomerically pure form on a multi-gram scale. We hope this method will be amenable to commercial production of these important amino alcohol products. The use of recyclable multimeric (salen)Co(III) catalysts would increase the practicality and lower the cost of this method on an industrial scale and should be the focus of future research.

2.4 Experimental

2.4.1 General information

All reactions were performed in vials or round-bottom flasks under ambient atmosphere unless otherwise noted. Stainless steel syringes were used to transfer air- and moisture-sensitive liquids. Column chromatography was performed on a Biotage Isolera automated purification system using silica gel 60 (230-400 mesh) from EM Science. Commercial reagents were purchased from Sigma Aldrich, TCI, Alfa Aesar, EMD, Silicycle, or Lancaster and used as received with the following exceptions: acetonitrile and dichloromethane were dried by passing through columns of activated alumina; pyridine was distilled from CaH_2 at 760 torr; phenyl carbamate was recrystalized from ethanol. Proton nuclear magnetic resonance (^{1}H NMR) and carbon nuclear magnetic resonance (^{13}C NMR) spectra were recorded on an Inova-500 (500 MHz) spectrometer. Proton and carbon chemical shifts are reported in parts per million downfield from tetramethylsilane and are referenced to residual protium in the NMR solvent ($CHCl_3$ = δ 7.27; CH_3OH = δ 3.31) or the carbon resonances of the NMR solvent ($CDCl_3$ = δ 77.0; CD_3OD = δ 49.15), respectively. NMR data are represented as follows: chemical shift,

multiplicity (br. = broad, s = singlet, d = doublet, t = triplet, q = quartet, m = multiplet), coupling constant in Hertz (Hz), integration. Infrared (IR) spectra were obtained using a Bruker Optics Tensor 27 FTIR spectrometer. Optical rotations were measured using a 1 mL cell with a 0.5 dm path length on a Jasco DIP 370 digital polarimeter. Mass spectroscopic (MS) data were obtained using an Agilent 6120 Single Quadrupole LC/MS instrument equipped with an ESI-APCI multimode source. Gas chromatography (GC) analysis was performed using an Agilent 7890A gas chromatograph with commercially available CycloSil and Chiraldex columns. High-performance liquid chromatography (HPLC) analysis was performed using an Agilent 1200 series quaternary HPLC system with commercially available ChiralPak and ChiralCel columns.

2.4.2 Preparation of (salen)Co–OTf catalysts

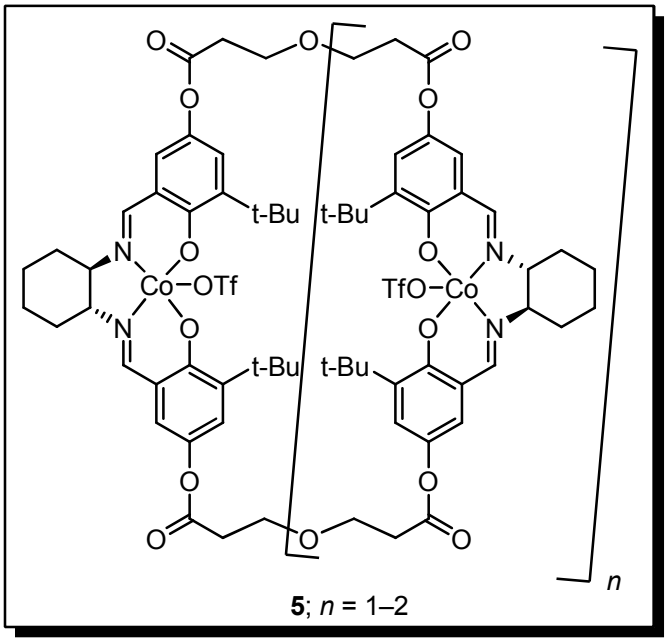

5; *n* = 1–2

Catalyst **5** was prepared according to a published procedure[9e-f]

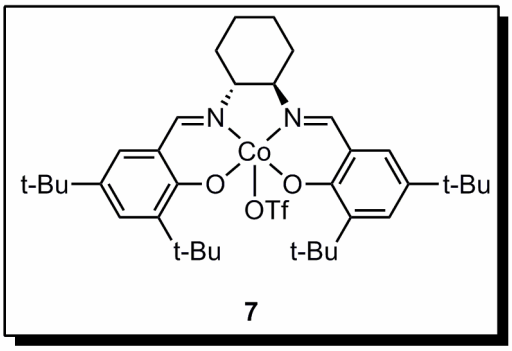

7

Catalyst **7** was prepared according to a published procedure[10]

2.4.3. Preparation of non-purchased epoxides

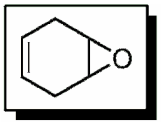

7-oxabicyclo[4.1.0]hept-3-ene

7-oxabicyclo[4.1.0]hept-3-ene was prepared according to a published procedure[9f,17]

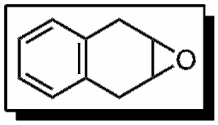

1a,2,7,7a-tetrahydronaphtho[2,3-b]oxirene

An oven-dried round-bottom flask was charged with a stir bar and 1,4-dihydronaphthalene (3.96 mL, 30.0 mmol, 1 equiv). CH_2Cl_2 (60 mL) was added, and the solution was cooled to 0 ℃. 3-Chloroperbenzoic acid (77% purity, 8.76 g, 39.0 mmol, 1.3 equiv) was added in one portion, and the reaction mixture was allowed to warm to room temperature with stirring for 24 h. The reaction was filtered to remove precipitated 3-chlorobenzoic acid, and the filtrate was washed

[17] Costero, A. M.; Rodriguez, S. *Tetrahedron* **1992**, *48*, 6265-6272.

with saturated $NaHCO_3$ (100 mL), 1 M Na_2SO_3, (100 mL), saturated $NaHCO_3$ (100 mL), and brine (100 mL), respectively. After drying over Na_2SO_4, solvent was removed by rotary evaporation. The crude product was purified using silica gel column chromatography, eluting with ethyl acetate/hexanes, to provide 2.60 g (17.8 mmol, 59% yield) of pure 1a,2,7,7a-tetrahydronaphtho[2,3-b]oxirene as a white solid. ^{1}H NMR (500 MHz, $CDCl_3$) δ = 7.19 - 7.13 (m, 2 H), 7.09 - 7.04 (m, 2 H), 3.49 (s, 2 H), 3.32 (d, *J* = 17.6 Hz, 2 H), 3.21 (d, *J* = 17.6 Hz, 2 H).

2.4.4 General procedures for carbamate addition to *meso*-epoxides

Method A (reaction optimization): A half-dram vial equipped with a screw-top cap was charged with a stir bar and either monomeric catalyst **7** (18.8 mg, 25.0 μmol, 0.05 equiv) or oligomeric catalyst **5** (4.1 mg, 5.0 μmol, 0.01 equiv). Cyclohexene oxide (75.9 μL, 0.75 mmol, 1.5 equiv) was added to the vial followed by MeCN (83 μL) and either phenyl carbamate (68.5 mg, 0.5 mmol, 1 equiv) or *tert*-butyl carbamate (58.5 mg, 0.5 mmol, 1 equiv). The vial cap was wrapped with Parafilm, and the reaction mixture was allowed to stir at the appropriate temperature for 24 h. The solution was passed through a short pad of silica gel into a 100 mL round-bottom flask, eluting with ethyl ether (70 mL). The solution was concentrated by rotary evaporation under reduced pressure to provide the crude residue. The yield of oxazolidinone product was obtained by analysis of the crude ^{1}H NMR spectrum using *p*-xylene as an internal standard. Purification by silica gel column chromatography then provided pure oxazolidinone product. The enantiomeric excess of the product was determined by GC analysis on a CycloSil-β column (150 °C isothermal, 7 psi).

Method B (substrate scope): A half-dram vial equipped with a screw-top cap was charged with a stir bar and oligomeric catalyst **7**. Epoxide was added to the vial followed by MeCN (167 μL) and phenyl carbamate (137 mg, 1.00 mmol, 1 equiv). The vial cap was wrapped with Parafilm, and the reaction mixture was allowed to stir at 50 °C for the specified reaction time. The solution was allowed to cool to room temperature. In selected cases (substrates **6**, **8**, and **9**), the solution was treated with cobalt scavenger Si-Triamine (6 equiv relative to cobalt catalyst) and 200 μL CH_2Cl_2 and stirred for 1 h. The reaction mixture was passed through a short pad of silica gel into a 100 mL round-bottom flask, eluting with ethyl ether (70 mL). The solution was concentrated by rotary evaporation under reduced pressure to provide the crude residue which was purified by silica gel column chromatography, eluting with ethyl ether/hexanes. The isolated yield of pure product was obtained, and the enantiomeric excess of the product was determined by GC or HPLC analysis on commercial chiral columns.

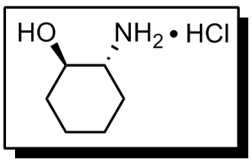

Method C (preparative-scale synthesis of (1*R*,2*R*)-2-aminocyclohexanol hydrochloride): A 200 mL round-bottom flask was charged with a stir bar and oligomeric catalyst **5** (409 mg, 0.50 mmol, 0.005 equiv). Cyclohexene oxide (15.2 mL, 150 mmol, 1.5 equiv) was added to the flask, followed by MeCN (16.7 mL) and phenyl carbamate (13.7 g, 100 mmol, 1 equiv). The flask was sealed with a plastic cap and wrapped with Parafilm. The reaction mixture was heated to 50 °C and allowed to stir at this temperature for 48 h at which point the solution was cooled to room temperature. Si-Triamine (2.33 g, 6 equiv relative to cobalt catalyst) and 100 mL CH_2Cl_2 were added, and the reaction mixture was allowed to stir for 1 h. The

reaction mixture was passed through a pad of silica gel, eluting with ether (1 L). The solution was concentrated by rotary evaporation and high vacuum. Full conversion of the phenyl carbamate starting material was observed by ^{1}H NMR, and the oxazolidinone was measured to be 97 % ee by GC analysis. To the crude reaction mixture was added ethanol:water (8:2, 500 mL), and the flask was placed in a water bath. KOH (56.1 g, 1.00 mol, 10 equiv) was added portion-wise over the course of 1 min. The flask was equipped with a reflux condenser and heated to 85 °C for 20 h. The reaction mixture was allowed to cool to room temperature, and the ethanol was removed by rotary evaporation under reduced pressure at 36 °C. The resulting aqueous solution was transferred to a separatory funnel, 200 mL of 10% aqueous KOH was added, and the aqueous layer was extracted with CH_2Cl_2 (3 x 300 mL). The combined organic extracts were dried over K_2CO_3, filtered over Celite, and concentrated by rotary evaporation and high vacuum. The crude amino alcohol was recrystallized by dissolving the solid in hot toluene (60 mL) and letting the solution cool to room temperature then 4 °C.[16] The resulting solid was collected by vacuum filtration, rinsing with cold toluene (3 x 4 mL) to provide 8.67 g (75.3 mmol) of pure amino alcohol. The amino alcohol was converted to the corresponding hydrochloride salt by adding CH_2Cl_2 (120 mL) followed by 2 M HCl in ether (150 mL, 300 mmol, 3 equiv) and hexanes (100 mL). A solid precipitate formed and was collected by vacuum filtration, rinsing the flask and washing the solid with hexanes (3 x 30 mL). The solid was transferred back to the original flask, using methanol to aid in the transfer, and concentrated to provide 11.1 g (72.9 mmol, 72.9% yield) of (1*R*,2*R*)-2-aminocyclohexanol hydrochloride as a tan solid. The material was determined to be >99% ee by HPLC analysis of the 2,4-dinitroaniline derivative of the free amino alcohol, which was obtained by reaction of 2-aminocyclohexanol

hydrochloride with Sanger's reagent and $NaHCO_3$ in DMF (ChiralCel OD-H, 25% IPA/hexanes, 1 mL/min, 254 nm). ^1H and ^{13}C NMR spectra are consistent with previously reported data.[16]

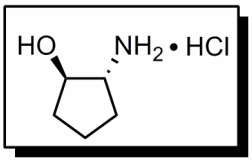

Method D (preparative-scale synthesis of (1*R*,2*R*)-2-aminocyclopentanol hydrochloride): A 1 L round-bottom flask was charged with a stir bar and oligomeric catalyst **3** (817 mg, 1.00 mmol, 0.01 equiv). Cyclopentene oxide (13.1 mL, 150 mmol, 1.5 equiv) was added to the flask, followed by MeCN (16.7 mL) and phenyl carbamate (13.7 g, 100 mmol, 1 equiv). The flask was sealed with a plastic cap and wrapped with Parafilm. The reaction mixture was heated to 50 °C and allowed to stir at this temperature for 48 h. The plastic cap was removed, and ethanol:water (8:2, 500 mL) and KOH (56.1 g, 1 mol, 10 equiv) were added. The flask was equipped with a reflux condenser and heated to 85 °C for 20 h. The reaction mixture was allowed to cool to room temperature, and the ethanol was removed by rotary evaporation under reduced pressure at 36 °C. 50% aqueous KOH (200 mL) was added, and the solution was transferred to a separatory funnel. The aqueous layer was extracted with CH_2Cl_2 (3 x 300 mL). The combined organic extracts were dried over K_2CO_3, filtered over Celite, and concentrated by rotary evaporation. To purify the crude amino alcohol, the corresponding hydrochloride salt was generated by adding toluene (10 mL) and 2 M HCl in ether (150 mL, 300 mmol, 3 equiv). A solid precipitate formed and was collected by vacuum filtration, rinsing the flask and washing the solid with hexanes (3 x 30 mL). The solid was transferred back to the original flask, using methanol to aid in the transfer, and concentrated to provide 13.8 g (100 mmol, 100% yield) of material that was ~97% pure by ^1H NMR. The free amino alcohol was obtained as a viscous brown oil by adding 50% aqueous KOH (100 mL), transferring the solution to a separatory

funnel, and extracting the mixture with CH_2Cl_2 (3 x 250 mL). The amino alcohol was recrystallized by dissolving the solid in hot toluene (30 mL), concentrating the solution to approximately 30 mL total volume and letting the solution cool to 4 °C then –30 °C.[16] The resulting solid was removed from the –30 °C freezer and collected quickly by vacuum filtration,[18] rinsing with cold toluene (3 x 4 mL). The solid was transferred back to the original flask, using CH_2Cl_2 to aid in the transfer and concentrated. The pure amino alcohol was converted to the corresponding hydrochloride salt by adding CH_2Cl_2 (90 mL) followed by 2 M HCl in ether (110 mL, 220 mmol, 2.2 equiv) and hexanes (90 mL). A solid precipitate formed and was collected by vacuum filtration, rinsing the flask and washing the solid with hexanes (3 x 25 mL). The solid was transferred back to the original flask, using methanol to aid in the transfer, and concentrated to provide 8.00 g (58.1 mmol, 58.1% yield) of (1*R*,2*R*)-2-aminocyclopentanol hydrochloride as a tan solid. The material was determined to be >99% ee by GC analysis of the *N*,*O*-bis-trifluoroacetyl derivative of the free amino alcohol, which was obtained by treatment of 2-aminocyclopentanol with TFAA and pyridine in CH_2Cl_2 (γ-TA, 100 °C isothermal, 7 psi). ^1H and ^{13}C NMR spectra are consistent with previously reported data.[16]

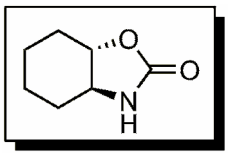

(3a*S*,7a*S*)-hexahydrobenzo[d]oxazol-2(3H)-one (6)

Followed method B using cyclohexene oxide (152 μL, 1.50 mmol, 1.5 equiv) and oligomeric catalyst **3** (8.2 mg, 0.01 mmol, 0.01 equiv) for 24 h. The reaction mixture was treated with cobalt scavenger Si-Triamine (47 mg, 6 equiv relative to cobalt catalyst) and 200 μL CH_2Cl_2 and stirred

[18] The solid was observed to melt slowly at room temperature, which is why the filtration was performed quickly using the cold solid.

for 1 h prior to further workup. The product was purified using silica gel column chromatography to provide 132 mg (0.936 mmol, 94% yield) of (3a*S*,7a*S*)-hexahydrobenzo[d]oxazol-2(3H)-one (**6**) as a white solid. This material was determined to be 96.2% ee by GC analysis (CycloSil-β, 150 °C isothermal, 7 psi), t_R(major) = 94.84 min, t_R(minor) = 101.7 min). IR (neat) 3278, 2939, 2873, 1742 (s), 1722 (s), 1382, 1247, 1229, 1118, 1030, 949, 933 cm^{-1}; ^1H NMR (500 MHz, $CDCl_3$) δ = 5.44 (br. s., 1 H), 3.89 (dt, *J* = 3.7, 11.4 Hz, 1 H), 3.32 (dt, *J* = 2.9, 11.0 Hz, 1 H), 2.25 - 2.15 (m, 1 H), 2.11 - 2.01 (m, 1 H), 1.98 - 1.88 (m, 1 H), 1.86 - 1.77 (m, 1 H), 1.66 (dq, *J* = 4.2, 12.0 Hz, 1 H), 1.53 - 1.28 (m, 3 H); $^{13}C\{^1H\}$ NMR (125 MHz, $CDCl_3$) δ = 160.7, 83.8, 60.9, 29.1, 28.5, 23.7, 23.5; MS (ESI-APCI) exact mass calculated for $[M+H]^+$ ($C_7H_{12}NO_2$) requires *m/z* 142.1, found *m/z* 142.2; $[\alpha]_D^{23}$ = +6.8 (c = 1.0, $CHCl_3$).

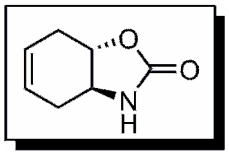

(3a*S*,7a*S*)-3a,4,7,7a-tetrahydrobenzo[d]oxazol-2(3H)-one (8)

Followed method B using 7-oxabicyclo[4.1.0]hept-3-ene (144 mg, 1.50 mmol, 1.5 equiv) and oligomeric catalyst **3** (16.3 mg, 0.02 mmol, 0.02 equiv) for 48 h. The reaction mixture was treated with cobalt scavenger Si-Triamine (94 mg, 6 equiv relative to cobalt catalyst) and 200 μL CH_2Cl_2 and stirred for 1 h prior to further workup. The product was purified using silica gel column chromatography to provide 116.4 mg (0.837 mmol, 84% yield) of (3a*S*,7a*S*)-3a,4,7,7a-tetrahydrobenzo[d]oxazol-2(3H)-one (**8**) as a white solid. This material was determined to be 96.1% ee by GC analysis (CycloSil-β, 140 °C isothermal, 7 psi), t_R(major) = 146.3 min, t_R(minor) = 154.8 min). IR (neat) 3283, 1736 (s), 1720 (s), 1373, 1317, 1236, 1147, 1124, 1026, 978, 948, 817 cm^{-1}; ^1H NMR (500 MHz, $CDCl_3$) δ = 5.82 (br. s., 1 H), 5.74 - 5.63 (m, 2 H), 4.15

(dt, *J* = 5.4, 11.0 Hz, 1 H), 3.56 (dt, *J* = 4.9, 11.0 Hz, 1 H), 2.67 - 2.56 (m, 1 H), 2.54 - 2.45 (m, 1 H), 2.45 - 2.36 (m, 1 H), 2.27 - 2.17 (m, 1 H); $^{13}C\{^{1}H\}$ NMR (125 MHz, $CDCl_3$) δ = 160.7, 124.9, 124.5, 79.9, 56.8, 30.8, 29.8; MS (ESI-APCI) exact mass calculated for $[M+H]^+$ ($C_7H_{10}NO_2$) requires *m/z* 140.1, found *m/z* 140.1; $[\alpha]_D^{24}$ = +216.3 (c = 1.0, $CHCl_3$).

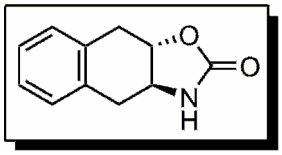

(3a*S*,9a*S*)-3a,4,9,9a-tetrahydronaphtho[2,3-d]oxazol-2(3H)-one (9)

Followed method B using 1a,2,7,7a-tetrahydronaphtho[2,3-b]oxirene (219 mg, 1.50 mmol, 1.5 equiv) and oligomeric catalyst **3** (16.3 mg, 0.02 mmol, 0.02 equiv) for 48 h and purified using silica gel column chromatography to provide 120 mg (0.634 mmol, 63% yield) of (3a*S*,9a*S*)-3a,4,9,9a-tetrahydronaphtho[2,3-d]oxazol-2(3H)-one (**9**) as a white solid. This material was determined to be 94.6% ee by HPLC analysis (ChiralPak AD-H, 5% IPA/hexanes, 1 mL/min, 210 nm, t_R(minor) = 22.40 min, t_R(major) = 24.91 min). IR (neat) 3311, 1747 (s), 1491, 1447, 1380, 1324, 1236, 1143, 1088, 1011, 952, 800 cm^{-1}; ^{1}H NMR (500 MHz, $CDCl_3$) δ = 7.25 - 7.14 (m, 4 H), 5.63 (br. s., 1 H), 4.34 (dt, *J* = 5.4, 11.5 Hz, 1 H), 3.76 (dt, *J* = 4.9, 11.5 Hz, 1 H), 3.35 (dd, *J* = 5.4, 15.1 Hz, 1 H), 3.22 (dd, *J* = 4.9, 15.1 Hz, 1 H), 3.19 - 3.11 (m, 1 H), 3.01 - 2.92 (m, 1 H); $^{13}C\{^{1}H\}$ NMR (125 MHz, $CDCl_3$) δ = 160.9, 132.6, 132.4, 130.4, 130.0, 127.0, 127.0, 80.2, 57.3, 34.5, 33.4; MS (ESI-APCI) exact mass calculated for $[M+H]^+$ ($C_{11}H_{12}NO_2$) requires *m/z* 190.1, found *m/z* 190.1; $[\alpha]_D^{24}$ = +198.1 (c = 1.0, $CHCl_3$).

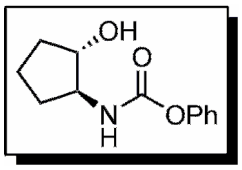

phenyl (1*S*,2*S*)-2-hydroxycyclopentylcarbamate (10)

Followed method B using cyclopentene oxide (131 μL, 1.50 mmol, 1.5 equiv) and oligomeric catalyst **3** (8.2 mg, 0.01 mmol, 0.01 equiv) for 24 h and purified using silica gel column chromatography to provide 146 mg (0.661 mmol, 66% yield) of phenyl (1*S*,2*S*)-2-hydroxycyclopentylcarbamate (**10**) as a white solid. This material was determined to be >99% ee by HPLC analysis (ChiralPak AD-H, 10% IPA/hexanes, 1 mL/min, 210 nm, t_R(minor) = 13.20 min, t_R(major) = 14.80 min). IR (neat) 3378, 3283, 2964, 1714, 1692 (s), 1547, 1533, 1490, 1207, 1169, 1023, 965 cm^{-1}; ^1H NMR (500 MHz, $CDCl_3$) δ = 7.38 (t, *J* = 7.3 Hz, 2 H), 7.23 (t, *J* = 7.3 Hz, 1 H), 7.14 (d, *J* = 7.8 Hz, 2 H), 5.25 (br. s., 1 H), 4.12 (q, *J* = 5.9 Hz, 1 H), 3.82 - 3.73 (m, 1 H), 3.56 (s, 1 H), 2.26 - 2.14 (m, 1 H), 2.13 - 2.02 (m, 1 H), 1.88 - 1.64 (m, 3 H), 1.49 (qd, *J* = 8.1, 13.2 Hz, 1 H); $^{13}C\{^1H\}$ NMR (125 MHz, $CDCl_3$) δ = 155.8, 150.7, 129.3, 125.6, 121.5, 79.3, 61.0, 32.5, 30.6, 21.0; MS (ESI-APCI) exact mass calculated for $[M+H]^+$ ($C_{12}H_{16}NO_3$) requires *m/z* 222.1, found *m/z* 222.1; $[\alpha]_D^{24}$ = –30.9 (c = 1.0, $CHCl_3$).

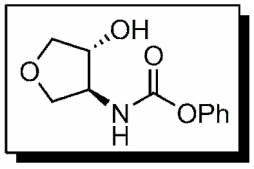

phenyl (3*S*,4*R*)-4-hydroxytetrahydrofuran-3-ylcarbamate (11)

Followed method B using 3,4-epoxytetrahydrofuran (104 μL, 1.50 mmol, 1.5 equiv) and oligomeric catalyst **3** (8.2 mg, 0.01 mmol, 0.01 equiv) for 24 h and purified using silica gel column chromatography to provide 110 mg (0.493 mmol, 49% yield) of phenyl (1*S*,2*S*)-2-hydroxycyclopentylcarbamate (**11**) as a white solid. This material was determined to be >99% ee by HPLC analysis (ChiralCel OD-H, 10% IPA/hexanes, 1 mL/min, 210 nm, t_R(major) = 23.68

min, t_R(minor) = not detected in enantioenriched sample; 35.55 min in racemic sample). IR (neat) 3398, 3349, 1701 (s), 1519, 1485, 1345, 1232, 1205, 1104, 1082, 1057, 1029, 974, 884, 805 cm^{-1}; ^1H NMR (500 MHz, CD_3OD) δ = 7.37 (t, *J* = 8.1 Hz, 2 H), 7.20 (t, *J* = 7.3 Hz, 1 H), 7.10 (d, *J* = 7.8 Hz, 2 H), 4.30 - 4.24 (m, 1 H), 4.09 (dd, *J* = 5.4, 9.3 Hz, 1 H), 4.04 - 3.97 (m, 2 H), 3.74 (dd, *J* = 2.2, 9.0 Hz, 1 H), 3.68 (dd, *J* = 1.5, 9.8 Hz, 1 H); $^{13}C\{^1H\}$ NMR (125 MHz, CD_3OD) δ = 156.9, 152.7, 130.5, 126.5, 122.8, 77.2, 74.8, 72.2, 61.0; MS (ESI-APCI) exact mass calculated for $[M+H]^+$ ($C_{11}H_{14}NO_4$) requires *m/z* 224.1, found *m/z* 224.1; $[\alpha]_D^{24}$ = –31.4 (c = 1.0, $CHCl_3$).

2.4.5 Absolute configuration determination

The absolute configuration of (1*S*,2*S*)-2-aminocyclohexanol hydrochloride and (1*S*,2*S*)-2-aminocyclopentanol hydrochloride were each assigned by comparison with experimental data provided in references 4b and 16. The absolute configuration of all other products was assigned by analogy.